Preliminary Report
of
The Hakuho Maru Cruise KH 86-2

April 21 - May 15, 1986

Geophysical and Geological Investigation of the
northeastern Part of the Sea of Japan and Japan Trench

(ODP Site Survey)

with

An Annex for Preliminary Report
of
The Tansei Maru Cruise KT 87-6

May 29 - June 4, 1987

Investigation on the Sea-Floor Spreading Tectonics
in the Northeastern Part of Japan Basin

(ODP Site Survey)

Ocean Research Institute
University of Tokyo
1988

Preliminary Report
of
The Hakuho Maru Cruise KH 86-2

April 21 - May 15, 1986

Geophysical and Geological Investigation of the
northeastern Part of the Sea of Japan and Japan Trench

(ODP Site Survey)

with

An Annex for Preliminary Report
of
The Tansei Maru Cruise KT 87-6

May 29 - June 4, 1987

Investigation on the Sea-Floor Spreading Tectonics
in the Northeastern Part of Japan Basin

(ODP Site Survey)

by

The Scientific Members of the Expedition

Edited by

Kazuo KOBAYASHI

PREFACE

Geological and geophysical features of the Sea of Japan have been extensively surveyed by a great number of scientists since long time ago. An unanimous understanding among them is that this area is a typical extinct backarc basin existing between the Japanese Islands and Asiatic continents. Nevertheless, enigmas have remained unsolved particularly concerning its origin. Difficulties in overall interpretation of the processes generating this area may be owing to its regional irregularities of magnetic anomalies, subbottom structure and geochemical composition of the crust. Although there exist numerous tracks of survey ships crossing the Sea of Japan, their spacings are in most places insufficient to reveal the regional irregularities. Precision of ships' positions in early time was unfortunately not so accurate as to reveal detailed features of the bottom structure using combined data of various projects. Accuracy of the ship's positions became sufficiently good only several years ago when the up-to-date Loran C electronic navigation device combined with the NNSS satellite navigation system was adopted.

This cruise KH 86-2 of the Research Vessel Hakuho Maru was greatly devoted to the comprehensive investigation of a few focused areas in the Sea of Japan by a well-controlled network of ship's tracks mostly parallel to one another with spacings shorter than a half-wavelength of the magnetic anomalies. Thus, lineaments of magnetic anomalies can be exactly correlated without any preassumption. The shape of survey tracks is similar to that adopted at our detailed mapping of the Japan Trenches by the Seabeam echo sounder of the French research vessel Jean Charcot. Although our ship Hakuho Maru has no Seabeam device on board during this cruise, most of the deep basins of the Sea of Japan are covered by thick sediments causing extremely flat bottom surface which makes narrow beam bathymetry useless. Seismic profiling has in contrast revealed some local variations in sediment structure.

The most extensive investigation was made in a region of 200 km x 150 km tripezoid located in the northeastern Japan Basin west of Matsumae Plateau. Total 20 parallel closedly spaced tracks with a length of approximately 200 km each were surveyed. Geomagnetic total force was precisely measured on all of the tracks together with single-channel seismic profiling on some of them. Magnetic anomaly patterns were firmly drawn based upon these data. On the flank of the Matsumae Plateau an offset of the subbottom topography was recognized by the profiler results. In addition, the multichannel seismic profiling was done along two couples of EW trending parallel tracks

at regions west off Okushiri Ridge (43°00'-42°50'N, 139°00'-139°45'E) and southwest off Musashi Tai (44°00'-44°10'N, 139°00'-139°45'E).

More than 10 station works including piston corings, dredge hauls, deep-sea photography and heat flow measurement were executed in the same region as well as at a few sites on the mouth of Tsugaru Straight and on the crest of the Erimo Seamount on our way from Tokyo. Samples collected by these operations were analyzed and labelled on board the ship and studied in the shore-based laboratories of some participants. Details of the operations and collected samples are described in this report.

Observation by Ocean Bottom Magnetometers(OBM) and related bottom-moored instruments was done for intervals of a few days to a week on the southeast edge of the tripezoid. The results are also useful to record the geomagnetic storms and other time variations for a controll of anomaly measurement.

In order to supplement the present magnetic and seismic reflection measurement by R.V. Hakuho Maru a short cruise of the research vessel Tansei Maru KT 87-6 was devoted to the same region. Preliminary report of this cruise is included in the present report as Annex.

A great portion of investigation presented in this report was undertaken aiming to the site survey of proposed drillings by the D. V. JOIDES Resolution for the Ocean Drilling Program. We are indebted to much invaluable advice and suggestion provided by members of the ODP/JOIDES committees and panels composed of many scientists and specialists from the international partner countries (USA, FRG, France, Canada, U.K., ESF and Japan). We are very grateful to general and financial support by the Ministry of Education, Science and Culture (MONBUSHO) to Japanese participation in the Ocean Drilling Program as well as the site survey efforts.

We wish to express our sincere thanks to Geological Survey of Japan and Hydrographic Department, Maritime Safety Agency of Japan for providing us their unpublished data. Great help of officers and crew of two research vessels, Hakuho Maru and Tansei Maru during these cruises is acknowledged, without which our survey was unable to be completed.

January 1988

Kazuo KOBAYASHI
Chief Scientist of KH 86-2

CONTENTS

1. SCIENTISTS ABOARD THE R.V. HAKUHO MARU FOR THE CRUISE KH 86-2

KOBAYASHI, Kazuo	(Chief Scientist) Ocean Research Institute, University of Tokyo
ASANUMA, Toshio*	Department of Earth Sciences, Chiba University
FURUTA, Toshio*	Ocean Research Institute, University of Tokyo
ISEZAKI, Nobuhiro**	Department of Earth Sciences, Kobe University
ISHII, Teruaki*	Ocean Research Institute, University of Tokyo
IYENGAR, R.V.	Ocean Research Institute, University of Tokyo
OUBIÑA, Jose Luis	Ocean Research Institute, University of Tokyo
KATO, Michio*	School of General Education, Kanazawa University
KITAMURA, Akitoshi	School of General Education, Kanazawa University
KOBAYASHI, Hiroaki	Department of Geology & Paleontology, Tohoku University
KOIZUMI, Kin-ichiro	Ocean Research Institute, University of Tokyo
KONISHI, Kenji*	Department of Geology, Kanazawa University
KURAMOTO, Shinichi*	Department of Geology, Kanazawa University
NAKANISHI, Masao	Ocean Research Institute, University of Tokyo
PARK, Chung-Hwa**	Ocean Research Institute, University of Tokyo
SAYANAGI, Keizo	Department of Earth Sciences, Kobe University
SEGAWA, Jiro	Ocean Research Institute, University of Tokyo
SUEMASU, Makoto*	Department of Earth Sciences, Chiba University
SUZAKI, Toshiaki*	Faculty of Science, Hirosaki University
TAMAKI, Kensaku**	Ocean Research Institute, University of Tokyo
TOKUYAMA, Hidekazu*	Ocean Research Institute, University of Tokyo
TOH, Hiroaki	Ocean Research Institute, University of Tokyo
TSUCHI, Ryuichi*	Department of Earth Sciences, Shizuoka University
WATANABE, Masaharu	Ocean Research Institute, University of Tokyo
YAMASHITA, Shigeru	Department of Earth Sciences, Chiba University

* from April 21 (Tokyo) to May 03 (Akita) only
** from May 05 (Akita) to May 15 (Tokyo) only

2. Index Maps of KH 86-2 and 1

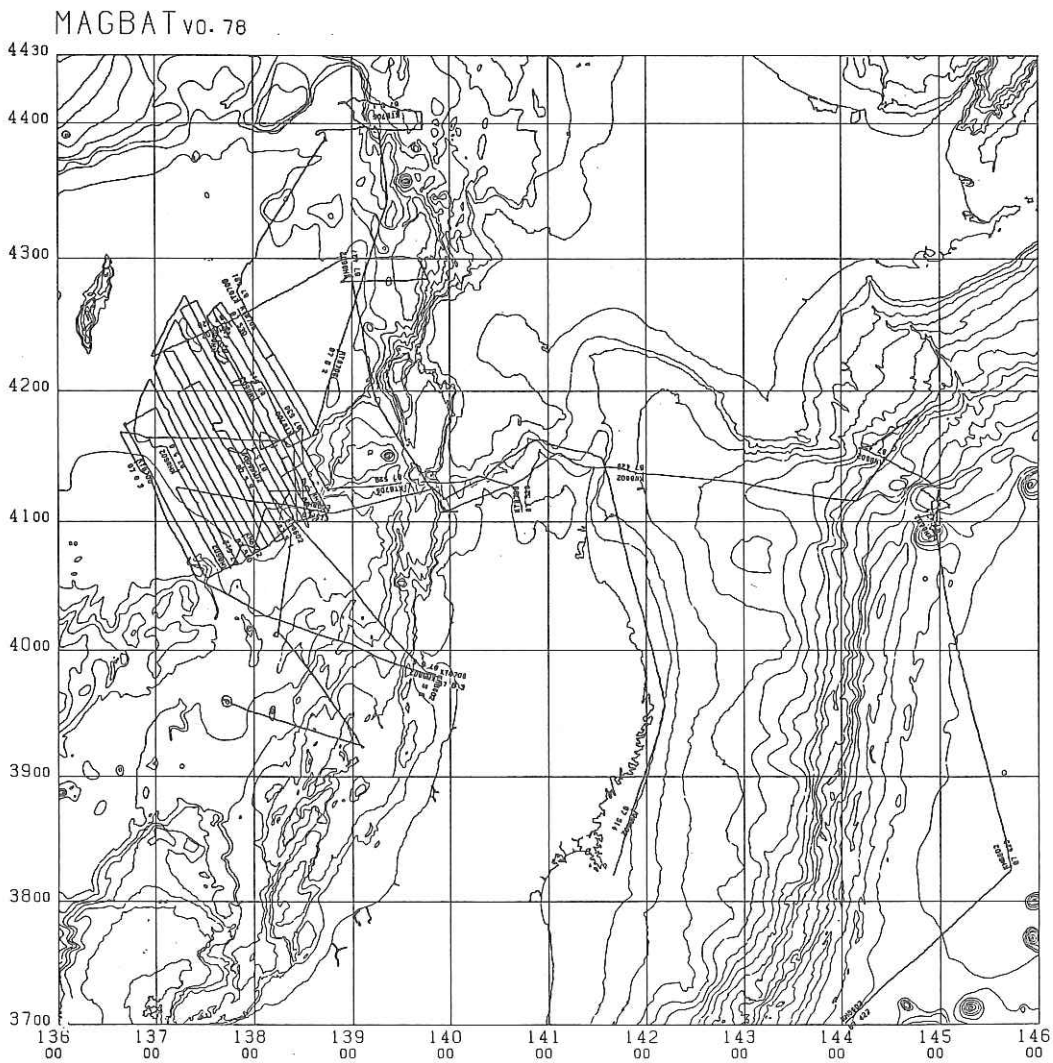

Fig. 2-1 Ship's tracks of the cruises KH 86-2 and KT 87-6 plotted in the Mercator projection. Numerical figures beside the tracks indicate positions at 00:00 (local time) of year-month-day. Contour interval 500 m. Bathymetry is based upon MAGBAT Data Base vo.78.

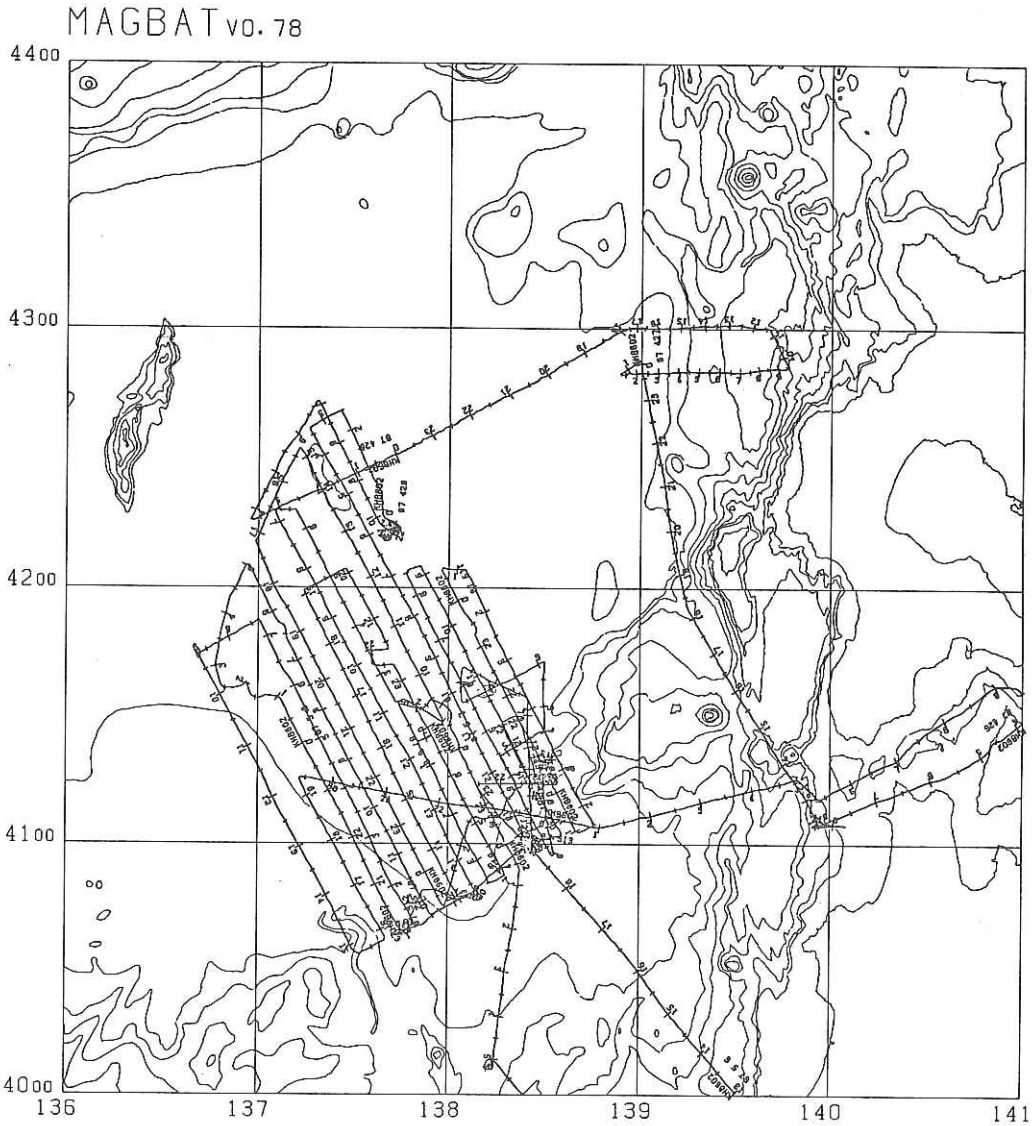

Fig. 2-2 Ship's tracks of the cruise KH 86-2 in the northeastern Sea of Japan plotted in the Mercator projection. Numerical figures indicate local time. Contour interval 500 m. Bathymetry is based upon our MAGBAT Data Base vo.78.

3. LIST OF RESEARCH STATIONS IN THE CRUISE KH 86-2

Site No.	Position Lat.(N)	Long.(E)	Investigation	Water Depth (M)	Date	& Time	Remarks
	[LEG 1:Tokyo to Akita]				April		
1	41°11.9'	144°53.4'	Piston Coring	7070	23	16:05	Hit on Bottom
2	40°54.1'	144°51.3'	Dredge Haul	3850	24	00:08	on Bottom(No.1)
	40°55.5'	144°50.9'		4080	24	00:56	on Bottom(No.2)
	40°56.2'	144°51.6'		4050	24	02:10	final on Bottom
3	40°58.7'	144°50.4'	Dredge Haul	4950	24	05:55	on Bottom
	40°57.4'	144°51.2'		4520	24	08:22	final on Bottom
4	40°56.1'	144°48.8'	Camera	4580	24	11:52	Start of Shots
	40°56.2'	144°48.9'			24	13:10	End of Shots
5	41°06.5'	139°55.6'	Piston Coring	510	26	09:30	Hit on Bottom
6	41°04.5'	139°55.8'	Piston Coring	580	26	11:23	Hit on Bottom
7	42°13.5'	137°39.4'	Piston Coring	3690	28	12:03	Hit on Bottom
7-2	42°13.6'	137°40.2'	Heat flow	3690	28	14:45	Hit on Bottom
	42°13.6'	137°40.1'				15:08	Hit
	42°13.6'	137°40.1'				15:15	Hit
	42°13.6'	137°40.2'				15:31	Hit
7-3	42°13.2'	137°40.1'	Camera	3690	28	18:15	Start of Shots
	42°13.3'	137°40.3'				19:30	End of Shots
JK1	40°59.7'	138°25.1'	set OBE-Z+OBC	3400	29	14:20	Lv surface
JK2	40°59.7'	138°25.9'	set OBP	3400	29	15:43	Lv surface
8	41°18.7'	138°28.8'	Piston Coring	3690	30	11:09	Hit on Bottom
8-2	41°19.9'	138°29.4'	Heat flow	3700	30	13:56	Hit
	41°19.9'	138°29.4'				14.02	Hit
	41°19.9'	138°29.4'				14.09	Hit
	41°19.9'	138°29.5'				14:32	Hit
	41°19.8'	138°29.4'				14:41	Hit
	41°19.8'	138°29.4'				15:03	Hit
8-3	41°16.8'	138°30.2'	Camera	3690	30	18:07	Start of Shots
	41°16.6'	138°31.6'		3690	30	19:21	End of Shots

					May	
9	39°18.6'	139°02.0'	Piston Coring	770	1	11:45 Hit on Bottom
10	39°14.0'	139°05.6'	Piston Coring	610	1	13:29 Hit on Bottom
10-2	39°14.2'	139°06.0'	Deep TV(failed,	600	1	14:08 Start of Work
	39°14.4'	139°06.7'	glass sphere broken)		1	15:19 End of Work
11	39°34.5'	137°43.0'	Dredge Haul	2170	1	23:21 on Bottom
	39°35.3'	137°41.7'		2060	2	02:00 final on Bottom

Port of Call at AKITA Harbor (Akita Shin-kou)
May 02 (Fri.) to May 06 (Tues.)

[LEG 2, Akita to Tokyo]

JK3	41°00.2'	138°25.1'	set OBM-S4	3380	6	19:14 Lv surface
JK4	40°49.0'	138°08.0'	set OBM-S1	3610	7	14:44 Lv surface
JK5	40°39.2'	137°44.5'	set OBM-S3	3320	7	18:18 Lv surface
12	41°12.4'	138°27.2'	Heat flow	3670	10	14:43 Hit Bottom
	41°12.5'	138°27.2'				15:07 Hit
	41°12.4'	138°27.3'				15:13 Hit
	41°12.4'	138°27.3'				15:34 Hit
12-2	41°12.7'	138°27.0'	Camera	3670	10	17:56 Start of Shots
	41°12.7'	138°27.9'		4440	10	19:11 End of Shots
JK2	40°59.6'	138°25.8'	retrieve OBP	3410	11	12:42 Release Wt
	40°59.8'	138°25.8'		3400	11	13:45 on Deck
JK1	40°59.6'	138°24.9'	retrieve OBE	3390	11	14:03 Release Wt
	40°59.8'	138°24.9'		3400	11	15:18 on Deck
JK3	41°00.2'	138°25.0'	retrieve OBM-S4	3380	11	15:31 Release Wt
	41°00.5'	138°25.2		3380	11	17:05 on Deck
JK4	40°49.0'	138°08.0'	retrieve OBM-S1	3600	11	18:41 Release Wt
	40°49.1'	138°08.4		3600	11	20:30 on Deck
JK5	40°39.0'	137°44.8'	retrieve OBM-S3	3320	12	00:44 on Deck

4. INDEX MAP OF RESEARCH STATIONS

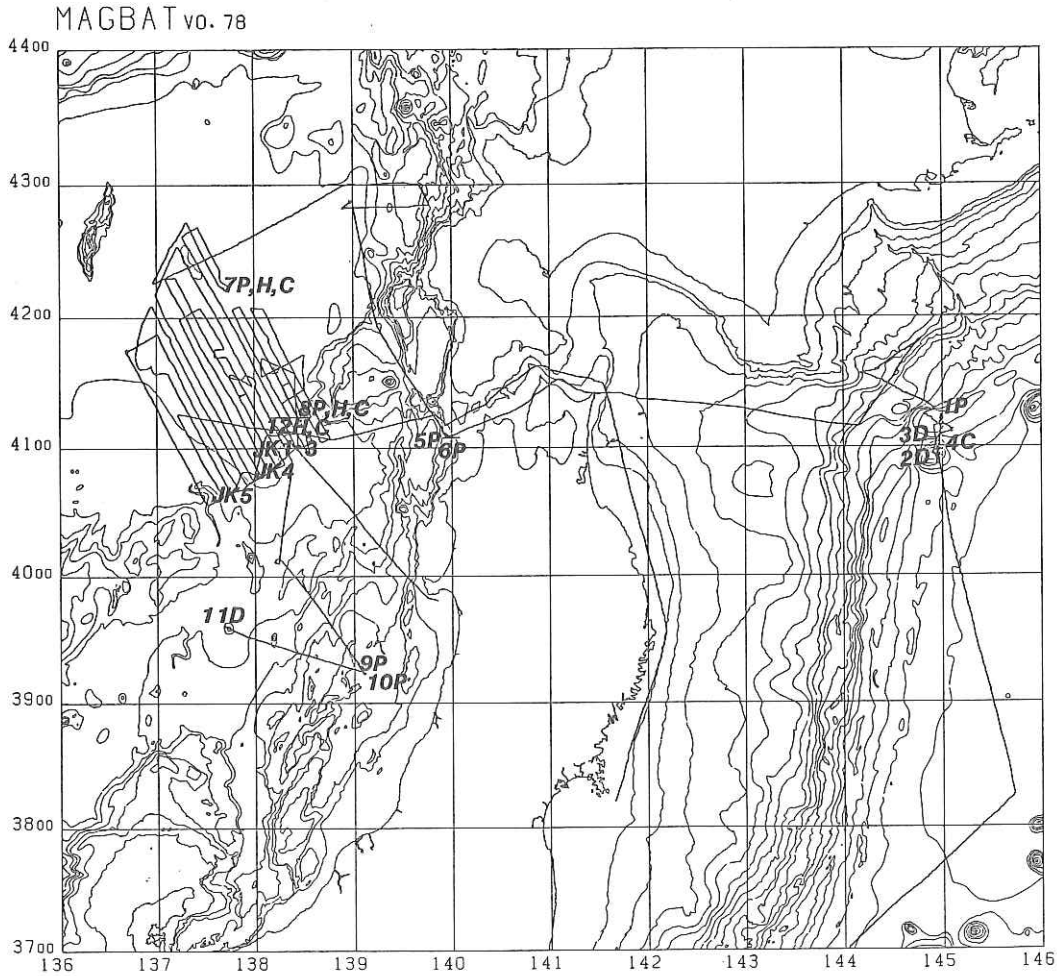

Fig. 4-1 Research stations in the cruise KH 86-2.
P: Piston coring, D: Dredge haul, H: Heat flow measurement,
C: Camera, JK: OBM, OBP, OBE, OBC

5. Measurement of Geomagnetic Total Force by A Proton Precession Magnetometer

K. Tamaki, K. Kobayashi, N. Isezaki, K. Sayanagi, M. Nakanishi, and C. H. Park

The age and spreading tectonics of the Japan Sea have been controversial for a long time because of poor development of magnetic anomaly lineations. Magnetic anomaly lineations of the Japan Sea have been regionally investigated since 1960's (Isezaki and Uyeda, 1973; Isezaki 1986). Overall feature of magnetic anomalies of the Japan Sea compiled by Isezaki (1986) from all the available data shows very complicated feature. Isezaki and Uyeda (1973) observed rather well developed lineations of ENE-WSW trend at the western part of the Japan Basin between the Yamato Bank and the Siberia Continent where the ENE-WSW trending configuration of the Japan Basin there suggests rather organized spreading history. The anomaly lineation sequence was identified by Isezaki (1986) to be from 20 Ma to 15 Ma. The eastern part of the Japan Basin, however, shows very complicated anomaly pattern on Isezaki's (1986) compiled magnetic anomaly contour map, suggesting poorly developed magnetic anomaly lineations. The complexity may partly be due to poor position fixing of old data of 1960's. We conducted a detailed magnetic anomaly mapping in an area of the eastern part of the Japan Basin during KH86-2 cruise to elucidate more real picture of magnetic anomaly lineations of the basin.

The detailed survey area was targeted at the area of the highest probability of the occurrence of magnetic anomaly lineations in the eastern half of the Japan Basin on the basis of the compilation of previous data of the Geological Survey of Japan, the Lamont-Doherty Geological Observatory, and the KH69-2 cruise data. The tracklines were designed with the direction of N30°W which was supposed to be normal to the direction of predicted magnetic anomaly lineations. The interval of each tracklines was set to be 4 nautical miles because the predicted minimum wavelength of magnetic anomaly lineations is about 5 nautical miles. Eighteen tracklines with length of 72 miles to 100 miles were designed. The resultant tracklines were shown in Fig. 5-1. Groups of fishery boats interrupted the execution of straight track lines very often and made some lack of tracklines. However, overall feature of the gridded tracklines was very successful.

A conventional proton precession magnetometer, Type ORI-Uchiyama, was used for the measurements of geomagnetic total forces. Data sampling interval was every 30 seconds. Composite position fixing by Loran C, NNSS, and GPS was used.

Figure 5-2 shows the result of the geomagnetic survey with the geomagnetic anomalies along tracklines. The amplitudes of magnetic anomalies are generally less than 300 nT except one locality at the southern end of the survey area where anomalies of 500 nT are observed. Most prominent magnetic anomaly lineations are developed at the mid part of the survey area with trend of N70°E which appears to be general trend of magnetic anomaly lineations in the survey area. All anomaly lineations are not continuous throughout all the tracks. The most continuous one is observed throughout 9 tracks. Most other anomaly lineations are observed throughout only 5 or less tracks. The discontinuity lines are not normal to the lineations but very oblique with the angle generally 45°. The oblique displacement of magnetic anomaly lineations are formed as a pseudofault of propagating ridge system (Hey, 1977). Our result suggests numerous occurrence of pseudofault in the lineation pattern. Such abundant occurrence of pseudofault indicates that ridge propagation was predominant in the spreading process along ridge axis of the eastern Japan Basin. The predominance of ridge propagation during the spreading of the Japan Basin may suggest very unstable stress state of back-arc spreading of the Japan Sea.

Northernmost lineations show the trend of N40°E which is quite different from major trend of N70°E. As the northern end of the survey area is at the center of the Japan Basin, the difference of the trends suggests that a remarkable reorganization of ridge system occurred at the later stage of the spreading process of the Japan Basin. Similar reorganization is observed in the Shikoku Basin (Kobayashi and Nakada, 1980) and the West Philippine Basin (Hilde and Lee, 1983). The trend of lineations also changes at the southern end of the survey area with trend of N45°E. This part is the margin of the basin and supposed to be oldest part of the Japan Basin lithosphere. This feature suggests that another reorganization of spreading ridge occurred at the early stage of spreading. Thus, we can elucidate two stages of major ridge reorganization.

A seamount was observed at the southeastern part of the survey area. The peak of the seamount is 2500 m deep and 1200 m high above the sea floor. As the sediment thickness of the surrounding area is about 1500 m (Ishiwada et al., 1984), the height of the seamount above the basement is about 2700 m. The magnetic anomalies, however, is not so high with the amplitudes less than 300 nT. The seamount is not conical but elongated parallel with the surrounding magnetic anomaly lineations. The seamount has steep scarps on the southern and the northern sides and rugged flat top. All these features suggest a possibility of continental fragment (Tamaki, 1985) as an origin of this seamount.

The exceptional highest peak at the southern end of the survey area is observed only on two tracklines. No topographic high is observed at the corresponding locality. One of the possible explanation of this high anomaly is the presence of an exceptionally thick oceanic crust caused by a large magma chamber. The large magma chamber may have caused an anomalously thick magnetized layer in the oceanic crust.

In conclusion, we are confirmed that the detailed survey of this kind is very effective of the analysis of magnetic anomaly lineation of the Japan Basin. The identification of pseudofaults is almost impossible without dense track survey of magnetics. Further study of the data obtained during this cruise will address lineation fabric of the spreading system and present valuable suggestions on spreading tectonics of the Japan Basin.

REFERENCES

Hey, R., A new class of "pseudofaults" and their bearing on plate tectonics, Earth Planet. Sci. Lett., 37, 321-325, 1977.

Hilde, T. W. C., and C-S. Lee, Origin and evolution of the west Philippine Basin: a new interpretation, Tectonophys., 102, 85-104, 1985.

Isezaki, N., A magnetic anomaly map of the Japan Sea, J. Geomag. Geoelectr., 38, 403-410, 1986.

Isezaki, N. and S. Uyeda, Geomagnetic anomaly pattern of the Japan Sea, Marine Geophys. Res., 2, 51-59, 1973.

Ishiwada, Y., E. Honza, and K. Tamaki, Sedimentary Basins of the Japan Sea, Proc. 27th Intern. Geol. Congr., 23, 43-65, 1984.

Kobayashi, K., and M. Nakada, Magnetic anomalies and tectonic evolution of the Shikoku inter-arc basin, J. Phys. Earth, 26, 391-402, 1978.

Tamaki, K., Two modes of back-arc spreading, Geology, 13, 475-478, 1985.

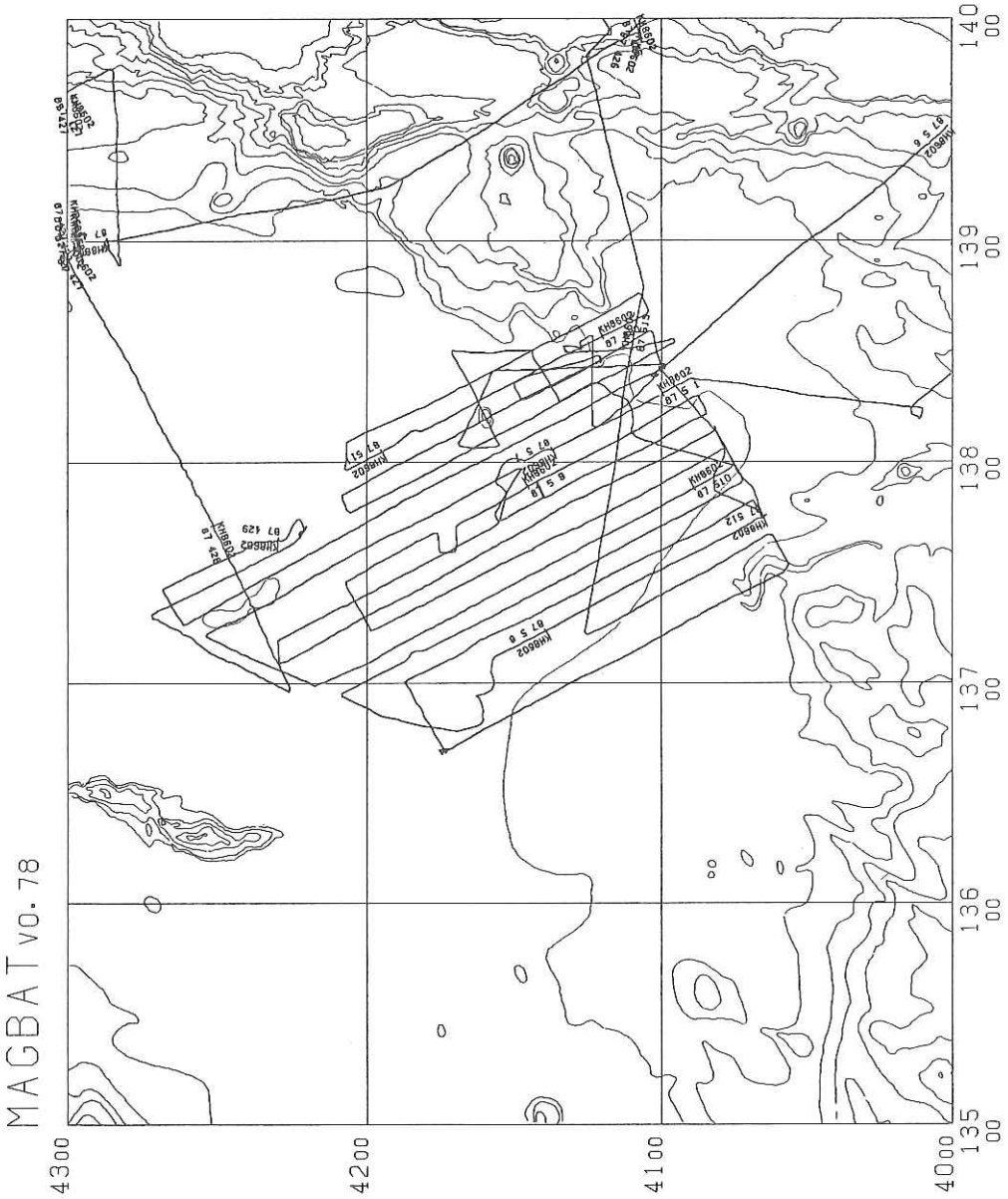

Fig. 5-1 Survey tracks of detailed geomagnetic survey. Interval of the tracks are generally 4 n.m.

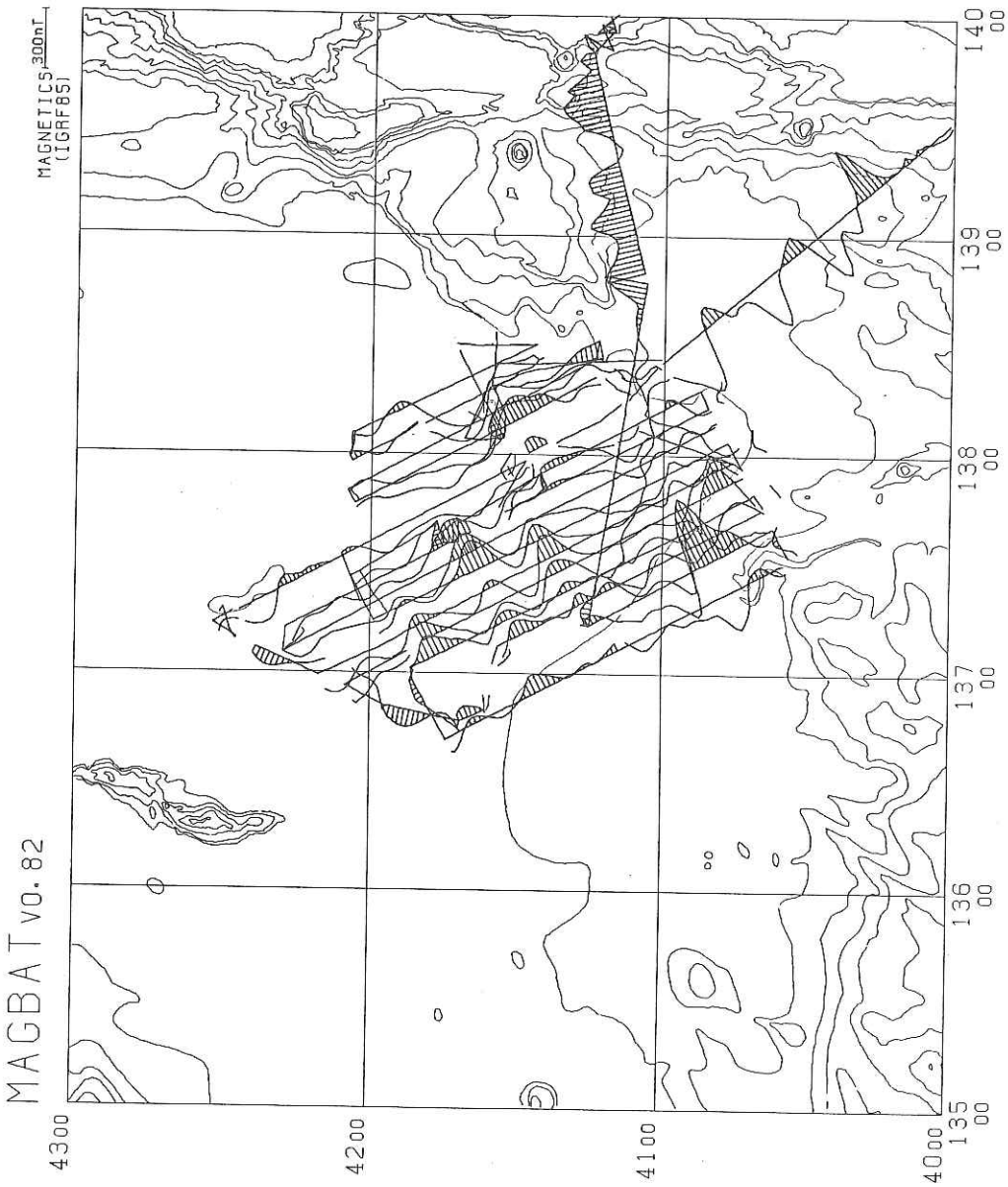

Fig. 5-2 Geomagnetic anomaly profiles along ship's tracks. Positive anomalies are hatched. Anomalies are based on IGRF1985.

6. THREE COMPONENT ANOMALIES OF GEOMAGNETIC FIELD MEASURED BY SCTM

K. Sayanagi and N. Isezaki

Three components of the geomagnetic field were measured by STCM (Shipboard Three Component Magnetometer) throughout the KH 86-2 cruise. Especially in the southeastern part of the Japan Basin, the detailed magnetic survey was carried out on 17 tracks which are 80 to 100 miles long with 4 mile interval by a proton magnetometer together with STCM. Because the strike of elongation of each magnetic anomaly can be determined by three component anomalies, the detail and precise feature of lineality of anomalies will be made clear.

Three component geomagnetic fields are obtained by eliminating the magnetic field induced by a ship's body from the observed magnetic field. In order to eliminate the induced magnetic field, 12 constants should be known relating to the magnetic susceptibility distribution, the permanent magnetization, the position of the sensors and the shape of a ship. These 12 constants are determined by three component data measured during rotation of a ship on an 8 shape track (e.g. a 360° rotation and a reversed 360° rotation). During the KH 86-2 cruise, 4 '8-shape' rotations were conducted as followed.

1. 24 April '86, 15h25m-15h55m, 41°06.7'N 145°03.7'E.
2. 27 April '86, 00h16m-00h45m, 42°51.2'N 139°00.1'E.
3. 6 May '86, 21h20m-21h55m, 41°00.4'N 138°24.8'E.
4. 12 May '86, 08h41m-09h11m, 41°44.3'N 136°41.6'E.

With these data sets, 12 constants and consequently three component anomalies will be calculated.

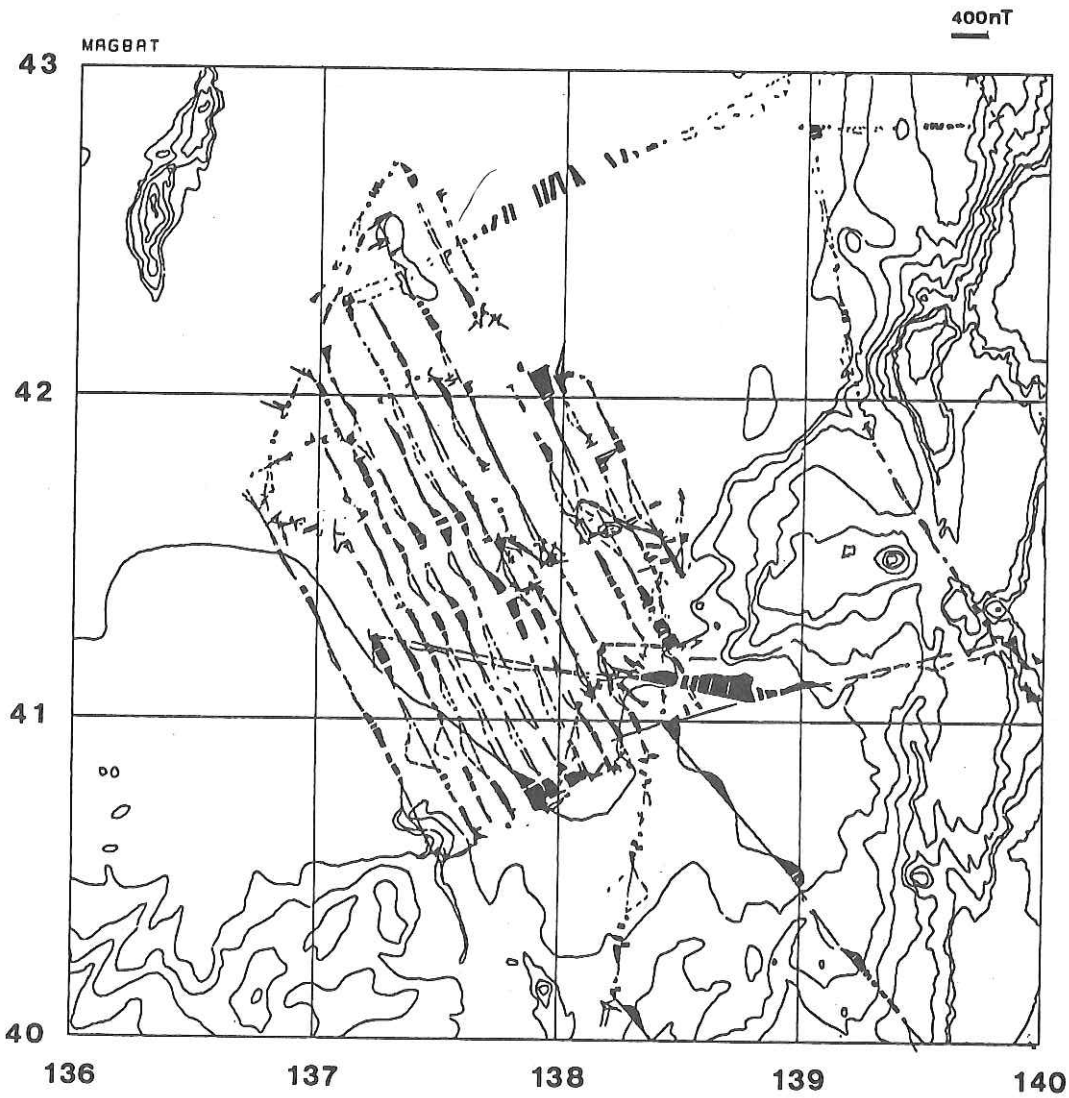

Fig. 6-1 The north component anomaly profiles projected on the ship's tracks. Positive anomalies are shaded.

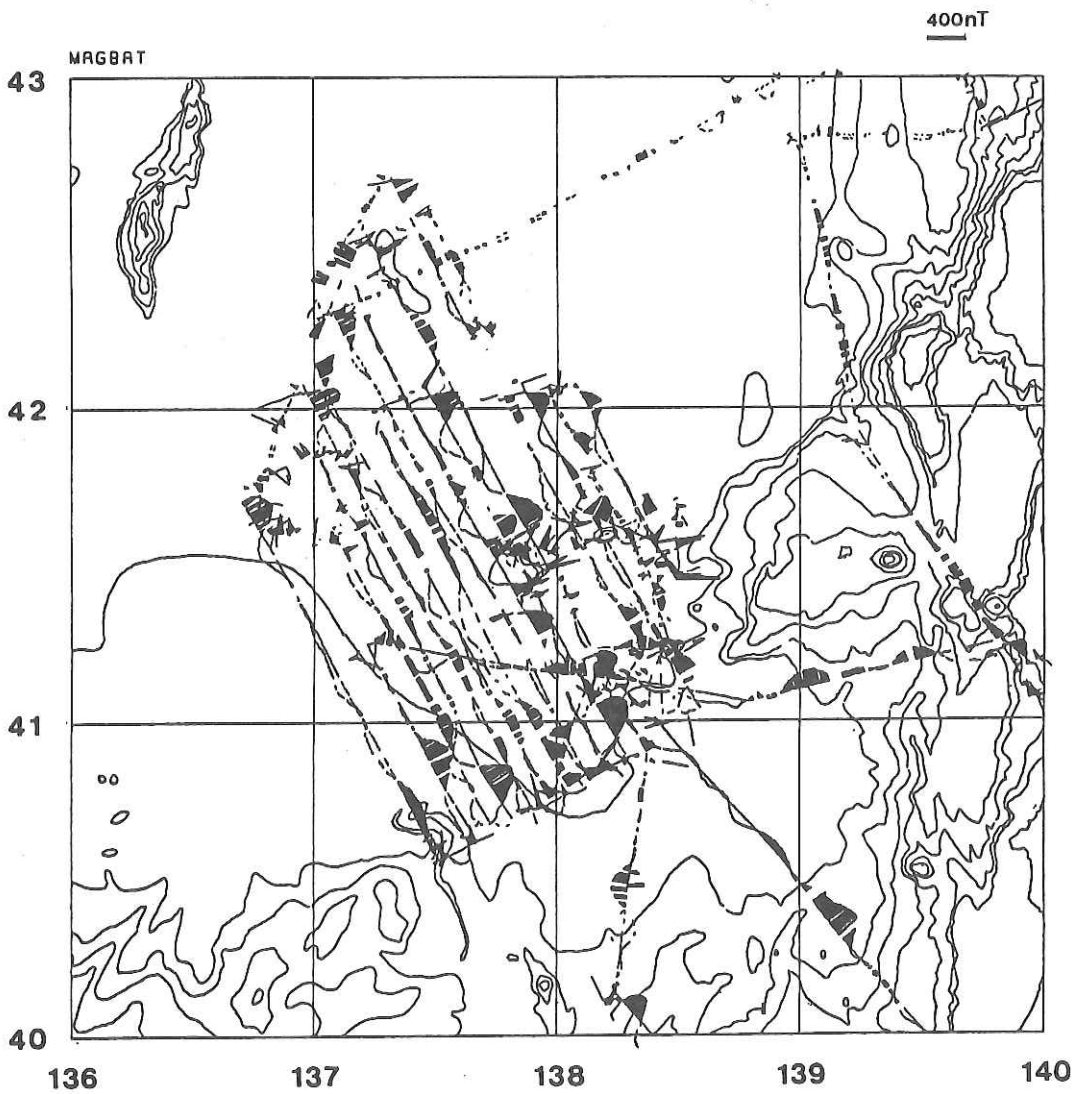

Fig. 6-2 The east component anomaly profiles projected on the ship's tracks. Positive anomalies are shaded.

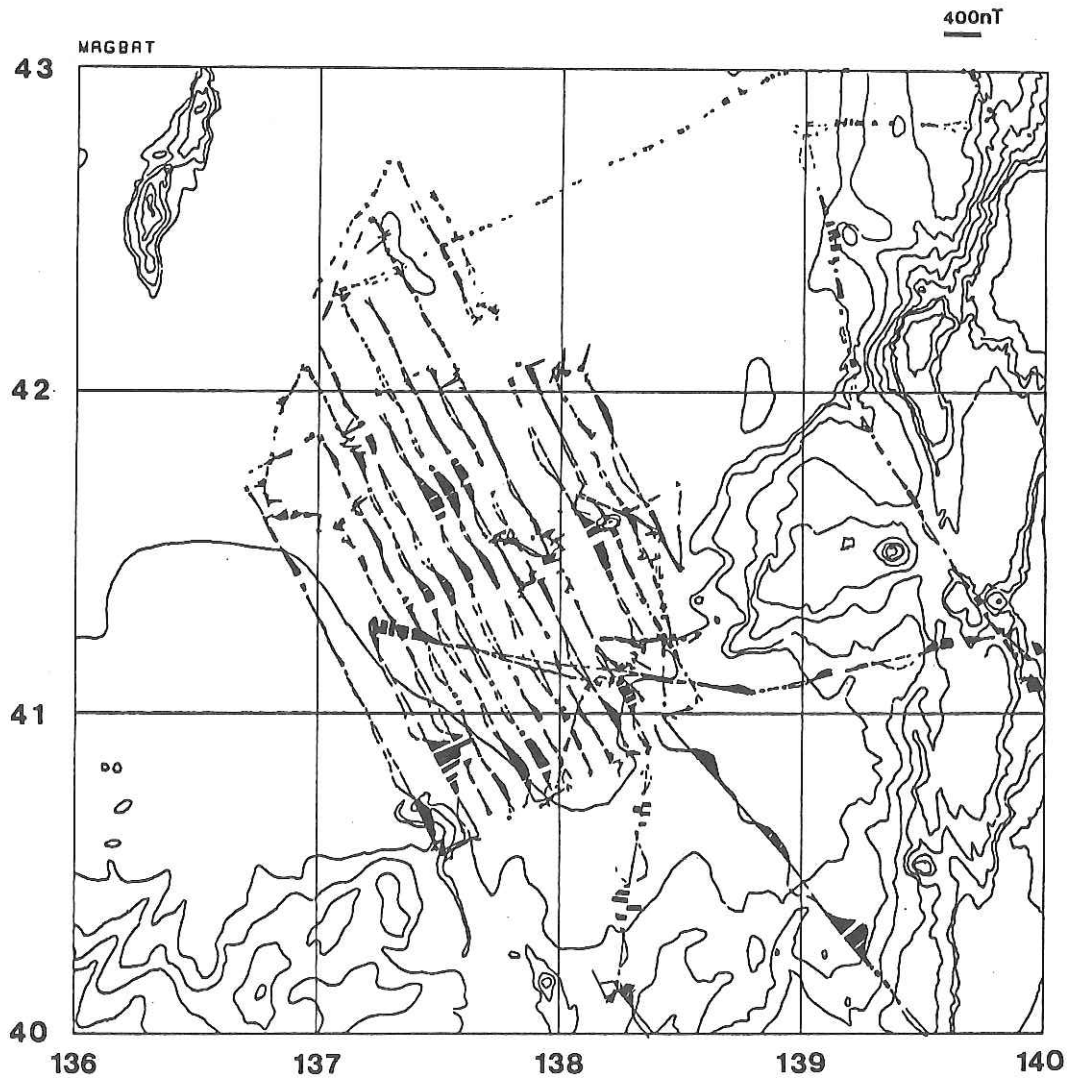

Fig. 6-3 The vertical component anomaly profiles projected on the ship's tracks. Positive anomalies are shaded.

7. GRAVITY MEASUREMENTS

K. Koizumi and J. Segawa

Outline of Measurements

A T.S.S.G. surface ship gravimeter was used for the measurement. The gravimeter sensor was of the string type Model 68-7-14 and the stabilized platform consisted of a vertical gyroscope Model 82-B with a pair of single degree of freedom gyros. Gravity data was processed by a Micro Nova computer using the program KAIKO-1 system(1984). Measurement of vertical acceleration of the ship was made with an interval of 0.02 sec. Free air gravity anomaly was obtained on board in real time by the aid of on-line Loran-C positioning data and the normal gravity obtained from the Normal Gravity formula. Bouguer anomaly was not calculated because bathymetric data was not available in real time. Gravity measurement was continued throughout the cruise except for the period from 13:00, 26 April to 03:00, 27 April when a failure of the power supply for the sensor exciting amplifier happened.

Calibration of gravity was carried out at Harumi wharf, Tokyo and Ohhama wharf, Akita. A LaCoste & Romberg G-type gravimeter(G-124) was used to measure gravity at the wharfs. A table for comparison of ship-board and land(wharf) gravity values is given in Table 7-1.

	LaCoste	T.S.S.G.	g
Harumi (Departure)	979.773 gal	979.779 gal (21 April)	+ 6 mgal
Ohhama	980.168 gal	980.161 gal (02 May)	- 7 mgal
Harumi (Arrival)	979.773 gal	979.776 gal (15 May)	+ 3 mgal

Table 7-1. Calibration of gravity values

Result of Measurements

T.S.S.G. gravimeter worked almost satisfactorily. Data consistency during a short period was better than 1 mgal. However Eotvos correction calculated from the position changes given by Loran-C receiver caused errors of ±5mgal with a period of approximately 10 min., resulting in

deterioration of the original gravity data. Some means to eliminate the short period fluctuation of Loran-C positioning or an improvement of filtering method of position data is necessary for the next operation.

As a preliminary report, two examples of Free air Anomaly Profile in Fig. 7-1 and Fig. 7-2 are described here. The free air gravity anomaly to be presented is modified values(thick solid line) from which the erroneous fluctuation was roughly smoothed out.

Free air anomaly across thrusting faults:

Two thrusting faults were found at 41° 12' N, 138° 28' E(A) and 41° 15' N, 138° 32' E(B) approximately. Both faults trend from NNE to SSW, and the basements of ESE side thrust over those WNW side. These faults are considered to be reversed faults from the bathymetry as well as the basement structure obtained by seismic profiling. Fig. 7-3 shows the positions of the faults(A and B) and Fig. 7-4 shows the profiles of free air gravity anomaly across the faults from the west to the east side(left to right in Fig. 7-4) together with sketches of subbottom structures obtained by seismic profiling. Bottom topographic and subbottom structures are well reflected on free air anomaly, showing a step of gravity anomaly to the order of magnitude 20 to 30 mgal.

Free air anomaly at a seamount:

A New seamount was found at about 41o 38' N, 138o 15' E. The top of the seamount is 2500m deep in the basin with a depth of 3700m. This mountain is elongated in the direction of WSW to ENE with a dimension of its base 10nm by 5nm. Fig. 7-5 shows a rough topography and the tracks of survey. Fig. 7-6 shows profiles of free air gravity anomaly along the tracks (NO. 1 to 5).

Free air anomaly in the central part of the mountain is positive with a maximum of +35mgal. Free air anomaly around the seamount shows a significant low relatively. Gravity is particularly low in the SSE and ENE sides, showing an unsymmetric feature.

Gravity anomaly of the new seamount is, generally speaking, very weak, and this fact together with the fact that it does not affect the magnetic anomaly may suggest that the seamount is composed of continental, light material. The significant sink of gravity at the foot of the mountain may further suggest that the mountain is well compensated isostatically.

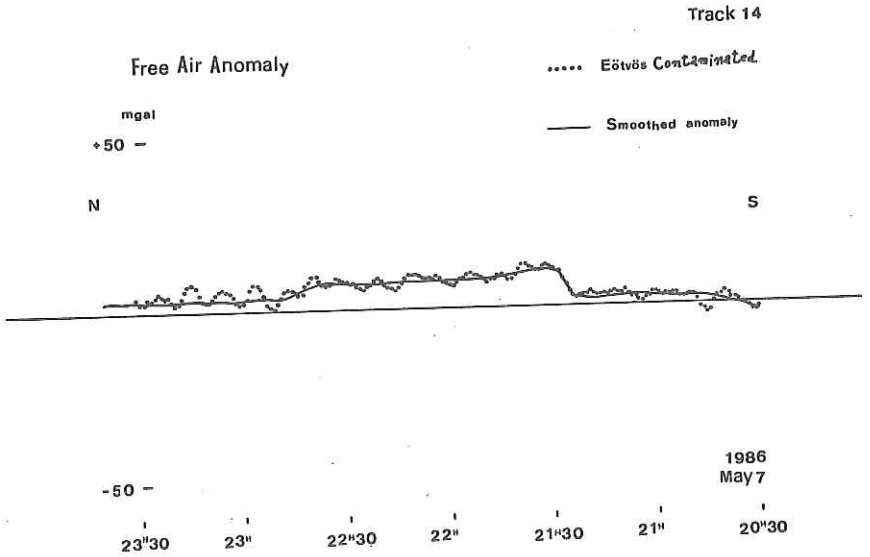

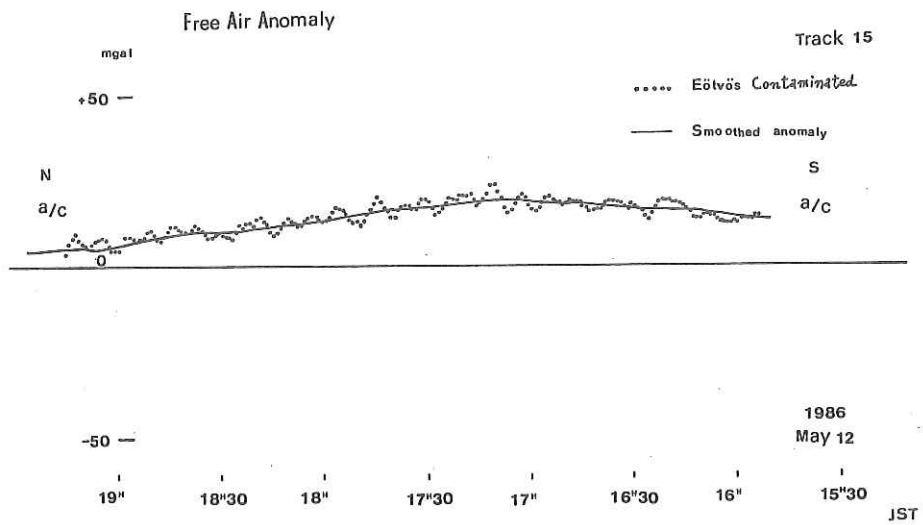

Fig. 7-1 (above) Free air gravity anomaly profile on a survey track 14 (20^h30^m to 23^h30^m of May 7, 1986) in the Japan Basin

Fig. 7-2 (below) Free air gravity anomaly profile on a survey track 15 (15^h30^m to 19^h00^m of May 12, 1986)

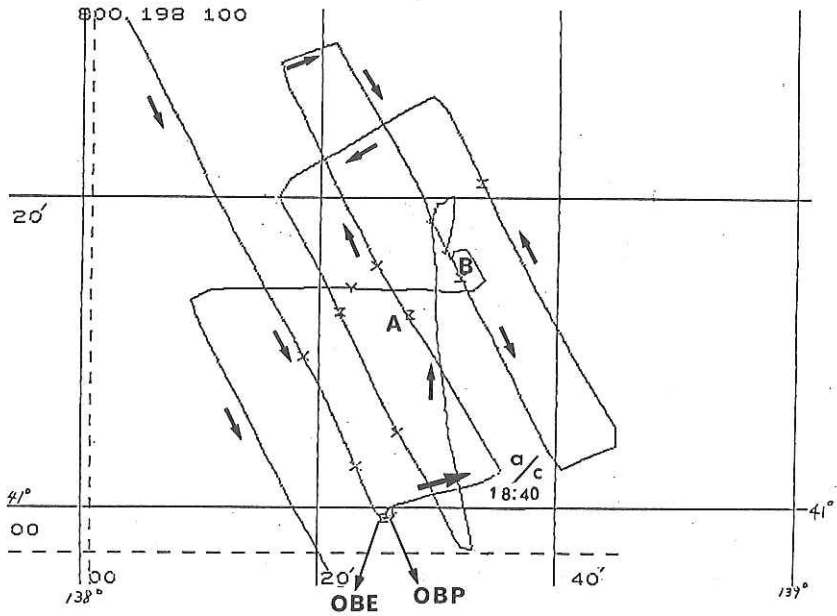

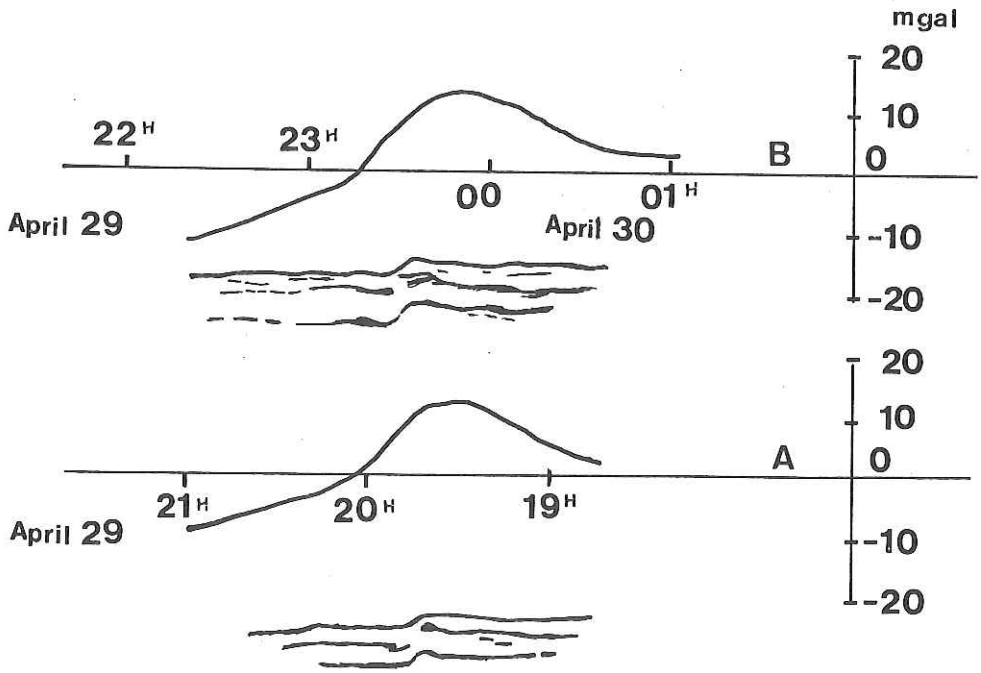

Fig. 7-3 (above) Ship's tracks surveying a newly discovered fault southwest of Matsumae Plateau.

Fig. 7-4 (below) Free air anomalies across a fault. Sketches under the gravity curves indicate seismic reflection profiles of the same cross-section showing the fault structure.

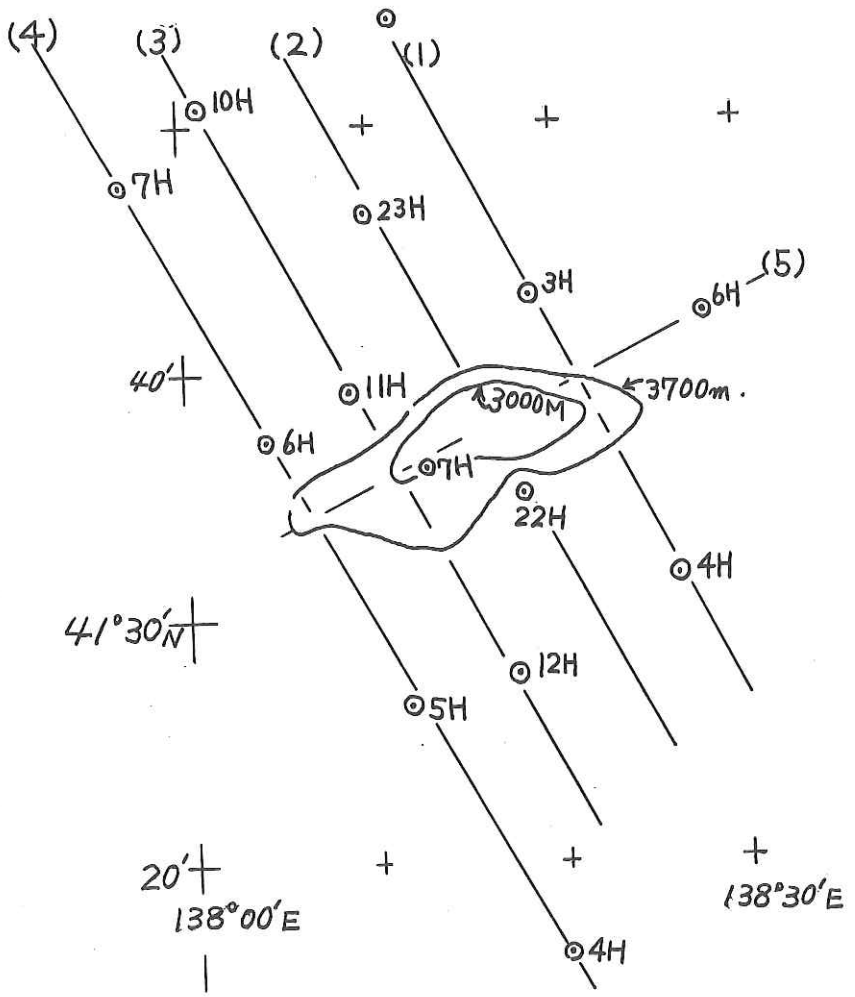

Fig. 7-5 Topography of a newly discovered Seamount in the eastern Japan Basin and its survey tracks in the cruise KH 86-2.

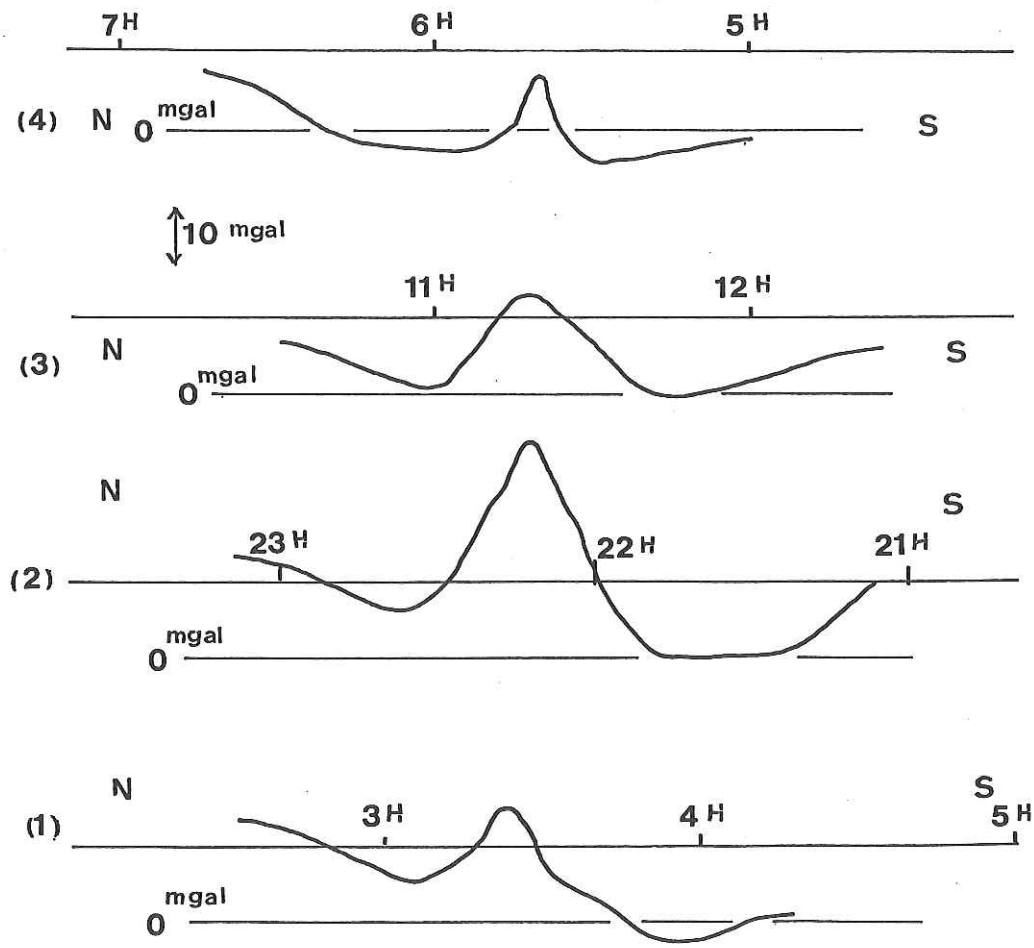

Fig. 7-6 Profiles of free air gravity anomalies on the tracks (1) to (4) shown in Fig. 7-5.

8. PISTON CORING

8-1. OPERATION LOGS

Date April 23,1986 Ship Hakuho Maru KH 86-2 Station 1
Latitude 41°11.9'N Longitude 144°53.4'E
Location West end of the Kurie Trench north of Erimo Smt (Be 10 site)
Sea small swell Weather 12m/s 135 (behind ship) rain
Bottom Topography flat Profiler no reflectors, very translucent

Length of Core Pipe 12 m Wall Thickness 7.5 mm Material Al
No. of pipe 1 ID of Pipe mm Core Head Wt. 480 Kg Trigger Wt. 50 Kg
Length Main Line 20 m Length Trigger Line 21 m Length Free Fall 9 m
Response at Hit clear in eyes Response at Pull-out none
Time Lowered 13 h 39 m; Uncorrected water Depth 7070 m
Time Hit 16 h 04 m; Uncorrected Water Depth 7070 m
Wire Angle at Hit 0 °; Wire-out at Hit 7188 m
Time Surfaced 19 h 36 m Uncorrected Water Depth 7070 m

Cored Length 0 cm (coarse sand attached)
Trigger Cored Length 0 cm
Method of Storage No. of Pipe filled 1
Length of Cores in Tray 1. cm, 2. cm, 3. cm, 4. cm, 5. cm, 6. cm.
No. of Cubic Samples for Paleomagnetism (No. No.)

Date April 26, 1986 Ship Hakuho Maru KH 86-2 Station 5
Latitude 41°01.5'N Longitude 139°55.6'E
Location W. off Tsugaru Str.
Sea calm Weather 2m/s, cloudy
Bottom Topography flat terrace (small) Profiler 3.5KHz layered structure

Length of Core Pipe 12 m Wall Thickness 7.5 mm Material Al
No. of pipe 1 ID of Pipe 65 mm Core Head Wt. 480 Kg Trigger Wt. 50 Kg
Length Main Line 20 m Length Trigger Line 21 m Length Free Fall 9 m
Response at Hit clear Response at Pull-out clear
Time Lowered 09 h 11 m; Uncorrected Water Depth 510 m
Time Hit 09 h 30 m; Uncorrected Water Depth 510 m
Wire Angle at Hit 0 °; Wire-out at Hit 484 m
Time Surfaced 9 h 47 m; Uncorrected Water Depth 510 m

Cored Length 717 cm (flow-in below 534cm)
Trigger Cored Length 26 cm (olive gray 5Y3/2 sandy silt)
Method of Storage No. of Pipe Filled 5
Length of Core in Tray 1. 47 cm, 2. 188 cm, 3. 187 cm, 4. 185 cm, 5. 110 cm, 6. cm.
No. of Cubic Samples for Paleomagnetism (No. 16601 - No. 16875)

Date April 26, 1986 Ship Hakuho Maru KH 86-2 Station 6
Latitude 41°04.5'N Longitude 139°55.8'E
Location SW of Stn KH 86-2-5
Sea calm Weather overcast
Bottom Topography edge of bench Profiler

Length of Core Pipe 12 m Wall Thickness 7.5 mm Material Al
No. of pipe 1 ID of Pipe mm Core Head Wt. 480 Kg Trigger Wt. 50 Kg
Length Main Line 20 m Length Trigger Line 21 m Length Free Fall 9 m
Response at Hit clear Lesponse at Pull-out clear
Time Lowered 10 h 56 m; Uncorrected Water Depth 590 m
Time Hit 11 h 12 m; Uncorrected Water Depth 580 m
Wire Angle at Hit 0 °; Wire-out at Hit 548 m
Time Surfaced 11 h 37 m; Uncorrected Water Depth 570 m

Cored Length 545 cm
Trigger Cored Length 8 cm (olive gray 5Y3/2 clay)
Method of Storage 2 m container with nyron rap No. of Pipe Filled 4
Length of Core in Tray 1. 127 cm, 2. 186 cm, 3. 191 cm, 4. 41 cm, 5. cm, 6. cm.
No. of Cubic Samples for Paleomagnetism (No. 16876 - No. 17111)

Date April 28, 1986 Ship Hakuho Maru KH 86-2 Station 7
Latitude 42°13.5'N Longitude 137°39.4'E
Location central Japan Basin, north margin of this survey area
Sea small swell Weather high overcast, 9m/s 240
Bottom Topography very flat Profiler slightly rough basement. bottom reflector
Length of Core Pipe 12 m Wall Thickness 7.5 mm Material Al
No. of pipe 1 ID of Pipe 65 mm Core Head Wt. 480 Kg Trigger Wt. 50 Kg
Length Main Line 20 m Length Trigger Line 21 m Length Free Fall 9 m
Response at Hit none-clear Response at Pull-out clear
Time Lowered 10 h 47 m; Uncorrected water Depth 3690 m
Time Hit 12 h 03 m; Uncorrected Water Depth 3690 m
Wire Angle at Hit 0 °; Wire-out at Hit 3640 m
Time Surfaced 13 h m; Uncorrected Water Depth 3690 m

Cored Length 1027 cm
Trigger Cored Length 115 cm (dark yellowish brown 10YR4/2 silt, cove top)
Method of Storage No. of Pipe filled 6
Length of Cores in Tray 1. 171 cm, 2. 182 cm, 3. 180 cm, 4. 183 cm, 5. 184 cm, 6. 127 cm.
No. of Cubic Samples for Paleomagnetism (No. 17201 - No. 17656)

Date April 30, 1986 Ship Hakuho Maru KH 86-2 Station 8
Latitude 41°18.7'N Longitude 138°28.8'E
Location weat margin of Japan Basin wind: 7m/s-10m/s 195
Sea calm, very small ripples Weather clear, slightly foggy
Bottom Topography downslope a faulted scarp Profiler good reflectors due to turbiditys & basement
Length of Core Pipe 12 m Wall Thickness 7.5 mm Material Al
No. of pipe 1 ID of Pipe 65 mm Core Head Wt. 480 kg Trigger Wt. 50 kg
Length Main Line 20 m Length Trigger Line 21 m Length Free Fall 9 m
Response at Hit clear Lesponse at Pull-out very clear
Time Lowered 09 h 58 m; Uncorrected Water Depth 3700 m
Time Hit 11 h 08 m; Uncorrected Water Depth 3700 m
Wire Angle at Hit 0 °; Wire-out at Hit 3634 m
Time Surfaced 12 h 18 m; Uncorrected Water Depth 3700 m

Cored Length 1010 cm
Trigger Cored Length 15 cm (dark yellowish brown 10YR4/2 clay)
Method of Storage No. of Pipe Filled 6
Length of Core in Tray 1. 158 cm, 2. 192 cm, 3. 187 cm, 4. 189 cm, 5. 189 cm, 6. 95 cm.
No. of Cubic Samples for Paleomagnetism (No. 18101 - No. 18462)

Date May 01, 1986 Ship Hakuho Maru KH 86-2 Station 9
Latitude 39°18.6'N Longitude 139°02.0'E
Location Mogami trough off SAKATA
Sea calm Weather wind 2m/s breeze, high overcast
Bottom Topography gentle slope between steep & carps Profiler clear reflectors
Length of Core Pipe 12 m Wall Thickness 7.5 mm Material Al
No. of pipe 1 ID of Pipe 65 mm Core Head Wt. 480 kg Trigger Wt. 50 kg
Length Main Line 20 m Length Trigger Line 21 m Length Free Fall 9 m
Response at Hit very clear Response atPull-out very clear
Time Lowered 11 h 16 m; Uncorrected water Depth 760 m
Time Hit 11 h 45 m; Uncorrected Water Depth 760 m
Wire Angle at Hit 0 °; Wire-out at Hit 728 m
Time Surfaced h m; Uncorrected Water Depth m

Cored Length 770 cm
Trigger Cored Length 60 cm (olive gray 5Y3/2 silt)
Method of Storage No. of Pipe filled 5
Length of Cores in Tray 1. 80 cm, 2. 192 cm, 3. 187 cm, 4. 189 cm, 5. 122 cm, 6. cm.
No. of Cubic Samples for Paleomagnetism (No. 17701 - No. 18037)

Date May 01,1986 Ship Hakuho Maru KH 86-2 Station 10
Latitude 39°14.0'N Longitude 139°05.6'E
Location Mogami Trough off SAKATA
Sea calm Weather 0m/s, overcast
Bottom Topography slope of gentle high Profiler clear reflectors

Length of Core Pipe 12 m Wall Thickness 7.5 mm Material Al
No. of pipe 1 ID of Pipe 65 mm Core Head Wt. 480 kg Trigger Wt. 50 kg
Length Main Line 20 m Length Trigger Line 21 m Length Free Fall 9 m
Response at Hit clear Response at Pull-out very clear
Time Lowered 13 h 06 m; Uncorrected water Depth 620 m
Time Hit 13 h 28 m; Uncorrected Water Depth 610 m
Wire Angle at Hit 0 °; Wire-out at Hit 580 m
Time Surfaced h m; Uncorrected Water Depth m

Cored Length 545 cm
Trigger Cored Length 12 cm (olive gray 5Y3/2 silt)
Method of Storage No. of Pipe filled 4
Length of Cores in Tray 1. 85 cm, 2. 191 cm, 3. 190 cm, 4. 79 cm, 5. 122 cm, 6. cm.
No. of Cubic Samples for Paleomagnetism (No. No.)

8-2. MEGASCOPIC CORE DESCRIPTION

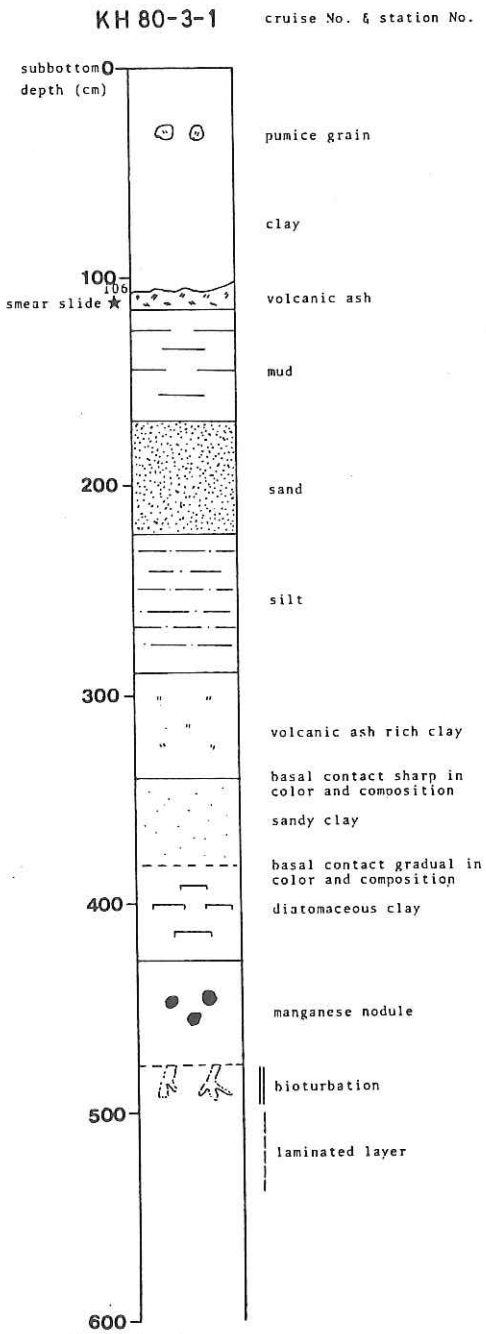

Fig. 8-2-1 Legend of core description.

Fig. 8-2-2 (from the next page to p.32) Megascopic description of cores collected in KH 86-2.

KH 86 - 2 - 5

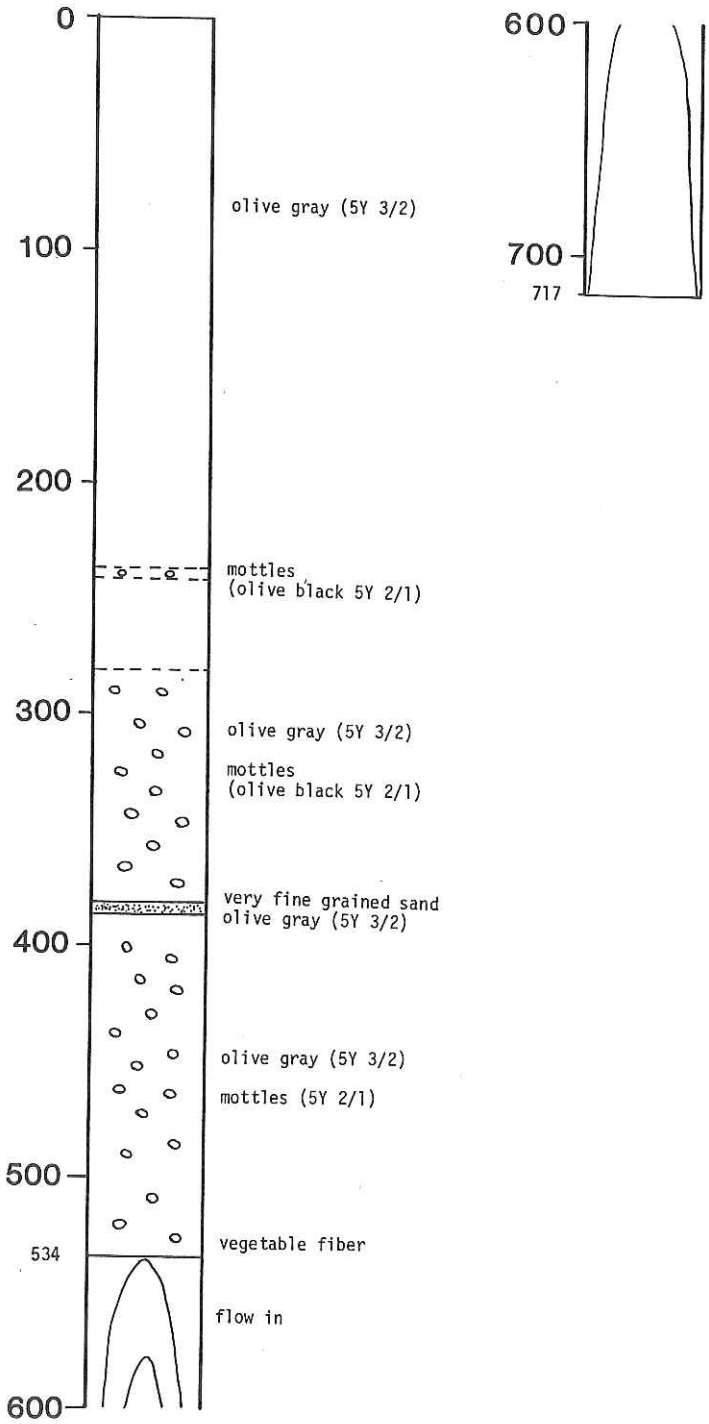
0
100
200
300
400
500
534
600
olive gray (5Y 3/2)
mottles
(olive black 5Y 2/1)
olive gray (5Y 3/2)
mottles
(olive black 5Y 2/1)
very fine grained sand
olive gray (5Y 3/2)
olive gray (5Y 3/2)
mottles (5Y 2/1)
vegetable fiber
flow in
600
700
717

KH 86 - 2 - 6

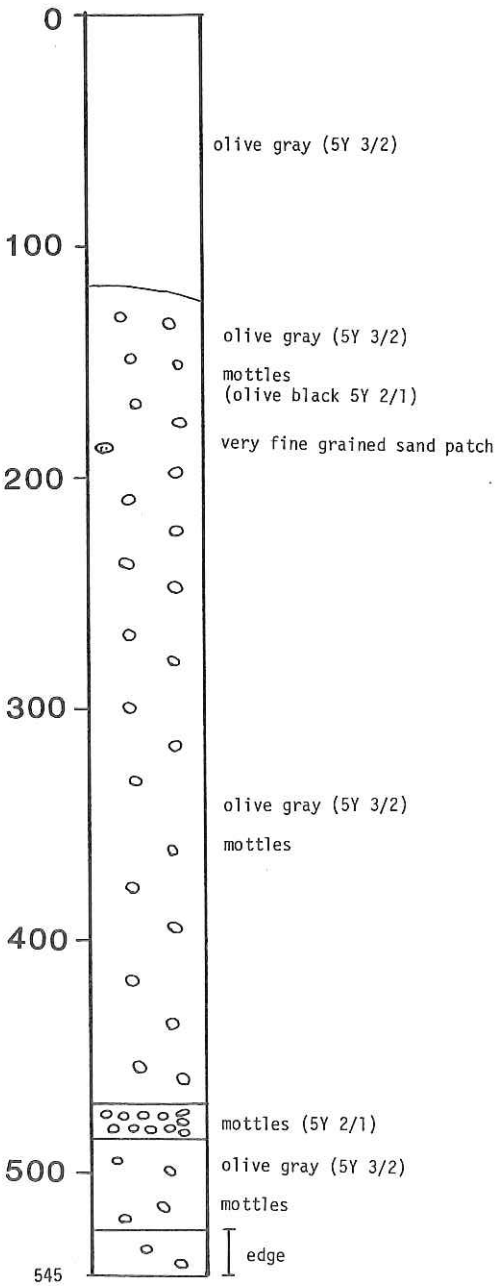
0
100
200
300
400
500
545
olive gray (5Y 3/2)
olive gray (5Y 3/2)
mottles
(olive black 5Y 2/1)
very fine grained sand patch
olive gray (5Y 3/2)
mottles
mottles (5Y 2/1)
olive gray (5Y 3/2)
mottles
edge

KH 86 - 2 - 7

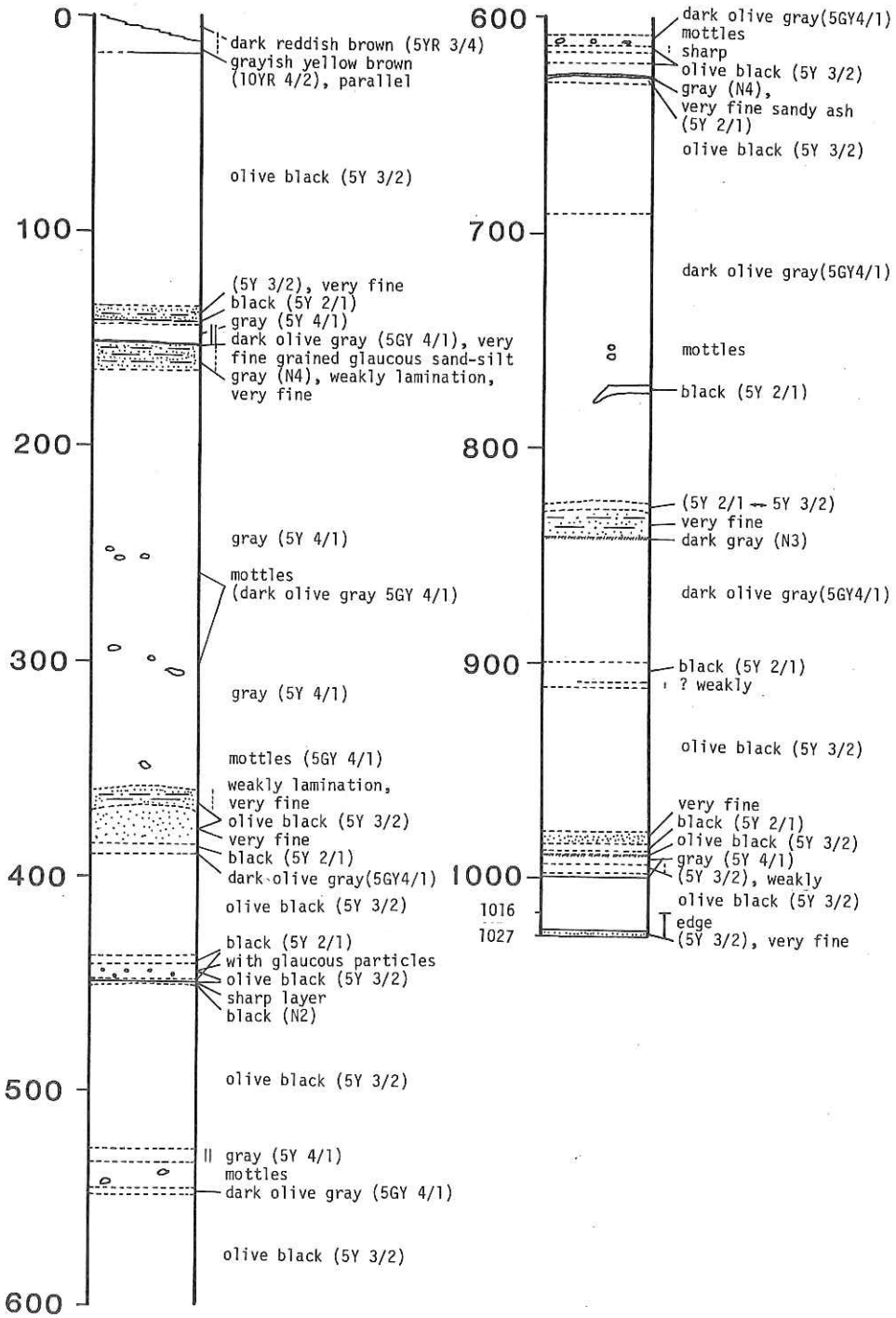
0
100
200
300
400
500
600
dark reddish brown (5YR 3/4)
grayish yellow brown (10YR 4/2), parallel
olive black (5Y 3/2)
(5Y 3/2), very fine
black (5Y 2/1)
gray (5Y 4/1)
dark olive gray (5GY 4/1), very fine grained glaucous sand-silt
gray (N4), weakly lamination, very fine
gray (5Y 4/1)
mottles (dark olive gray 5GY 4/1)
gray (5Y 4/1)
mottles (5GY 4/1)
weakly lamination, very fine
olive black (5Y 3/2)
very fine
black (5Y 2/1)
dark olive gray(5GY4/1)
olive black (5Y 3/2)
black (5Y 2/1)
with glaucous particles
olive black (5Y 3/2)
sharp layer
black (N2)
olive black (5Y 3/2)
gray (5Y 4/1)
mottles
dark olive gray (5GY 4/1)
olive black (5Y 3/2)
600
700
800
900
1000
1016
1027
dark olive gray(5GY4/1)
mottles
sharp
olive black (5Y 3/2)
gray (N4), very fine sandy ash (5Y 2/1)
olive black (5Y 3/2)
dark olive gray(5GY4/1)
mottles
black (5Y 2/1)
(5Y 2/1 ~ 5Y 3/2)
very fine
dark gray (N3)
dark olive gray(5GY4/1)
black (5Y 2/1)
? weakly
olive black (5Y 3/2)
very fine
black (5Y 2/1)
olive black (5Y 3/2)
gray (5Y 4/1)
(5Y 3/2), weakly
olive black (5Y 3/2)
edge
(5Y 3/2), very fine

KH 86 - 2 - 8

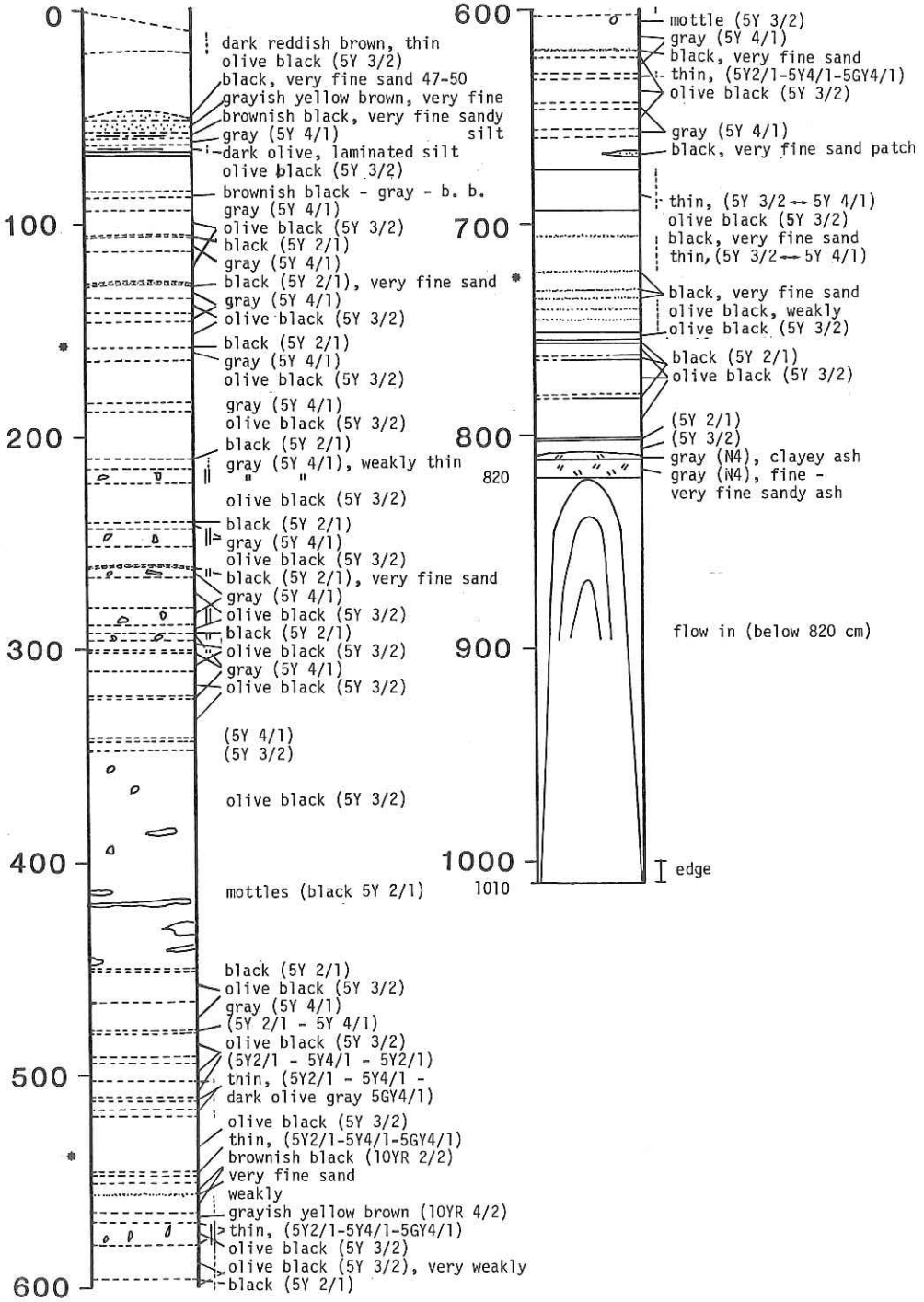
0
100
200
300
400
500
600
dark reddish brown, thin
olive black (5Y 3/2)
black, very fine sand 47-50
grayish yellow brown, very fine
brownish black, very fine sandy
gray (5Y 4/1) silt
dark olive, laminated silt
olive black (5Y 3/2)
brownish black - gray - b. b.
gray (5Y 4/1)
olive black (5Y 3/2)
black (5Y 2/1)
gray (5Y 4/1)
black (5Y 2/1), very fine sand
gray (5Y 4/1)
olive black (5Y 3/2)
black (5Y 2/1)
gray (5Y 4/1)
olive black (5Y 3/2)
gray (5Y 4/1)
olive black (5Y 3/2)
black (5Y 2/1)
gray (5Y 4/1), weakly thin
" "
olive black (5Y 3/2)
black (5Y 2/1)
gray (5Y 4/1)
olive black (5Y 3/2)
black (5Y 2/1), very fine sand
gray (5Y 4/1)
olive black (5Y 3/2)
black (5Y 2/1)
olive black (5Y 3/2)
gray (5Y 4/1)
olive black (5Y 3/2)
(5Y 4/1)
(5Y 3/2)
olive black (5Y 3/2)
mottles (black 5Y 2/1)
black (5Y 2/1)
olive black (5Y 3/2)
gray (5Y 4/1)
(5Y 2/1 - 5Y 4/1)
olive black (5Y 3/2)
(5Y2/1 - 5Y4/1 - 5Y2/1)
thin, (5Y2/1 - 5Y4/1 -
dark olive gray 5GY4/1)
olive black (5Y 3/2)
thin, (5Y2/1-5Y4/1-5GY4/1)
brownish black (10YR 2/2)
very fine sand
weakly
grayish yellow brown (10YR 4/2)
thin, (5Y2/1-5Y4/1-5GY4/1)
olive black (5Y 3/2)
olive black (5Y 3/2), very weakly
black (5Y 2/1)
600
700
800
820
900
1000
1010
mottle (5Y 3/2)
gray (5Y 4/1)
black, very fine sand
thin, (5Y2/1-5Y4/1-5GY4/1)
olive black (5Y 3/2)
gray (5Y 4/1)
black, very fine sand patch
thin, (5Y 3/2 ↔ 5Y 4/1)
olive black (5Y 3/2)
black, very fine sand
thin, (5Y 3/2 ↔ 5Y 4/1)
black, very fine sand
olive black, weakly
olive black (5Y 3/2)
black (5Y 2/1)
olive black (5Y 3/2)
(5Y 2/1)
(5Y 3/2)
gray (N4), clayey ash
gray (N4), fine -
very fine sandy ash
flow in (below 820 cm)
edge

KH 86 - 2 - 9

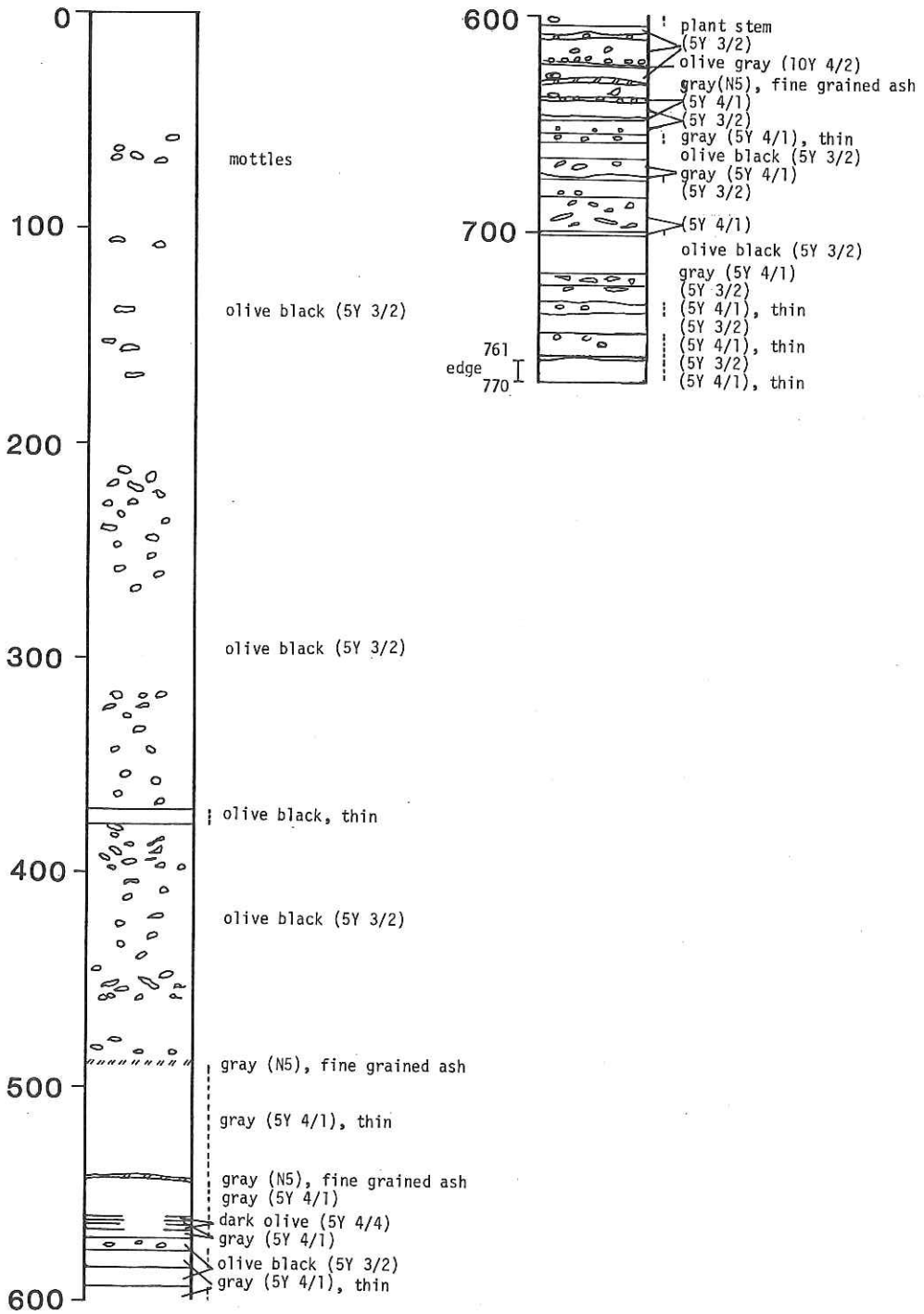
0
100
200
300
400
500
600
mottles
olive black (5Y 3/2)
olive black (5Y 3/2)
olive black, thin
olive black (5Y 3/2)
gray (N5), fine grained ash
gray (5Y 4/1), thin
gray (N5), fine grained ash
gray (5Y 4/1)
dark olive (5Y 4/4)
gray (5Y 4/1)
olive black (5Y 3/2)
gray (5Y 4/1), thin
600
700
761
edge
770
plant stem
(5Y 3/2)
olive gray (10Y 4/2)
gray(N5), fine grained ash
(5Y 4/1)
(5Y 3/2)
gray (5Y 4/1), thin
olive black (5Y 3/2)
gray (5Y 4/1)
(5Y 3/2)
(5Y 4/1)
olive black (5Y 3/2)
gray (5Y 4/1)
(5Y 3/2)
(5Y 4/1), thin
(5Y 3/2)
(5Y 4/1), thin
(5Y 3/2)
(5Y 4/1), thin

KH 86 - 2 - 10

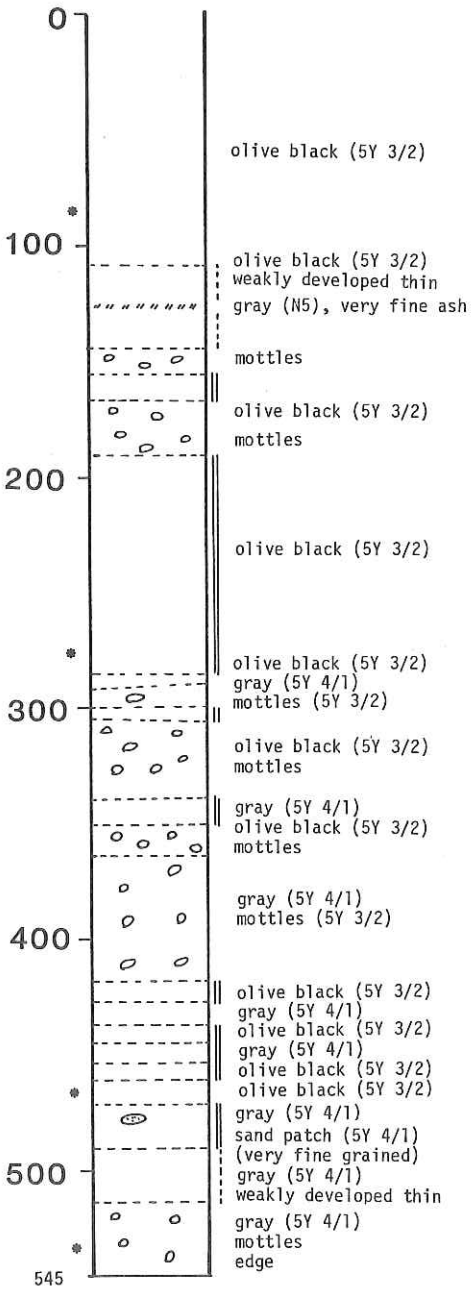
0
100
200
300
400
500
545
olive black (5Y 3/2)
olive black (5Y 3/2)
weakly developed thin
gray (N5), very fine ash
mottles
olive black (5Y 3/2)
mottles
olive black (5Y 3/2)
olive black (5Y 3/2)
gray (5Y 4/1)
mottles (5Y 3/2)
olive black (5Y 3/2)
mottles
gray (5Y 4/1)
olive black (5Y 3/2)
mottles
gray (5Y 4/1)
mottles (5Y 3/2)
olive black (5Y 3/2)
gray (5Y 4/1)
olive black (5Y 3/2)
gray (5Y 4/1)
olive black (5Y 3/2)
olive black (5Y 3/2)
gray (5Y 4/1)
sand patch (5Y 4/1)
(very fine grained)
gray (5Y 4/1)
weakly developed thin
gray (5Y 4/1)
mottles
edge

8-3. CHEMICAL COMPOSITION OF TEPHTA LAYERS

Toshio Furuta

Petrographic and geochemical characteristics as well as field occurrences of deep-sea tephra layers play an important role in identifing them in submarine sediments and correlating one layer with others at a remote places. Study of the characteristics also provides several informations on eruptions of the source volcanoes. Some widespread submarine tephra layers around the Japanese Islands are recognized in deep-sea sediments as well as on lands. In the poston cores, some tephra layers can be visually or petrographycally recognized by the constituents, grain size, and colour. Core KH86-2-7 has been identified five layers, level from top; 140, 380, 672, 835, and 980 cm. However three of them don't be composed by the materials of volcanic origin. Core KH86-2-9 has three identificiable tephra layers, 489, 542, and 632 cm. In core KH86-2-10 one layer is identified, 126 cm. Chemical compositions of volcanic glass shards in each tephra layer are tabulated in Table 8-3-1.

One of them (KH86-2-9, 632) can be correlated to the AT-tephra layer which is one of the most dicumented layer on and near the Japanese Islands (Furuta et al., 1986).

Reference.

Furuta T., K. Fujioka, and F. Arai. 1986. Widespread submarine tephras around Japan - Petrographic and chemical properties. Marine Geology, 72, 125-142.

Table 8-3-1. Chemical composition of volcanic glass shards in KH86-2 cores.

core	interval	SiO_2	TiO_2	Al_2O_3	FeO*	MnO	MgO	CaO	Na_2O	K_2O	Total	N
KH86-2-7	835-836	74.70	0.11	11.66	1.25	0.06	0.15	1.12	3.56	3.11	95.57	4
"	980-981	73.26	0.09	11.31	1.28	0.04	0.09	0.74	3.59	4.09	94.55	2
KH86-2-9	489-490	75.16	0.03	11.58	1.38	0.04	0.29	1.36	3.95	2.67	96.49	29
"	542-543	69.51	0.07	14.16	1.59	0.04	0.50	1.74	4.48	3.02	95.11	7
"	632-633	73.83	0.03	11.60	1.20	0.03	0.16	1.11	3.63	3.25	94.86	31
KH86-2-10	126-127	68.05	0.03	14.80	1.72	0.07	0.70	2.25	4.68	2.69	95.00	13

9. DREDGE HAULS

9-1. OPERATION LOGS

Date April 23-24, 1986 Ship Hakuho Maru KH 86-2 Station No. 2
Location Erimo Seamount
Weather rain Wind 14m/s Sea rough, large swells
Bottom Topography fairly steep slope
Type of Dredge Nalwalk chain bag with backet Add.Wt. kg
Time lowered 22 h 40 m Uncorr. Water Depth 4200 m
Initial Time on Bottom 0 h 07 m Uncorr. Water Depth 3850 m
Wire Length 4025 m Wire Angle
Ship Position Lat. 40°54.1' Long. 144°51.3'
Direction of Haul NE Ship Speed 0.8 kt. (till 2 h 00 m)
Speed Wire-in 0.3 m/sec (from 2 h 00 m) Winch No. 5
Final Time on Bottom 2 h 10 m Uncorr. Water Depth 4100 m
Wire Length 4300 m Wire Angle 0°
Ship Position Lat. 40°56.2' Long. 144°51.6'
Time Surfaced 03 h 36 m
Dredged Materials Several granules of trachyandesite lava, phosphorite and others.
Note Dredge subnavigation transponder was installed at about 100 m above the dredge.

Date April 24, 1987 Ship Hakuho Maru KH 86-2 Station No. 3
Location Northern slope of the down faulted block, Erimo Seamount
Weather rain Wind 2m/sec Sea huge swell
Bottom Topography slope
Type of Dredge Nalwalk chain bag with backet Add.Wt. 50x2kg+chain
Time lowered 04 h 15 m Uncorr.Water Depth 4600 m
Initial Time on Bottom 05 h 55 m Uncorr. Water Depth 4950 m
Wire Length 5250 m Wire Angle 20°
Ship Position Lat. 40°58.7' Long. 144°50.4'
Direction of Haul 155°-200° Ship Speed 0.6 kt. (till 08 h 22 m)
Speed Wire-in 0.5 m/sec (from 08 h 22 m) Winch No. 5
Final Time on Bottom 08 h 22 m Uncorr. Water Depth 4520 m
Wire Length 5300 m Wire Angle
Ship Position Lat. 40°57.4' Long. 144°51.2'
Time Surfaced 09 h 47 m (lost top 72m of wire w/dredges)
Dredged Material No recovery, "break down" (lost top 72 m of wire with dredge)

Date May 01-02, 1986 Ship Hakuho Maru KH 86-2 Station No. 11
Location Meiyo Daini Seamount
Weather overcast, rainy Wind 2m/s SE - 9m/s Sea calm
Bottom Topography SE side slope(steep)
Typeof Dredge Nalwalk chain bag Add.Wt. 50x2kg+chain
Time Towered 21 h 47 m Uncorr. Water Depth m
Initial Time on Bottom 22 h 50 m Uncorr. Water Depth 2560 m
Wire Length 2690 m Wire Angle 10-12
Ship Position Lat. 39°34.5' Long. 137°43.0'
Direction of Haul 300°-360° Ship Speed kt. (till 01 h 38 m)
Speed Wire-in 0.1 m/sec (from 01 h 38 m) Winch No. 5
Final Time on Bottom 02 h 00 m Uncorr. Water Depth 2080 m
Wire Length 2380 m Wire Angle 60°
Ship Position Lat. 39°35.3' Long. 137°41.7'
Time Surfaced 02 h 44 m
Dredged Materials More than 1000 gravels of andesite, rhyolite and detrital granite.
Note Dredge subnavigation transponder was installed at about 300 m above the dredge.

9-2. POSITION OF DREDGE HAULS

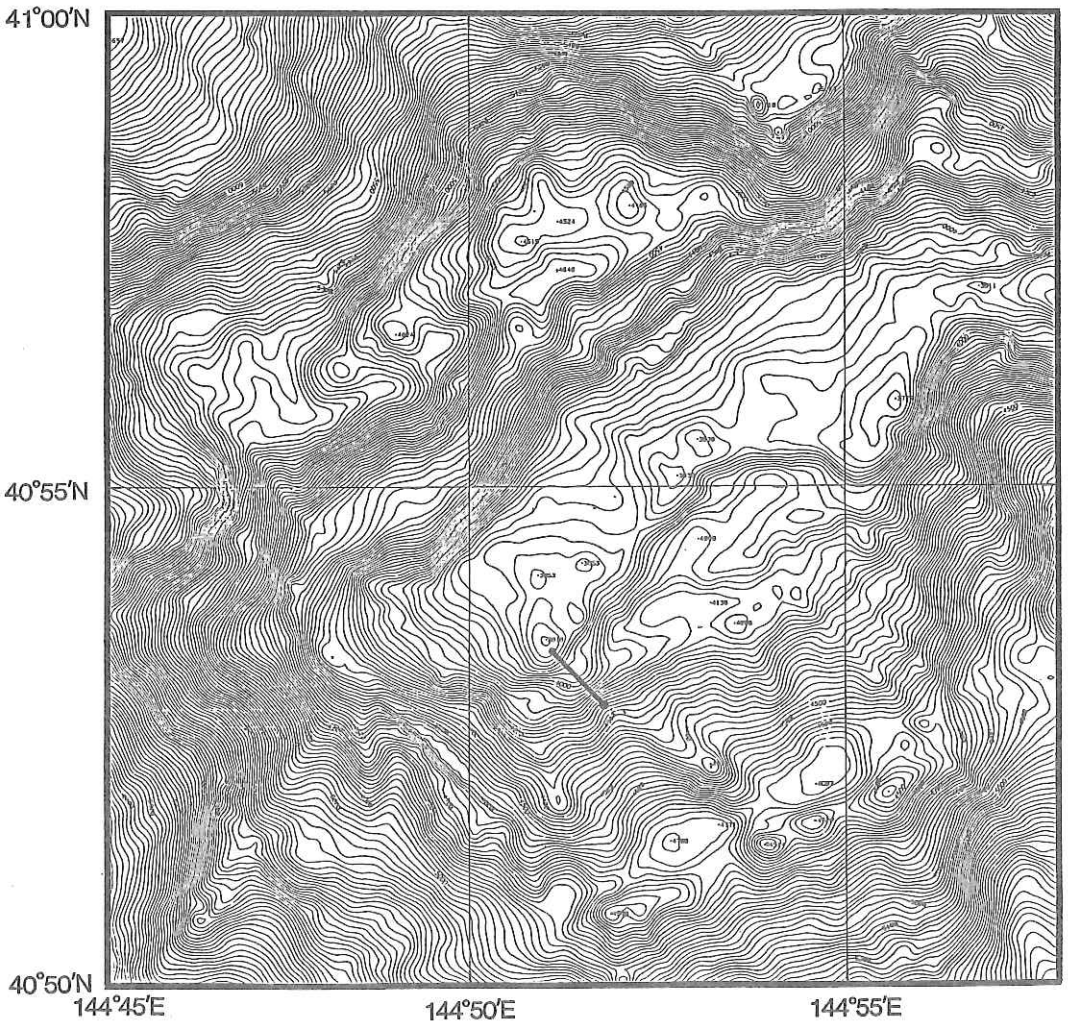

Fig. 9-2-1 Location of dredge hauls at the Erimo Seamount during KH 86-2.

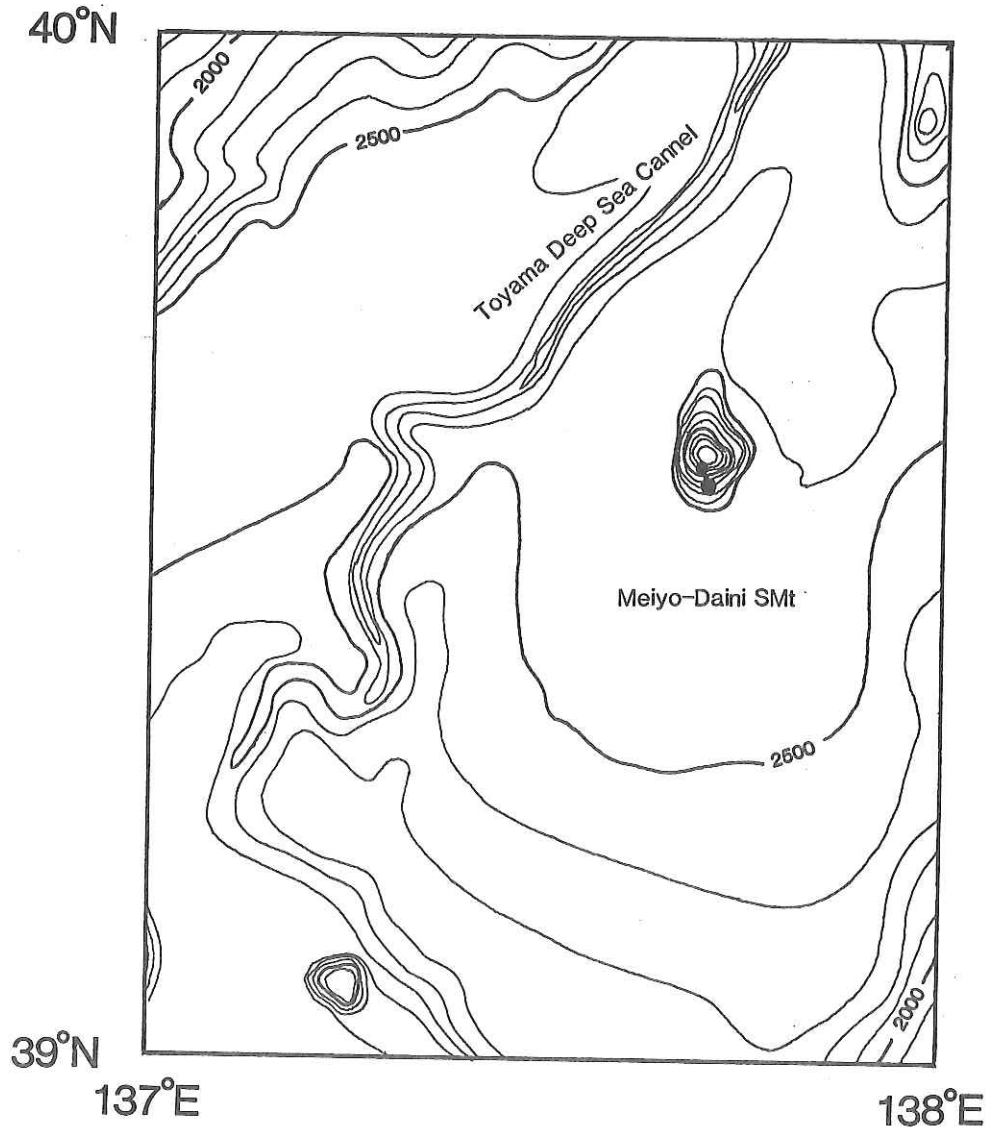

Fig. 9-2-2 Location of dredge hauls at the Meiyo Daini Seamount in the Sea of Japan during KH 86-2.

9-3. LIST OF DREDGED MATERIALS DURING KH 86-2

Sample No.	Diameter(mm) L	M	S	Round-ness	Wt(kg)	Mn-coating(mm)	Lithology & Remarks
A-001	280	220	170	0.4	12.8	N	andesite, v, (pl+cpx+ol)
002	310	120	70	0.2	3.5	N	andesite, v, (pl+cpx)
003	190	180	80	0.3	2.9	N	"
004	200	100	80	0.2	2.0	N	"
005	150	100	90	0.4	2.3	N	"
006	170	130	100	0.4	2.2	N	"
007	130	120	110	0.5	2.4	N	andesite, v, (pl+cpx), including gabbroic xenolith
008	120	100	70	0.4	1.4	N	andesite, v, (pl+cpx)
009	130	110	70	0.4	1.5	N	andesite, v
010	190	140	50	0.3	1.6	N	"
011	170	120	100	0.3	1.5	N	andesite, v, alt
012	110	110	60	0.5	0.96	N	andesite, v
013	130	110	100	0.5	1.9	N	andesite, v
014	150	110	90	0.5	1.4	N	andesite, v, (pl+cpx)
015	130	80	70	0.6	1.3	N	andesite, v, (pl+cpx+mt)
016	130	90	70	0.6	1.3	N	andesite, v,
017	170	80	80	0.4	1.4	N	"
018	130	100	60	0.3	1.4	N	andesite, v, (pl+cpx), alt
019	140	120	80	0.5	1.9	N	andesite, v
020	140	100	50	0.4	1.2	N	andesite, v, (pl+cpx), including basaltic & gabbroic xenolith
021	130	90	70	0.3	1.1	N	"
022	70	60	60	0.3	0.65	N	andesite, v, h.alt
023	230	130	12	0.3	4.5	N	andesite, v, alt
024	190	160	100	0.3	3.0	N	andesite, v, (pl+cpx), including basaltic xenolith
025	150	120	120	0.4	3.7	N	andesite, v, (pl+cpx+ol)
026	210	140	80	0.3	3.4	N	andesite, v, (pl+cpx)
027	170	150	90	0.4	2.1	N	andesite, v, alt
028	120	110	110	0.2	2.5	N	andesite, v
029	190	170	100	0.3	2.7	N	andesite, v, alt
030	160	100	80	0.3	1.5	N	andesite, v, (pl+cpx), including basaltic & gabbroic xenolith
031	120	70	70	0.4	1.3	N	andesite, v, h.alt
032	140	80	70	0.4	1.0	N	andesite, v, (pl+cpx)
033	140	90	80	0.5	1.1	N	andesite, v, alt
034	140	90	70	0.3	1.9	N	andesite, v, (pl+cpx), including gabbroic xenolith
035	120	100	70	0.3	1.6	N	"
036	170	120	50	0.5	1.4	N	andesite, v, (pl+cpx)
037	170	130	50	0.3	1.4	N	"
038	160	100	80	0.5	1.3	N	andesite, v, h.alt
039	170	110	70	0.4	1.5	N	"
040	120	90	90	0.5	1.2	N	andesite, v
041	100	80	80	0.3	1.1	N	andesite, v, (pl+cpx)
042	130	90	40	0.4	0.9	N	andesite, v
043	120	100	70	0.5	1.4	N	andesite, v, (pl+cpx)

Sample No.	Diameter(mm) L	M	S	Round-ness	Wt(kg)	Mn-coating(mm)	Lithology & Remarks
A-044	120	80	40	0.6	0.8	N	andesite, v, (pl+cpx)
045	120	110	80	0.6	1.0	N	andesite, v
046	140	140	40	0.5	0.9	N	"
047	120	120	50	0.4	0.8	N	andesite, v, (pl+cpx)
048	110	90	50	0.3	0.9	N	"
049	110	90	60	0.5	0.9	N	"
050	120	80	50	0.6	0.9	N	andesite, v
051	100	70	70	0.4	0.6	N	andesite, v, (pl+cpx), including basaltic xenolith
052	150	60	30	0.5	0.5	N	andesite, v
053	90	80	30	0.3	0.6	N	"
054	110	70	30	0.6	0.5	N	andesite, v, (pl+cpx)
055	80	40	30	0.5	0.4	N	andesite, v
056	120	60	50	0.5	0.7	N	andesite, v, (pl+cpx)
057	80	60	20	0.5	0.3	N	andesite, v, alt
058	250	210	160	0.4	10.5	N	andesite, v
059	270	200	125	0.3	5.7	N	andesite, v, (pl+cpx), including basaltic & gabbroic xenolith
060	130	80	60	0.4	890(g)	N	andesite, v, (pl+cpx), alt
061	120	80	40	0.5	600	N	andesite, v, (pl+cpx)
062	120	110	70	0.5	850	N	andesite, v, h.alt
063	110	90	60	0.4	910	N	andesite, v, (pl+cpx)
064	120	80	30	0.6	550	N	andesite, v, (pl+cpx), h.alt
065	110	100	80	0.3	880	N	andesite, v
066	140	110	60	0.3	770	N	andesite, v, alt
067	140	70	50	0.5	540	N	andesite, v, (pl+cpx)
068	120	100	40	0.4	630	N	andesite, v, h.alt
069	110	90	40	0.6	680	N	andesite, v, (pl+cpx)
070	100	90	50	0.3	650	N	andesite, v
071	120	90	50	0.6	670	N	andesite, v, (pl+cpx)
072	110	80	70	0.4	680	N	andesite, v, h.alt
073	150	50	50	0.5	730	N	andesite, v, alt
074	110	100	100	0.3	740	N	andesite, v, (pl+cpx)
075	140	110	40	0.3	670	N	andesite, v, alt
076	150	90	60	0.5	710	N	andesite, v, (pl+cpx), including basaltic xenolith
077	110	80	60	0.4	700	N	andesite, v, (pl+cpx)
078	110	100	40	0.4	600	N	andesite, v
079	110	80	50	0.4	740	N	"
080	110	90	50	0.3	650	N	andesite, v, (pl+cpx), including gabbroic xenolith
081	120	70	70	0.4	660	N	andesite, v, alt
082	110	100	40	0.2	500	N	"
083	130	60	40	0.4	590	N	andesite, v, (pl+cpx), including gabbroic xenolith
084	100	90	40	0.5	420	N	andesite, v, (pl+cpx), alt
085	100	60	40	0.4	450	N	andesite, v, (pl+cpx)
086	100	60	50	0.4	610	N	andesite, v, (pl+cpx), alt
087	130	80	50	0.3	760	N	andesite, v, (pl+cpx)
088	110	70	60	0.3	460	N	andesite, v
089	90	60	60	0.4	550	N	"

Sample No.	Diameter(mm) L	M	S	Round-ness	Wt(g)	Mn-coating(mm)	Lithology & Remarks
A-090	120	70	60	0.4	570	N	andesite, v, h.alt
091	120	70	40	0.5	440	N	andesite, v, (pl+cpx)
092	120	70	40	0.4	500	N	"
093	120	70	40	0.4	500	N	andesite, v, h.alt
094	120	70	50	0.3	580	N	andesite, v, (pl+cpx), h.alt
095	120	70	30	0.4	450	N	andesite, v, (pl+cpx)
096	110	100	40	0.3	510	N	andesite, v, alt
097	80	80	40	0.4	510	N	andesite, v, (pl+cpx), including basaltic xenolith
098	120	60	40	0.4	450	N	andesite, v
099	120	80	30	0.6	430	N	andesite, v, alt
100	90	70	50	0.3	470	N	"
101	120	80	40	0.5	450	N	andesite, v, (pl+cpx)
102	90	70	30	0.5	340	N	"
103	110	70	50	0.3	400	N	"
104	130	60	50	0.5	450	N	andesite, v, h.alt
105	110	60	40	0.4	440	N	andesite, v, (pl+cpx)
106	100	70	40	0.4	350	N	"
107	100	60	40	0.7	340	N	andesite, v
108	90	70	50	0.5	340	N	andesite, v, alt
109	90	50	40	0.4	370	N	andesite, v, (pl+cpx), including basaltic xenolith
110	120	50	50	0.4	360	N	"
111	110	60	40	0.4	360	N	andesite, v, (pl+cpx)
112	100	60	40	0.4	350	N	andesite, v, (pl+cpx), alt
113	70	70	60	0.4	400	N	andesite, v, h.alt
114	100	60	30	0.5	290	N	andesite, v, (pl+cpx)
115	110	80	40	0.2	390	N	andesite, v
116	120	50	40	0.5	330	N	andesite, v, (pl+cpx), alt
117	90	90	30	0.3	270	N	andesite, v, (pl+cpx), including basaltic xenolith
118	90	60	30	0.5	260	N	andesite, v, (pl+cpx)
119	110	60	40	0.3	270	N	andesite, v
120	80	60	30	0.4	250	N	"
121	120	70	30	0.3	270	N	andesite, v, alt
122	90	50	40	0.5	250	N	"
123	130	90	70	0.4	980	N	andesite, v, (pl+cpx+ol)
124	130	90	60	0.4	760	N	andesite, v
125	120	80	70	0.5	800	N	"
126	110	90	80	0.5	730	N	andesite, v, (pl+cpx+ol), including basaltic xenolith
127	110	90	70	0.4	650	N	"
128	110	80	60	0.5	590	N	"
129	110	80	60	0.6	520	N	andesite, v
130	100	100	40	0.5	400	N	andesite, v, h.alt
131	110	90	40	0.4	440	N	"
132	120	70	70	0.5	710	N	"
133	100	90	80	0.5	630	N	andesite, v
134	110	80	60	0.2	500	N	andesite, v, (pl+cpx)
135	90	70	60	0.5	350	N	andesite, v, (pl+cpx+ol)
136	80	70	50	0.5	310	N	andesite, v
137	100	90	50	0.4	380	N	"

Sample No.	Diameter(mm) L	M	S	Round-ness	Wt(g)	Mn-coating(mm)	Lithology & Remarks
A-138	100	90	80	0.3	880	N	andesite, v
139	100	80	40	0.3	480	N	"
140	110	80	80	0.4	690	N	"
141	110	80	70	0.4	610	N	"
142	100	80	60	0.4	430	N	andesite, v, alt
143	100	80	30	0.2	290	N	"
144	110	70	60	0.6	500	N	andesite, v
145	110	70	50	0.5	420	N	andesite, v, h.alt
146	110	90	40	0.5	370	N	andesite, v, alt
147	110	60	40	0.6	320	N	andesite, v, (pl+cpx)
148	110	50	40	0.5	340	N	andesite, v, alt
149	90	60	30	0.4	310	N	andesite, v, (pl+cpx), alt
150	80	80	40	0.5	300	N	andesite, v, alt
151	110	70	50	0.5	460	N	andesite, v, (pl+cpx)
152	90	60	50	0.4	340	N	andesite, v
153	90	60	50	0.4	290	N	andesite, v, (pl+cpx+ol)
154	100	70	30	0.5	280	N	andesite, v
155	90	70	30	0.4	350	N	"
156	90	60	30	0.4	270	N	"
157	130	70	40	0.5	360	N	andesite, v, h.alt
158	110	70	50	0.4	370	N	andesite, v, (pl+cpx)
159	90	70	50	0.4	310	N	andesite, v, h.alt
160	120	50	40	0.4	350	N	andesite, v, alt
161	100	60	60	0.3	340	N	"
162	110	90	60	0.6	460	N	"
163	120	50	30	0.5	320	N	andesite, v, h.alt
164	90	80	40	0.4	320	N	"
165	100	70	50	0.5	290	N	"
166	100	70	40	0.4	320	N	andesite, v, (pl+cpx)
167	90	60	50	0.4	320	N	" (")
168	90	70	30	0.4	280	N	andesite, v, alt
169	90	80	40	0.6	310	N	andesite, v, (pl+cpx)
170	90	60	30	0.4	230	N	andesite, v, h.alt
171	110	60	60	0.4	340	N	andesite, v, (pl+cpx) including gabbroic xenolith
172	90	60	40	0.3	250	N	andesite, v, h.alt
173	80	80	40	0.5	230	N	"
174	90	70	40	0.5	270	N	"
175	90	70	20	0.2	230	N	andesite, v
176	80	50	40	0.3	210	N	andesite, v, h.alt
177	110	60	40	0.4	280	N	andesite, v, alt
178	110	80	40	0.4	310	N	andesite, v, (pl+cpx), alt, including basaltic xenolith
179	90	60	40	0.5	360	N	"
180	110	70	60	0.4	430	N	andesite, v, h.alt
181	90	80	60	0.4	440	N	"
182	100	60	50	0.5	370	N	"
183	100	50	30	0.5	300	N	"
184	100	60	50	0.4	330	N	"
185	100	60	30	0.3	250	N	"
186	100	60	30	0.3	300	N	andesite, v
187	80	60	40	0.5	290	N	"

Sample No.	Diameter(mm) L	M	S	Round-ness	Wt(g)	Mn-coating(mm)	Lithology & Remarks
A-188	100	60	50	0.5	350	N	andesite, v
189	80	70	40	0.3	300	N	andesite, v, h.alt
190	90	60	40	0.5	320	N	"
191	90	70	40	0.4	370	N	andesite, v, (pl+cpx+ol)
192	90	70	50	0.4	310	N	andesite, v
193	80	70	40	0.4	270	N	"
194	90	60	40	0.3	250	N	"
195	90	60	30	0.4	260	N	andesite, v, h.alt
196	80	60	30	0.5	240	N	"
197	80	70	40	0.4	260	N	andesite, v, (pl+cpx), alt, including basaltic inclusion
198	100	70	40	0.4	280	N	andesite, v
199	110	60	40	0.5	260	N	"
200	100	70	40	0.4	280	N	"
201	110	90	40	0.4	450	N	andesite, v, (pl+cpx+ol)
202	90	70	40	0.4	240	N	andesite, v, (pl+cpx), alt, including basaltic inclusion
203	80	60	40	0.4	270	N	andesite, v, alt
204	90	70	30	0.4	280	N	andesite, v
205	90	70	30	0.3	260	N	"
206	90	60	30	0.4	240	N	andesite, v, h.alt
207	100	60	50	0.2	260	N	"
208	80	50	50	0.3	290	N	andesite, v, (pl+cpx+ol)
209	60	60	50	0.5	240	N	andesite, v, h.alt
210	80	70	40	0.3	210	N	andesite, v
211	70	70	30	0.5	210	N	andesite, v, alt
212	90	50	40	0.3	240	N	andesite, v, h.alt
213	90	70	30	0.2	200	N	andesite, v
214	90	60	40	0.4	260	N	andesite, v, h.alt
215	80	60	40	0.4	260	N	andesite, v, alt
216	90	70	40	0.4	260	N	"
217	80	60	40	0.4	220	N	andesite, v, (pl+cpx), alt, including basaltic xenolith
218	90	70	40	0.5	280	N	andesite, v, alt
219	90	60	40	0.3	210	N	"
220	100	50	40	0.4	220	N	andesite, v, h.alt
221	70	50	50	0.4	220	N	"
222	90	60	40	0.3	210	N	"
223	80	60	40	0.3	210	N	"
224	100	80	20	0.3	220	N	andesite, v
225	90	70	30	0.4	200	N	andesite, v, alt
226	70	50	30	0.5	210	N	andesite, v
227	70	60	40	0.4	190	N	andesite, v, alt
228	100	50	40	0.4	200	N	"
229	70	60	40	0.5	200	N	"
230	80	60	10	0.3	150	N	andesite, v
231	80	70	30	0.3	190	N	"
232	80	60	30	0.4	190	N	"
233	90	50	30	0.4	170	N	"
234	60	50	40	0.4	170	N	"
235	60	60	20	0.4	140	N	andesite, v, alt
236	70	60	40	0.4	190	N	"

Sample No.	Diameter(mm) L	M	S	Roundness	Wt(g)	Mn-coating(mm)	Lithology & Remarks
A-237	80	50	50	0.4	210	N	andesite, v
238	70	50	40	0.5	180	N	"
239	70	40	40	0.5	160	N	andesite, v, alt
240	80	50	20	0.4	140	N	"
241	60	60	50	0.2	170	N	andesite, v
242	70	60	20	0.3(2?)	150	N	"
243	90	50	30	0.4	230	N	andesite, v, alt
244	80	50	30	0.5	160	N	"
245	80	70	30	0.4	180	N	"
246	80	50	40	0.5	160	N	andesite, v
247	80	50	40	0.4	210	N	"
248	80	50	20	0.4	160	N	"
249	90	60	40	0.4	270	N	"
250	100	60	40	0.5	250	N	"
251	80	70	30	0.3	240	N	"
252	80	70	40	0.3	260	N	"
253	90	60	20	0.4	200	N	"
254	70	60	50	0.5	210	N	andesite, v, alt
255	80	60	30	0.3	200	N	"
256	100	70	40	0.3	300	N	andesite, v
257	70	50	50	0.4	230	N	andesite, v, alt
258	70	60	40	0.4	220	N	andesite, v
259	70	50	40	0.6	180	N	andesite, v, alt
260	90	70	20	0.3	160	N	"
261	100	40	30	0.2	120	N	andesite, v
262	100	50	30	0.3	180	N	"
263	80	60	40	0.4	240	N	"
264	60	60	30	0.4	190	N	andesite, v, alt
265	80	60	30	0.4	200	N	"
266	70	40	40	0.4	210	N	andesite, v
267	80	50	40	0.5	200	N	andesite, v, alt
268	80	70	30	0.4	180	N	"
269	80	60	30	0.4	190	N	"
270	120	50	30	0.4	160	N	"
271	90	60	40	0.3	190	N	"
272	80	40	40	0.4	200	N	andesite, v
273	70	60	30	0.4	190	N	andesite, v, alt
274	90	60	40	0.4	180	N	"
275	80	60	40	0.4	170	N	"
276	100	60	30	0.3	180	N	andesite, v
277	70	60	30	0.5	150	N	andesite, v, alt
278	80	50	40	0.3	180	N	andesite, v
279	100	40	30	0.3	140	N	andesite, v, alt
280	80	40	40	0.4	160	N	"
281	70	50	30	0.5	160	N	"
282	80	60	30	0.4	170	N	"
283	80	60	30	0.5	180	N	andesite, v
284	100	50	40	0.3	170	N	andesite, v, alt
285	80	60	20	0.3	160	N	"
286	70	60	30	0.2	150	N	"
287	70	60	30	0.3	150	N	andesite, v
288	70	50	40	0.3	170	N	andesite, v, alt

Sample No.	Diameter(mm) L	M	S	Roundness	Wt(g)	Mn-coating(mm)	Lithology & Remarks
A-289	70	60	20	0.4	140	N	andesite, v, alt
290	70	50	30	0.3	150	N	"
291	90	70	30	0.4	170	N	"
292	90	40	30	0.3	130	N	"
293	100	40	30	0.4	140	N	"
294	60	50	40	0.3	170	N	"
295	80	60	50	0.4	230	N	"
296	90	60	30	0.5	170	N	"
297	90	60	30	0.3	160	N	"
298	80	40	30	0.2	140	N	andesite, v
299	160	80	70	0.4	1180	N	"
300	140	80	80	0.3	1290	N	andesite, v, (pl+cpx), alt, including basaltic inclusion
301	110	80	30	0.3	310	N	andesite, v
302	80	80	30	0.4	200	N	andesite, v, alt
303	50	40	30	0.4	160	N	"
304	90	60	30	0.3	240	N	"
305	70	50	40	0.3	190	N	andesite, v
306	80	70	40	0.3	220	N	"
307	90	60	40	0.4	370	N	"
308	80	70	30	0.4	250	N	"
309	80	40	40	0.4	260	N	"
310	80	80	40	0.4	270	N	"
311	80	50	40	0.5	220	N	"
312	60	60	30	0.5	170	N	"
313	80	40	40	0.3	220	N	"
314	80	50	40	0.3	240	N	"
315	80	50	40	0.4	270	N	"
316	80	60	30	0.5	200	N	"
317	70	40	40	0.4	190	N	"
318	80	40	40	0.3	220	N	"
319	60	60	60	0.5	230	N	"
320	70	60	30	0.3	200	N	"
321	60	40	40	0.6	160	N	"
322	60	40	30	0.4	110	N	"
323	60	40	40	0.4	110	N	"
324	60	50	40	0.4	150	N	"
325	80	60	50	0.4	210	N	"
326	60	50	40	0.4	160	N	"
327	60	50	40	0.4	140	N	"
328	70	40	40	0.4	160	N	"
329	60	50	30	0.5	120	N	"
330	80	60	50	0.4	310	N	"
331	70	50	40	0.4	240	N	"
332	70	60	30	0.5	160	N	"
333	70	50	30	0.3	160	N	"
334	70	50	40	0.4	180	N	"
335	60	60	50	0.5	170	N	"
336	60	50	30	0.5	150	N	"
337	70	60	40	0.4	130	N	"
338	40	40	40	0.4	100	N	"
339	50	40	40	0.5	120	N	"

Sample No.	Diameter(mm) L	M	S	Round-ness	Wt(g)	Mn-coating(mm)	Lithology & Remarks
A-340	60	50	40	0.4	140	N	andesite, v
341	60	40	30	0.4	120	N	"
342	70	50	30	0.4	110	N	"
343	60	50	40	0.3	130	N	"
344	60	50	30	0.5	100	N	"
345	70	50	30	0.4	120	N	"
346	60	50	30	0.4	90	N	"
347	70	50	30	0.4	140	N	"
348	70	50	30	0.3	110	N	"
349	70	60	40	0.3	150	N	"
350	60	40	40	0.4	110	N	"
351	50	30	30	0.3	90	N	"
352	40	40	40	0.3	110	N	"
353	60	50	30	0.4	120	N	"
354	60	50	30	0.3	110	N	"
355	80	40	40	0.3	140	N	andesite
356	50	50	50	0.5	260	N	andesite, v
357	80	40	30	0.3	140	N	andesite, v, alt
358	50	50	40	0.4	110	N	"
359	80	50	30	0.3	140	N	"
360	90	60	20	0.3	140	N	"
361	70	50	20	0.4	90	N	andesite, v
362	70	50	40	0.3	110	N	"
363	80	70	20	0.2	130	N	andesite, v, alt
364	60	40	40	0.4	110	N	"
365	90	60	20	0.4	120	N	"
366	60	50	40	0.4	120	N	andesite, v
367	80	40	30	0.4	100	N	andesite, v, alt
368	70	60	20	0.3	110	N	andesite, v
369	70	40	40	0.5	140	N	andesite, v, alt
370	90	60	20	0.2	120	N	andesite, v
371	60	50	20	0.4	90	N	andesite, v, alt
372	60	40	30	0.3	120	N	andesite, v
373	80	60	30	0.5	110	N	andesite, v, h.alt
374	60	50	30	0.4	90	N	"
375	70	40	30	0.4	80	N	andesite, v, alt
376	70	40	30	0.4	130	N	andesite, v
377	60	50	30	0.2	110	N	"
378	100	30	20	0.3	110	N	andesite, v, alt
379	50	40	30	0.4	90	N	"
380	60	40	20	0.4	80	N	"
381	70	40	40	0.3	130	N	andesite, v
382	70	60	40	0.5	150	N	"
383	70	50	40	0.3	180	N	"
384	80	50	30	0.4	180	N	andesite, v, alt
385	60	50	40	0.4	160	N	andesite, v
386	60	50	40	0.4	150	N	andesite?, h.alt
387	60	50	40	0.4	140	N	andesite, v
388	60	50	30	0.4	120	N	andesite, h.alt
389	60	50	40	0.3	120	N	andesite, v
390	70	50	50	0.3	110	N	"
391	60	40	40	0.4	110	N	"

Sample No.	Diameter(mm) L	M	S	Roundness	Wt(g)	Mn-coating(mm)	Lithology & Remarks
A-392	70	40	40	0.3	130	N	andesite, v
393	60	50	40	0.3	130	N	andesite, v, h.alt
394	70	50	20	0.3	110	N	andesite, v
395	80	50	40	0.3	120	N	"
396	70	50	30	0.3	130	N	"
397	70	60	30	0.4	120	N	andesite, v, h.alt
398	80	50	40	0.3	130	N	"
399	70	50	30	0.5	110	N	andesite, v
400	70	50	40	0.4	130	N	andesite, v, h.alt
401	70	60	30	0.4	160	N	andesite, v, alt
402	90	60	50	0.4	220	N	andesite, v
403	70	60	40	0.4	190	N	andesite, v, alt
404	80	60	30	0.3	150	N	"
405	70	60	40	0.4	150	N	andesite, v
406	80	70	40	0.5	170	N	andesite, v, alt
407	70	50	40	0.4	140	N	andesite, v
408	80	70	30	0.4	160	N	andesite, v, alt
409	80	60	40	0.4	140	N	andesite, v
410	70	50	40	0.4	160	N	andesite, h.alt
411	90	60	20	0.4	130	N	andesite, v, alt
412	70	60	40	0.4	170	N	andesite, v
413	70	50	30	0.3	130	N	andesite, v, alt
414	90	50	30	0.3	120	N	andesite, h.alt
415	60	50	40	0.4	140	N	andesite, v
416	80	50	30	0.4	150	N	andesite, h.alt
417	80	40	40	0.5	150	N	andesite, v
418	60	50	40	0.5	130	N	"
419	70	60	40	0.4	160	N	andesite, v, alt
420	70	40	20	0.5	100	N	"
421	80	40	30	0.4	120	N	andesite, v, h.alt
422	60	40	30	0.4	140	N	andesite, v
423	70	60	40	0.3	170	N	andesite, h.alt
424	80	60	30	0.3	170	N	andesite, v
425	70	50	40	0.3	120	N	andesite, v, alt
426	90	60	30	0.4	120	N	andesite?, h.alt
427	80	50	40	0.5	180	N	"
428	70	40	40	0.4	190	N	"
429	70	70	50	0.3	170	N	andesite, v, alt
430	90	50	20	0.3	110	N	andesite, v
431	70	40	40	0.4	140	N	andesite, v, alt
432	80	50	40	0.4	150	N	andesite, v
433	70	50	30	0.4	140	N	"
434	80	50	20	0.4	120	N	"
435	80	50	30	0.4	140	N	"
436	60	50	30	0.5	130	N	andesite, h.alt
437	90	50	30	0.4	140	N	andesite, v, alt
438	60	50	30	0.4	120	N	"
439	60	40	20	0.3	100	N	andesite, v
440	80	50	30	0.4	120	N	"
441	70	40	30	0.3	110	N	andesite, v, alt
442	60	50	30	0.4	130	N	"
443	90	50	30	0.3	130	N	"

Sample No.	Diameter(mm) L	M	S	Roundness	Wt(g)	Mn-coating(mm)	Lithology & Remarks
A-444	60	50	40	0.4	150	N	andesite?, h.alt
445	80	60	20	0.4	100	N	"
446	80	60	20	0.4	100	N	"
447	70	40	20	0.4	140	N	andesite, v, alt
448	70	50	40	0.4	150	N	"
449	80	60	30	0.4	140	N	"
450	80	60	30	0.3	100	N	"
451	70	50	30	0.3	100	N	"
452	70	50	30	0.3	120	N	"
453	60	50	40	0.4	130	N	andesite, v
454	100	40	20	0.4	140	N	andesite?, h.alt
455	60	40	20	0.4	90	N	andesite, alt
456	70	40	30	0.4	100	N	andesite, v, alt
457	50	40	40	0.4	90	N	"
458	80	50	20	0.4	110	N	andesite?, v, h.alt
459	70	40	30	0.3	120	N	andesite, v, alt
460	90	40	30	0.3	110	N	andesite?, h.alt
461	80	40	30	0.4	120	N	andesite, v
462	50	40	40	0.4	90	N	"
463	60	50	30	0.3	75	N	"
464	50	50	40	0.3	70	N	"
465	60	40	40	0.3	110	N	"
466	80	50	30	0.3	120	N	andesite, v, alt
467	70	40	30	0.3	100	N	andesite, v
468	90	60	20	0.3	130	N	andesite, v, alt
469	60	50	30	0.4	95	N	"
470	60	50	30	0.4	90	N	"
471	70	50	30	0.4	95	N	andesite, v, h.alt
472	70	60	40	0.3	90	N	andesite, v
473	70	50	30	0.4	120	N	andesite, h.alt
474	70	40	30	0.4	120	N	"
475	60	40	30	0.3	95	N	"
476	70	40	30	0.3	110	N	andesite, v, alt
477	70	50	20	0.3	95	N	andesita?, h.alt
478	70	40	30	0.4	100	N	andesite, v
479	60	40	30	0.4	110	N	"
480	60	50	20	0.3	100	N	"
481	60	50	20	0.4	90	N	andesite, v, h.alt
482	50	50	20	0.4	95	N	andesite, v, alt
483	50	40	40	0.4	105	N	"
484	60	40	30	0.4	110	N	"
485	60	50	30	0.4	140	N	andesite, v
486	70	30	30	0.3	110	N	andesite, h.alt
487	50	40	10	0.2	65	N	andesite, v
488	50	50	20	0.4	70	N	"
489	70	50	40	0.4	120	N	"
490	60	50	30	0.3	130	N	"
491	60	60	40	0.4	110	N	andesite, h.alt
492	70	50	20	0.4	130	N	"
493	70	50	30	0.3	130	N	andesite, v
494	60	40	30	0.4	100	N	"
495	80	50	30	0.4	120	N	"

Sample No.	Diameter(mm) L	M	S	Round-ness	Wt(g)	Mn-coating(mm)	Lithology & Remarks
A-496	70	40	20	0.5	65	N	andesite, v
497	50	50	40	0.3	110	N	"
498	60	50	20	0.4	100	N	andesite, h.alt
499	70	50	20	0.4	105	N	andesite, v
500	80	50	30	0.4	125	N	andesite, h.alt
501	70	30	30	0.4	90	N	"
502	70	50	30	0.4	120	N	"
503	60	50	20	0.3	75	N	"
504	70	50	40	0.4	90	N	"
505	70	50	30	0.4	150	N	andesite
506	70	60	40	0.4	160	N	"
507	70	50	40	0.3	170	N	"
508	80	60	20	0.3	140	N	"
509	60	50	40	0.4	180	N	"
510	70	40	40	0.3	160	N	"
511	70	60	20	0.3	140	N	"
512	70	40	30	0.3	130	N	"
513	60	50	30	0.4	110	N	"
514	60	40	20	0.4	100	N	"
515	70	60	40	0.2	125	N	"
516	90	40	20	0.3	100	N	"
517	70	50	40	0.4	160	N	"
518	60	50	40	0.3	120	N	"
519	70	40	30	0.3	105	N	"
520	40	40	40	0.3	100	N	"
521	60	50	30	0.3	110	N	"
522	60	40	30	0.2	90	N	"
523	70	40	30	0.2	105	N	"
524	60	40	30	0.4	120	N	"
525	70	40	30	0.3	130	N	"
526	60	40	30	0.2	105	N	"
527	60	40	40	0.4	120	N	"
528	60	30	30	0.3	100	N	"
529	60	40	40	0.5	130	N	"
530	70	30	20	0.2	70	N	"
531	60	40	30	0.3	75	N	"
532	40	40	30	0.2	65	N	"
533	70	50	30	0.2	95	N	"
534	60	40	30	0.3	90	N	"
535	50	50	30	0.4	60	N	"
536	60	50	30	0.3	90	N	"
537	80	40	30	0.3	90	N	"
538	70	50	20	0.3	90	N	"
539	70	50	30	0.2	95	N	"
540	70	50	30	0.4	85	N	"
541	50	40	30	0.4	55	N	"
542	60	50	30	0.4	120	N	"
543	60	60	20	0.4	95	N	"
544	60	50	30	0.5	110	N	"
545	80	40	20	0.3	85	N	"
546	70	40	20	0.2	70	N	"
547	70	30	20	0.3	70	N	"

Sample No.	Diameter(mm) L	M	S	Roundness	Wt(g)	Mn-coating(mm)	Lithology & Remarks
A-548	70	50	50	0.4	160	N	andesite
549	40	40	40	0.3	100	N	"
550	60	40	30	0.4	80	N	"
551	50	40	40	0.3	105	N	"
552	50	40	30	0.3	110	N	"
553	60	50	40	0.4	105	N	"
554	70	40	20	0.4	85	N	"
555	60	50	20	0.3	80	N	"
556	60	50	30	0.5	75	N	"
557	70	40	30	0.2	70	N	"
558	70	40	30	0.3	75	N	"
559	70	40	20	0.2	60	N	"
560	60	40	30	0.4	80	N	"
561	60	50	40	0.4	115	N	"
562	60	40	30	0.4	95	N	"
563	80	40	20	0.2	85	N	"
564	50	40	30	0.4	95	N	"
565	70	40	20	0.3	95	N	"
566	60	30	20	0.3	85	N	"
567	60	40	30	0.3	80	N	"
568	60	40	20	0.2	75	N	"
569	60	40	40	0.4	85	N	"
570	60	40	30	0.3	95	N	"
571	60	40	40	0.5	105	N	"
572	60	30	30	0.3	80	N	"
573	60	50	30	0.3	85	N	"
574	60	40	30	0.3	75	N	"
575	50	40	20	0.5	70	N	"
576	60	40	30	0.4	70	N	"
577	60	40	30	0.4	75	N	"
578	60	50	20	0.4	80	N	"
579	50	30	30	0.4	75	N	"
580	60	30	30	0.3	80	N	"
581	60	40	30	0.3	70	N	"
582	50	50	30	0.5	90	N	"
583	50	40	30	0.5	80	N	"
584	60	40	20	0.3	70	N	"
585	50	30	20	0.3	65	N	"
586	50	40	30	0.3	65	N	"
587	60	50	30	0.3	75	N	"
588	70	40	30	0.3	85	N	"
589	60	40	30	0.4	75	N	"
590	50	40	40	0.3	90	N	"
591	50	40	30	0.3	70	N	"
592	30	30	30	0.4	75	N	"
593	60	40	30	0.3	85	N	"
594	60	50	20	0.3	75	N	"
595	70	30	10	0.2	60	N	"
596	50	40	20	0.3	70	N	"
597	70	40	20	0.2	60	N	"
598	60	50	30	0.3	65	N	"
599	50	50	30	0.4	75	N	"

Sample No.	Diameter(mm) L	M	S	Round-ness	Wt(g)	Mn-coating(mm)	Lithology & Remarks
A-600	70	30	20	0.3	60	N	andesite
601	60	50	10	0.3	60	N	"
602	60	40	30	0.4	70	N	"
603	60	40	20	0.4	55	N	"
604	50	50	40	0.4	80	N	"
605	50	40	30	0.3	70	N	"
606	50	40	30	0.3	75	N	"
607	50	40	30	0.4	65	N	"
608	50	40	30	0.3	70	N	"
609	70	40	30	0.3	65	N	"
610	60	40	30	0.3	50	N	"
611	50	40	20	0.4	50	N	"
612	50	30	30	0.4	65	N	"
613	50	30	20	0.3	50	N	"
614	50	30	30	0.3	65	N	"
615	50	30	20	0.3	40	N	"
616	50	40	20	0.3	50	N	"
617	50	30	20	0.2	55	N	"
618	60	40	20	0.3	55	N	"
619	60	30	20	0.3	50	N	"
620	60	30	20	0.3	50	N	"
621	50	40	20	0.3	50	N	"
622	60	30	20	0.3	55	N	"
623	50	40	30	0.3	55	N	"
624	50	20	20	0.3	50	N	"
625	40	30	20	0.3	55	N	"
626	60	30	20	0.3	50	N	"
627	50	30	30	0.3	50	N	"
628	50	30	20	0.3	50	N	"
629	50	20	20	0.2	50	N	"
630	50	30	30	0.4	50	N	"
631	40	30	30	0.3	45	N	"
632	60	20	10	0.3	45	N	"
633	60	40	30	0.3	90	N	"
634	50	40	40	0.3	90	N	"
635	50	40	40	0.4	95	N	"
636	60	60	30	0.5	105	N	"
637	50	50	30	0.4	60	N	"
638	60	50	40	0.3	120	N	"
639	60	50	20	0.4	80	N	"
640	60	40	30	0.3	90	N	"
641	50	40	40	0.3	105	N	"
642	70	50	30	0.3	100	N	"
643	60	40	30	0.5	95	N	"
644	60	40	30	0.4	100	N	"
645	60	50	30	0.4	105	N	"
646	60	40	20	0.3	90	N	"
647	70	50	20	0.3	80	N	"
648	50	50	40	0.4	95	N	"
649	60	40	30	0.3	75	N	"
650	50	40	30	0.3	65	N	"
651	50	50	20	0.4	75	N	"

Sample No.	Diameter(mm) L	M	S	Roundness	Wt(g)	Mn-coating(mm)	Lithology& Remarks
A-652	50	30	30	0.3	80	N	andesite
653	50	40	30	0.4	95	N	"
654	50	40	30	0.4	80	N	"
655	60	40	40	0.3	65	N	"
656	60	40	30	0.4	75	N	"
657	50	40	40	0.3	75	N	"
658	60	50	30	0.2	90	N	"
659	60	40	30	0.3	70	N	"
660	70	40	40	0.3	80	N	"
661	60	50	20	0.3	75	N	"
662	60	40	20	0.3	65	N	"
663	50	40	20	0.3	60	N	"
664	60	30	20	0.2	70	N	"
665	40	40	30	0.3	70	N	"
666	60	40	30	0.4	70	N	"
667	60	40	20	0.4	70	N	"
668	40	40	30	0.4	60	N	"
669	50	40	30	0.4	75	N	"
670	50	40	20	0.3	60	N	"
671	40	40	30	0.3	60	N	"
672	50	30	30	0.3	65	N	"
673	50	30	30	0.2	60	N	"
674	60	50	20	0.4	70	N	"
675	60	40	30	0.2	55	N	"
676	50	30	20	0.3	60	N	"
677	40	30	30	0.2	50	N	"
678	60	40	30	0.2	60	N	"
679	40	40	20	0.3	50	N	"
680	70	20	10	0.3	50	N	"
681	60	30	20	0.3	40	N	"
682	60	30	20	0.3	40	N	"
683	60	30	20	0.2	50	N	"
684	40	40	30	0.2	35	N	"
685	50	40	20	0.3	50	N	"
686	60	40	20	0.3	60	N	"
687	60	40	20	0.3	50	N	"
688	50	40	30	0.4	80	N	"
689	50	40	10	0.3	55	N	"
690	50	40	30	0.3	60	N	"
691	50	30	20	0.3	55	N	"
692	50	40	20	0.2	60	N	"
693	60	30	20	0.3	55	N	"
694	70	20	10	0.2	30	N	"
695	50	30	20	0.4	55	N	"
696	50	40	20	0.3	55	N	"
697	70	30	20	0.2	45	N	"
698	50	40	20	0.2	60	N	"
699	50	40	30	0.4	75	N	"
700	50	20	20	0.2	45	N	"
701	50	30	10	0.3	40	N	"
702	50	30	20	0.2	45	N	"
703	40	40	20	0.3	50	N	"

Sample No.	Diameter(mm) L	M	S	Roundness	Wt(g)	Mn-coating(mm)	Lithology & Remarks
A-704	50	30	30	0.3	65	N	andesite
705	50	40	30	0.4	65	N	"
706	40	30	30	0.4	55	N	"
707	40	40	20	0.4	50	N	"
708	60	40	20	0.4	55	N	"
709	40	30	20	0.4	60	N	"
710	50	40	30	0.4	70	N	"
711	50	50	10	0.3	45	N	"
712	50	30	20	0.2	50	N	"
713	40	30	30	0.4	60	N	"
714	40	40	20	0.3	65	N	"
715	50	30	20	0.4	60	N	"
716	50	40	20	0.2	50	N	"
717	50	40	20	0.4	60	N	"
718	50	40	20	0.2	50	N	"
719	50	30	10	0.3	40	N	"
720	30	30	30	0.3	30	N	"
721	40	40	6	0.2	20	N	"
722	60	30	20	0.3	40	N	"
723	50	40	10	0.2	40	N	"
724	40	30	20	0.3	40	N	"
725	40	40	30	0.5	60	N	"
726	40	30	20	0.4	60	N	"
727	50	30	20	0.4	50	N	"
728	40	30	20	0.3	40	N	"
729	50	30	20	0.3	40	N	"
730	40	30	20	0.3	35	N	"
731	50	30	20	0.4	45	N	"
732	50	30	20	0.2	30	N	"
733	60	30	20	0.3	30	N	"
734	60	30	20	0.3	30	N	"
735	40	30	30	0.2	35	N	"
736	40	30	20	0.4	35	N	"
737	50	30	20	0.3	30	N	"
738	70	20	10	0.2	30	N	"
739	40	30	30	0.3	30	N	"
740	40	30	20	0.2	30	N	"
741	50	20	10	0.4	30	N	"
742	40	30	30	0.3	40	N	"
743	40	30	20	0.2	40	N	"
744	50	40	20	0.2	40	N	"
745	40	30	20	0.4	45	N	"
746	40	30	20	0.2	40	N	"
747	40	30	30	0.3	50	N	"
748	40	30	30	0.4	50	N	"
749	40	30	20	0.4	45	N	"
750	50	40	10	0.3	45	N	"
751	40	40	20	0.4	45	N	"
752	50	30	20	0.3	40	N	"
753	60	30	20	0.4	40	N	"
754	50	30	20	0.4	40	N	"
755	40	30	30	0.3	45	N	"

Sample No.	Diameter(mm) L	M	S	Roundness	Wt(g)	Mn-coating(mm)	Lithology & Remarks
A-756	40	40	20	0.4	40	N	andesite
757	60	30	20	0.2	40	N	"
758	40	30	20	0.4	40	N	"
759	50	30	10	0.3	30	N	"
760	50	30	20	0.4	40	N	"
761	30	30	20	0.3	40	N	"
762	40	30	20	0.4	40	N	"
763	30	20	20	0.3	40	N	"
764	40	30	20	0.3	35	N	"
765	50	20	20	0.2	30	N	"
766	50	20	20	0.3	35	N	"
767	50	30	20	0.3	30	N	"
768	60	40	10	0.3	35	N	"
769	40	30	20	0.4	35	N	"
770	50	20	10	0.2	30	N	"
771	50	30	10	0.3	35	N	"
772	40	30	20	0.3	40	N	"
773	50	30	20	0.4	40	N	"
774	40	40	20	0.3	35	N	"
775	40	30	20	0.3	35	N	"
776	40	20	20	0.3	35	N	"
777	40	30	10	0.2	30	N	"
778	30	20	20	0.4	30	N	"
779	30	30	20	0.3	30	N	"
780	40	30	20	0.3	30	N	"
781	40	20	10	0.3	30	N	"
782	40	10	10	0.2	25	N	"
783	40	20	20	0.3	25	N	"
784	40	30	20	0.3	25	N	"
785	40	30	20	0.3	25	N	"
786	40	30	10	0.4	30	N	"
787	40	20	20	0.3	25	N	"
788	40	20	10	0.4	30	N	"
789	30	20	10	0.3	20	N	"
790	40	20	10	0.3	20	N	"
791	60	50	7	0.1	25	N	"
792	40	30	10	0.4	30	N	"
793	30	20	10	0.3	20	N	"
794	40	20	10	0.2	20	N	"
795	40	20	10	0.2	20	N	"
796	40	20	7	0.2	25	N	"
797	40	20	10	0.3	20	N	"
798	40	20	10	0.3	20	N	"
799	40	20	10	0.2	15	N	"
800	30	20	20	0.2	20	N	"
801	30	20	10	0.3	20	N	"
802	60	20	10	0.3	20	N	"
803	40	20	10	0.4	20	N	"
804	30	20	20	0.2	20	N	"
805	30	20	10	0.4	15	N	"

Sample No.	Diameter(mm) L	M	S	Roundness	Wt(kg)	Mn-coating(mm)	Lithology & Remarks
B-001	220	120	110	0.5	6.2	N	rhyolite, alt, including basaltic xenolith
002	180	170	110	0.5	3.4	N	"
003	150	140	70	0.5	1.9	N	"
004	130	100	80	0.4	1.4	N	"
005	140	70	50	0.5	1.0	N	"
006	130	70	70	0.4	1.5	N	"
007	120	90	70	0.6	1.0	N	"
008	140	100	70	0.5	1.0	N	"
009	260	130	100	0.8	4.1	N	"
010	260	180	70	0.6	4.5	N	"
011	280	120	90	0.5	3.8	N	"
012	220	130	90	0.6	3.6	N	"
013	150	90	50	0.5	1.1	N	"
014	120	80	50	0.7	0.6	N	"
015	100	60	60	0.6	0.6	N	"
016	220	160	70	0.5	3.0	N	"
017	190	130	60	0.5	1.7	N	rhyolite, alt
018	200	110	90	0.4	1.5	N	rhyolite, alt, including basaltic xenolith
019	160	90	80	0.5	1.6	N	rhyolite, alt
020	180	110	70	0.4	1.0	N	"
021	110	100	80	0.5	1.3	N	"
022	120	110	70	0.4	1.2	N	"
023	110	80	70	0.5	0.8	N	rhyolite, alt, including basaltic xenolith
024	120	90	50	0.4	0.5	N	rhyolite, alt
025	140	60	50	0.4	0.5	N	"
026	400	250	200	0.4	20.0	N	rhyolite, (K-feld+cpx+mt), alt, including basaltic xenolith
027	280	200	120	0.4	9.8	N	"
028	350	160	120	0.5	7.8	N	rhyolite, alt
029	250	200	100	0.4	5.1	N	rhyolite, (K-feld+cpx+mt), alt, including basaltic xenolith
030	300	160	150	0.4	7.4	N	rhyolite, alt
031	270	180	130	0.5	6.1	N	"
032	250	180	110	0.6	5.1	N	"
033	200	180	100	0.6	2.5	N	rhyolite, (K-feld+cpx+mt), alt, including basaltic xenolith
034	120	90	50	0.5	0.4	N	rhyolite, alt
035	125	110	75	0.4	750(g)	N	rhyolite, alt, including basaltic xenolith
036	140	120	60	0.3	600	N	"
037	140	80	70	0.4	670	N	rhyolite, alt
038	110	90	70	0.6	510	N	"
039	120	90	60	0.4	530	N	"
040	120	70	60	0.6	640	N	"
041	130	80	50	0.2	500	N	"
042	120	90	60	0.3	550	N	rhyolite, (K-feld+cpx+mt), alt
043	120	100	40	0.3	600	N	rhyolite, (K-feld+cpx+mt), alt, including basaltic xenolith

Sample No.	Diameter(mm) L	M	S	Round-ness	Wt(g)	Mn-coating(mm)	Lithology & Remarks
B-044	130	80	50	0.6	650	N	rhyolite, alt, including basaltic xenolith
045	100	70	70	0.6	590	N	"
046	120	90	60	0.4	430	N	"
047	80	70	40	0.5	250	N	"
048	120	60	50	0.5	370	N	rhyolite, (K-feld+cpx+mt), alt, including basaltic xenolith
049	90	60	40	0.6	250	N	rhyolite, alt
050	120	90	50	0.5	530	N	"
051	100	80	40	0.5	230	N	"
052	100	80	40	0.4	310	N	rhyolite, alt, including basaltic xenolith
053	90	70	50	0.6	340	N	"
054	70	60	30	0.3	270	N	rhyolite, alt
055	130	70	30	0.4	310	N	"
056	120	60	50	0.5	260	N	"
057	90	80	40	0.4	240	N	rhyolite, alt including basaltic xenolith
058	80	70	60	0.3	280	N	rhyolite, alt
059	90	60	30	0.4	220	N	"
060	80	60	40	0.4	250	N	"
061	80	60	50	0.5	280	N	"
062	80	70	40	0.4	210	N	"
063	80	60	40	0.4	220	N	rhyolite, alt, including basaltic xenolith
064	90	70	60	0.5	310	N	"
065	90	60	50	0.4	220	N	rhyolite, alt
066	70	50	40	0.4	150	N	"
067	90	50	30	0.3	140	N	"
068	80	70	30	0.4	200	N	"
069	90	70	30	0.4	170	N	rhyolite, alt, including basaltic xenolith
070	80	70	40	0.4	200	N	"
071	90	40	40	0.4	150	N	rhyolite, alt
072	70	60	30	0.5	150	N	"
073	70	60	40	0.4	150	N	"
074	100	40	30	0.4	150	N	"
075	90	60	30	0.5	140	N	"
076	80	60	20	0.5	130	N	"
077	90	50	30	0.3	130	N	"
078	80	60	30	0.3	120	N	"
079	80	40	20	0.4	150	N	"
080	80	60	40	0.4	150	N	"
081	70	50	40	0.4	150	N	"
082	80	50	20	0.4	110	N	"
083	70	50	40	0.3	120	N	"
084	80	50	30	0.5	140	N	"
085	80	40	20	0.4	90	N	"
086	80	60	20	0.5	100	N	"
087	70	40	30	0.6	110	N	"
088	70	50	30	0.4	100	N	"
089	70	60	40	0.4	120	N	"

Sample No.	Diameter(mm) L	M	S	Round-ness	Wt(g)	Mn-coating(mm)	Lithology & Remarks
B-090	70	60	20	0.5	100	N	rhyolite, alt
091	60	60	30	0.5	90	N	"
092	60	50	40	0.5	110	N	"
093	60	40	30	0.4	80	N	"
094	70	50	40	0.4	80	N	"
095	60	40	20	0.3	40	N	"
096	70	40	20	0.3	60	N	"
097	130	120	70	0.4	610	N	rhyolite,(K-feld+cpx+mt), alt, including basaltic xenolith
098	70	50	40	0.6	130	N	rhyolite, alt
099	80	60	20	0.4	140	N	"
100	80	40	40	0.5	115	N	"
101	70	50	30	0.4	105	N	rhyolite, alt, including basaltic xenolith
102	80	60	40	0.5	160	N	"
103	70	50	40	0.5	150	N	rhyolite, alt
104	70	40	20	0.4	70	N	"
105	70	40	40	0.4	100	N	"
106	80	30	30	0.4	85	N	"
107	60	30	30	0.6	90	N	"
108	60	50	30	0.6	100	N	"
109	60	50	30	0.4	90	N	"
110	80	40	30	0.3	115	N	"
111	70	40	30	0.4	95	N	rhyolite, (K-feld+cpx+mt), alt, including basaltic xenolith
112	60	50	30	0.4	80	N	rhyolite, alt
113	60	40	30	0.3	70	N	"
114	60	40	40	0.5	110	N	"
115	50	40	20	0.6	55	N	"
116	40	40	40	0.4	55	N	"
117	70	40	20	0.4	70	N	"
118	50	40	30	0.4	85	N	"
119	70	40	30	0.5	70	N	"
120	50	50	40	0.4	90	N	"
121	50	40	30	0.6	70	N	"
122	60	40	20	0.4	65	N	"
123	80	40	30	0.4	85	N	"
124	60	50	30	0.4	80	N	"
125	60	40	30	0.5	60	N	"
126	60	50	30	0.4	50	N	"
127	60	40	30	0.5	75	N	"
128	40	40	30	0.5	50	N	"
129	60	30	20	0.4	40	N	"
130	70	20	20	0.3	35	N	"
131	50	30	20	0.4	40	N	"
132	40	40	20	0.5	40	N	"
133	50	40	20	0.3	45	N	"
134	50	30	10	0.3	30	N	"
135	60	40	20	0.4	50	N	"
136	40	40	10	0.3	20	N	"
137	40	30	10	0.3	20	N	"
138	30	20	20	0.3	20	N	"

Sample No.	Diameter(mm) L	M	S	Round-ness	Wt(g)	Mn-coating(mm)	Lithology & Remarks
B-139	30	20	20	0.4	20	N	rhyolite, alt
140	30	30	20	0.3	15	N	"
141	30	20	10	0.4	15	N	"
142	30	20	20	0.3	10	N	"
143	30	20	10	0.4	10	N	"
144	40	10	10	0.2	10	N	"
145	110	92	65	0.3	500	N	basaltic xenolith included in rhyolite, v, (kamp+pl+cpx+mt)
146	70	40	40	0.3	110	N	"

Sample No.	Diameter(mm) L	M	S	Round-ness	Wt(g)	Mn-coating(mm)	Lithology & Remarks
C-001	300	150	70	0.4	7500	N	scoria, alt
002	300	200	120	0.2	6500	N	"
003	280	120	70	0.2	3200	N	"
004	100	80	50	0.2	530	N	"
005	90	70	50	0.1	290	N	"
006	100	60	50	0.1	330	N	"
007	100	50	30	0.1	190	N	"
008	100	70	40	0.2	300	N	"
009	100	70	30	0.2	240	N	"
010	90	40	40	0.1	130	N	"
011	90	50	30	0.2	150	N	"
012	70	50	30	0.1	130	N	"
013	50	50	50	0.2	130	N	"
014	50	40	30	0.1	65	N	"
015	70	60	40	0.1	155	N	"
016	60	30	20	0.1	60	N	"
017	50	40	20	0.2	110	N	"
018	50	40	30	0.1	70	N	"
019	60	40	30	0.1	60	N	"
020	60	50	30	0.1	70	N	"
021	50	50	30	0.2	65	N	"
022	60	40	30	0.1	65	N	"
023	40	30	30	0.1	60	N	"
024	40	30	20	0.1	50	N	"
025	40	20	20	0.1	45	N	"
026	40	30	20	0.1	40	N	"
027	40	30	10	0.1	40	N	"
028	30	20	10	0.1	35	N	"

Sample No.	Diameter(mm) L	M	S	Round-ness	Wt(g)	Mn-coating(mm)	Lithology & Remarks
D-001	-	-	-	-	3500	N	mud (10YR4/2)
002	-	-	-	-	6000	N	" (")

Sample No.	Diameter(mm) L	M	S	Round-ness	Wt(g)	Mn-coating(mm)	Lithology & Remarks
E-001	130	80	55	0.8	680	N	basalt, alt
002	130	70	50	0.8	540	N	diorite
003	95	60	55	0.7	460	N	"
004	95	65	35	0.7	240	N	"
005	75	60	50	0.7	310	N	granite porphyry
006	95	50	50	0.7	300	N	basalt
007	85	60	40	0.7	320	N	basalt, aphyric
008	85	55	55	0.7	240	N	diorite
009	85	60	30	0.7	180	N	granite, porphyry
010	80	45	45	0.6	250	N	"
011	85	50	40	0.7	280	N	granite
012	80	80	20	0.6	180	N	sandstone
013	85	60	25	0.6	160	N	mudstone
014	90	55	35	0.7	150	N	diorite?, alt
015	55	50	35	0.7	100	N	diorite
016	80	40	30	0.6	120	N	diorite?, alt
017	85	40	35	0.6	130	N	basalt?, alt
018	60	50	35	0.7	130	N	basalt
019	75	55	15	0.6	100	N	basalt?, h.alt
020	50	45	20	0.7	60	N	no cutting
021	40	30	20	0.7	36	N	"
022	45	25	15	0.7	23	N	"
023	45	30	20	0.6	21	N	"
024	35	20	15	0.6	18	N	"
025	40	30	15	0.7	19	N	"
026	30	25	10	0.7	14	N	"
027	45	30	10	0.6	15	N	"
028	35	20	10	0.6	14	N	"
029	35	30	7	0.7	10	N	"
030	30	25	15	0.8	9	N	"
031	45	15	10	0.8	12	N	"
032	30	15	15	0.7	7	N	"
033	30	25	6	0.7	6	N	"
034	30	25	7	0.9	10	N	"
035	30	25	10	0.7	10	N	"
036	30	20	10	0.8	7	N	"
037	25	25	15	0.8	10	N	"
038	40	15	10	0.8	8	N	"
039	30	15	10	0.7	7	N	"
040	25	15	10	0.7	6	N	"
041	25	20	7	0.8	4	N	"
042	20	15	12	0.8	4	N	"
043	–	–	–	–	3	N	wood chip

Sample No.	Diameter(mm) L	M	S	Roundness	Wt(g)	Mn-coating(mm)	Lithology & Remarks
F-001	170	60	60	0.4	1200	N	dacite?
002	100	100	40	0.6	580	N	dacite?, alt
003	205	115	50	0.1	1000	N	dacite?
004	130	90	60	0.3	1050	N	dacite?, h.alt
005	110	100	60	0.3	730	N	"
006	100	80	70	0.4	440	N	"
007	100	65	65	0.4	380	N	"
008	95	60	40	0.4	210	N	"
009	75	55	30	0.3	150	N	"
010	75	55	40	0.3	190	N	dacite
011	60	50	35	0.3	90	N	dacite?, h.alt
012	70	50	40	0.4	180	N	dacite, alt
013	60	40	25	0.3	100	N	dacite
014	70	50	45	0.4	180	N	diorite?, alt
015	90	50	15	0.3	120	N	diorite
016	80	50	35	0.6	160	N	basalt?, aphyric
019	45	30	20	0.4	10	N	pumice
020	70	60	40	0.4	160	N	tuff breccia

Note

- v : vesicular
- alt : altered
- h.alt : highly altered
- ( ) : phenocryst assemblage
- pl : plagioclase
- cpx : clinopyroxene
- ol : olivine
- mt : magnetite
- K-feld : potasium feldspar
- kamp : kaersutite

9-4. DESCRIPTION OF DREDGED SAMPLES FROM ERIMO SEAMOUNT AND MEIYO-DAINI SEAMOUNT (JAPAN SEA), DURING KH 86-2 CRUISE

T. Ishii, S. Yamashita, H. Kobayashi, A. Kitamura,
T. Shimizu, K. Konishi, R. Tsuchi and K. Kobayashi

More than one thousand rocks (about 400 kg weight in total) were dredged in this cruise from three dredge sites. Two sites (Station No. 2 and 3) and one site (Station No.11) were selected for the investigation of dredge hauls of Erimo Seamount and Meiyo-Daini Seamount (northwestern Japan Sea), respectively. Precise position, depths of each station and other information are given at the operation logs ofdredge haul(9-1), and positions are shown in the bathymetric charts (Fig. 9-2-1 and 9-2-2).

Improved new type of Nalwalk chain-bag dredges with backet (Ishii et al., 1985) were operated to collect boulder to granule rock samples as well as psammitic to pelitic soft sediments. Newly prepared dredge pinger-transponder (DPT-1030) was firstly installed at 100-300 meters above the dredge to confirm for dredge hitting sea bottom. The DPT-1030 is reported by Ishii et al. in this volume. Because most of the dredged rock-samples were more or less covered with soft sediment and/or Mn-coating, these rocks were at first separated from soft sediments by washing, and cut into two or more piéces for observation and description of visual features inside each sample. Washed samples were classified into several groups according to lithologic characteristics. After numbering the samples (in the order of size), diameter (L, M and S), roundness, weight and thickness of Mn-coating, the lithology and remarks of each sample were observed on board as well as on land and described as shown in Table 9-3, excluding data on soft sediments. In the table, roundness is described after Powers' system (Powers, 1953), that is 0.10=very angular, 0.20=angular, 0.30=subangular, 0.40=subrounded, 0.60=rounded and 0.85=well-rounded. Wet chemical analyses of dredged rocks and related rocks are listed in Table 9-4-1, and are shown in the variation diagrams (Kuno, 1954) and alkali-silica diagram in Fig. 9-4-1 and Fig. 9-4-2, respectively.

Erimo Seamount

Erimo Seamount have been surveyed by many research vessels during the last fifteen years. It was also an important target of the Nautile Dives of Japan-France KAIKO Project. Considering those previous studies, stations of dredge hauls were decided. One gravel of relatively fresh plagioclase-phyric trachyandesite (KH 86-2-2-1) was recovered at Station No. 2. Major element chemistries of this rock as well as Nautile' s samples are listed in Table 9-4-1 and are shown in Fig. 9-4-1 with Kitano's (1970)

data. Dredge hauls at Erimo Seamount are more precisely reported by Konishi et al. in this volume.

Meiyo-Daini Seamount

More than one thousand rocks including andesitic rocks, rhyolitic rocks and granitic rocks were collected from south eastern steep slope of Meiyo-Daini Seamount. All granitic gravels are rounded and those Powers' number are obviously larger than andesitic and rhyolitic rock (Table 9-3). It is reasonable to consider that those gravels were ice raft products or detrital products from some provinces.

Relatively fresh andesitic rocks were selected for wet chemical analyses, and these results are shown in Table 9-4-2 and Fig. 9-4-1. Precise petrological studies on the above andesitic rocks are reported by Yamashita in this volume.

Acknowledgements

We thank Mr. H. Haramura, University of Tokyo, for his wet chemical analyses. Thanks are due to Mr. T. Hiroi, Dr. M. Nomura and Mr. A. Uchiyama for computer programs, Ms. T. Hatanaka for her help in preparation of polished thin sections, and Ms. D. Van de Rijt and T. Mizutani in typewriting.

References

Ishii, T., Kobayashi, K., Shibata, T., Naka, J., Jhonson, K., Ikehara, K., Iguchi, M., Konishi, K., Wakita, H., Zhang, F., Nakamura, Y. and Kayane, H., 1985. Description of samples from Ogasawara fore-arc. Ogasawara Plateau and Mariana Trough, during KH 84-1 Cruise. In Preliminary Report of the Hakuho-Maru Cruise KH84-1 (Ocean Research Institute, University of Tokyo), 105-165.

Kitano, K., 1970. Alkaline basalts from the Erimo Seamount. Jour. Geol. Soc. Japan, 76, 399-404.

Kuno, H., 1954. Volcanoes and volcanic rocks, Iwanami-syoten, Tokyo(in Japanese), pp. 255.

Powers, M.C., 1953. A new roundness scale for sedimentary particles. J. Sed. Pet., 23, 117-119.

Table 9-4-1. The wet chemical analyses of igneous rocks collected from Meiyo Daini seamount and Erimo seamount by Hakuho Maru and Nautile (Analyst: H. Haramura)

	Meiyo-Daini Seamount				Erimo Seamount									
Anal.No.	1	2	3	4	5	6	7	8	9	10	11	12	13	14
Sample No.	KH86-2 11A059	KH86-2 11A114	KH86-2 11A128	KH86-2 11A201	KH86-2 2-1	KAIKO 49-1	KAIKO 50-1	KAIKO 50-2	KAIKO 50-3	KAIKO 50-4	KAIKO 50-5A	KAIKO 50-6	KH69-2 18-02I	KH69-2 18-31I
SIO2	56.44	57.92	56.67	56.44	54.30	58.42	43.36	42.08	44.54	41.19	43.38	44.86	56.36	45.75
TIO2	.91	.83	.81	.84	.97	1.23	3.74	4.26	4.14	4.34	3.79	4.20	1.73	2.67
AL2O3	19.82	19.34	19.03	19.15	17.75	17.90	13.03	15.41	15.29	16.46	13.65	14.55	17.73	13.08
FE2O3	2.84	3.80	2.12	1.83	4.23	4.72	6.09	7.45	7.21	8.63	6.38	7.41	4.86	5.78
FEO	2.07	1.05	3.90	3.66	3.63	.89	6.50	2.04	3.10	1.74	5.77	2.88	1.06	4.04
MNO	.12	.05	.14	.14	.13	.26	.17	.10	.17	.14	.17	.14	.13	.14
MGO	1.62	1.28	1.62	1.41	3.96	1.34	9.50	4.12	5.71	3.59	8.62	5.91	1.37	6.81
CAO	5.51	5.08	5.00	4.82	7.85	4.42	9.79	11.37	10.66	10.09	10.23	10.76	5.64	14.05
NA2O	4.63	5.18	4.67	4.70	3.85	6.45	3.15	3.56	3.75	3.08	3.29	3.54	6.01	2.52
K2O	2.55	3.01	3.03	3.07	1.09	3.36	1.14	1.77	1.39	1.53	1.23	1.46	3.54	.90
P2O5	.32	.37	.29	.29	.27	.36	.78	2.89	.84	3.06	.75	.94	.76	.45
H2O+	2.45	1.65	2.65	2.83	1.14	.38	2.38	3.35	2.70	3.95	2.08	2.33	.84	3.15
H2O-	1.07	.88	.55	.53	.62	.13	.55	1.35	.87	2.07	.90	1.15	.28	.85
TOTAL	100.35	100.44	100.48	99.71	99.79	99.86	100.18	99.75	100.37	99.87	100.24	100.13	100.31	100.19
NI(ppm)	22	17	19	21	36	19	207	119	205	217	136	132	12	124
CR(ppm)	51	62	49	43	47	31	264	317	294	330	297	297	23	326
CIPW NORM														
Q	6.56	5.10	3.93	4.03	7.09	.00	.00	.00	.00	.00	.00	.00	.00	.00
OR	15.56	18.17	18.41	18.83	6.57	19.98	6.93	11.00	8.49	9.63	7.47	8.93	21.09	5.53
AB	40.46	44.76	40.62	41.27	33.23	54.21	21.41	29.94	24.04	27.77	20.15	26.06	48.60	19.00
AN	26.07	21.07	22.63	22.85	28.49	10.03	18.56	21.93	21.47	28.31	19.38	20.17	11.04	22.58
NE	.00	.00	.00	.00	.00	.39	3.25	.95	4.74	.00	4.59	2.67	1.45	1.72
WO	.00	.92	.39	.00	3.94	3.89	10.92	4.46	10.73	.00	11.60	10.72	3.98	19.55
EN	.00	.79	.18	.00	2.99	3.36	9.13	3.86	9.27	.00	10.02	9.27	3.44	16.90
FS	.00	.00	.20	.00	.55	.00	.40	.00	.00	.00	.00	.00	.00	.00
EN	4.17	2.46	3.96	3.64	7.07	.00	.00	.00	.00	8.94	.00	.00	.00	.00
FS	.18	.00	4.26	4.24	1.30	.00	.00	.00	.00	.00	.00	.00	.00	.00
FO	.00	.00	.00	.00	.00	.00	10.65	4.86	3.80	.41	8.45	4.18	.00	.51
FA	.00	.00	.00	.00	.00	.00	.52	.00	.00	.00	.00	.00	.00	.00
MT	4.25	1.17	3.16	2.75	6.26	.15	9.08	.00	.00	.00	8.40	.00	.00	5.97
IL	1.78	1.61	1.58	1.66	1.88	2.35	7.30	4.76	7.14	4.23	7.40	6.60	2.54	5.27
AP	.77	.88	.69	.70	.64	.84	1.86	7.04	2.01	7.55	1.79	2.25	1.78	1.08
C	.20	.00	.00	.03	.00	.00	.00	.00	.00	.00	.00	.00	.00	.00
HM	.00	3.08	.00	.00	.00	4.65	.00	7.84	7.45	9.20	.77	7.67	4.90	1.89
OT	.00	.00	.00	.00	.00	.15	.00	3.36	.88	3.96	.00	1.48	1.20	.00

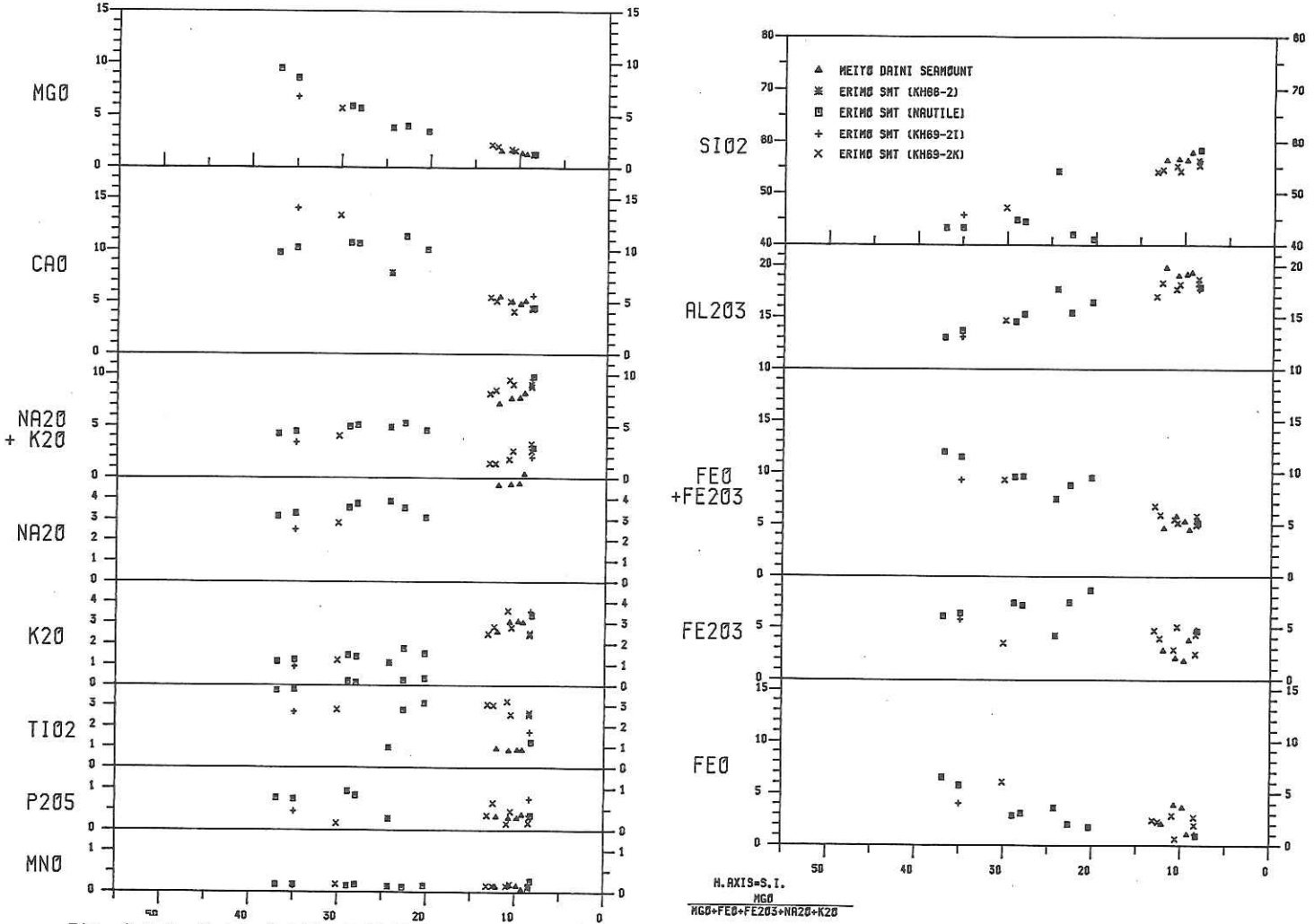

Fig. 9-4-1. Oxide (wt%)--Solidification Index (SI) diagram (Kuno, 1954) of wet chemical analyses of igneous rocks collected from Meiyo Daini and Erimo seamounts. Analyst; X: Erimo Seamount (KH 69-2) by Kitano (1970), the others by Haramura (Table 9-4-1).

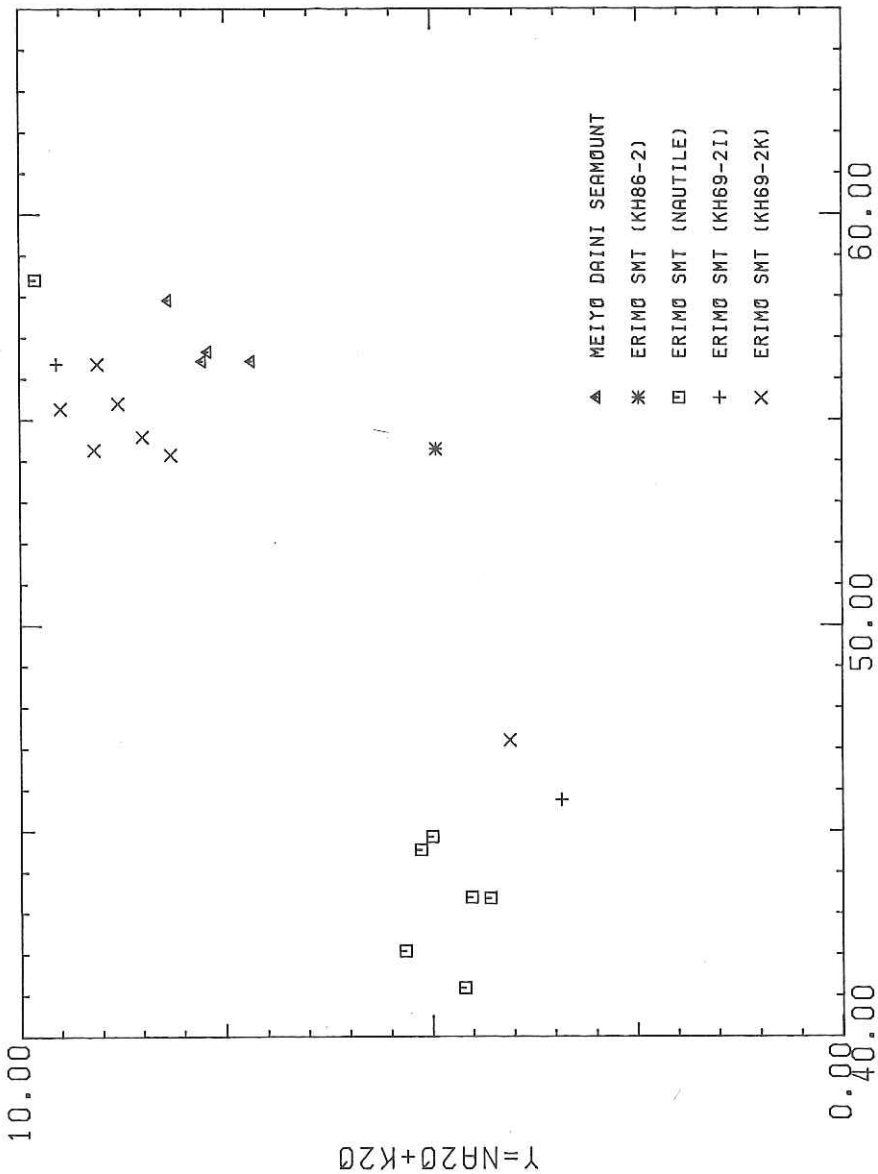

Fig. 9-4-2. Alkali-silica diagram of wet chemical analyses of igneous rocks collected from Meiyo Daini seamount and Erimo seamount. Analyst; X: Kitano (1970), the others: Haramura (new data).

9-5. NOTE ON DREDGE SAMPLES FROM ERIMO SEAMOUNT

K. Konishi, R. Tsuchi, T. Ishii, H. Kobayashi,
K. Kitamura, S. Kuramoto and S. Yamashita

Purpose

Four dredge sites were originally proposed at Erimo Seamount area during the present cruise. They were selected for the purpose to (1) settle the age of the shallow-water carbonate cap as well as its basaltic basement, and (2) reinforce the interpretation that Erimo Seamount was and most probably is still being broken down neotectonically, from both biostratigraphic and lithologic evidence. The reported K-Ar dates for the basaltic basement of Erimo Seamount range from 80Ma to 83Ma(Ozima et al., 1970), while a non-unequivocal age of a new species of gastropod, Nerinea (Plesioptygmatis) ryofuae, has been assigned to Campanian (Tsuchi and Kuroda, 1973). If accepted, both ages are exceptionally younger than those of the seamounts hither to known in the northwestern Pacific region, especially near Japan. As it is always possible that K-Ar data tends to yield a "minimum age", it is highly desirable to cross-check the date independently with index fossils such as large benthonic foraminifers in orderto verify the result of the radiometric dating.

Following the detailed seabeam mapping of submarine topography by R/V Jean-Charcot (Cadet, Kobayashi et al., 1985), a dive of the submersible, NAUTILE in the summer of 1985 (Kobayashi et al., 1987) observed E-W trending depression tectonically active, north of which appears to have been down-faulted. Whether the breakdown of seamount may occur in general along trench like Daiichi-Kashima and Erimo needs to be examined rigorously. Supporting evidence for such contention should be provided from biostratigraphic correlation and lithological coincidence for shallow-water carbonate caps between the main body and supposedly down-faulted block of Erimo Seamount. Also it was focussed on the western part of the seamount in order to fill a gap of our knowledge. Almost all the dredge records were so far restricted to its eastern part.

Operation

Details of the operation at St. 2 whence a transponder was installed 100 m above the dredge are described elsewhere in this report.

Result

Because of shortage of time available, only two dredge hauls were carried out with Norwalk chain bag type of dredger. Furthermore, the samples were recovered only from one station (St. 2), as the dredger was lost during operation at the other station (St. 3)(Fig. 9-2-1).

Besides some 1.7 kg of greyish olive mud, 34 rock fragments of various size and rock types together with several small round pebbles were recovered from St. 2, which covers an area about 4.2 km long from the southwestern flat top down to the upper slope northwestwards. These small round pebbles (Sample Nos. 02-07) are considered to be ice-rafted, because of their high value of roundness and "exotic" lithologies.

Preliminary petrographic study revealed that the collection includes one pebble of basalt and the other one of Mn-coated phosphorite. This subangular fragment of basalt is believed to come from a presumably faulted outcrop along the northern upper slope. The phosphorite with whitish cream color has been almost entirely altered but still preserves relict of original phenocrysts after basalt. Rest of the samples consists of ferro-manganese crusts and nodules. Some of them were grown on pieces of fossil sponge (Sample Nos. 21-23 & 27). It is difficult to conclude from the present results alone whether carbonate-cap does occur on the western summit or not. If it occurs, however, it should be limited to the southernmost area as a veneer, as the sample from St. 2 may suggest.

9-6. ANDESITIC LAVA RECOVERED FROM MEIYO DAINI SEAMOUNT IN YAMATO BASIN DURING KH 86-2 CRUISE

S. Yamashita

A series of seamounts exists in the midst of Yamato Basin. The rock fragments have ever recovered from these seamounts consist mainly of andesitic lava (KH84-3 Cruise Report, 1984,MS). Kaneoka (1986) reported their K-Ar ages about 12-14Ma. Those andesitic volcanism is interesting in relation to the evolution of Yamato Basin, because of following respects: (1)Ages of the volcanism nearly correspond to that of opening of Japan Sea, proposed by Otofuji et al. (1986). (2)These seamounts show the configuration as a chain in the midst of Yamato Basin.

One dredge haul was carried out at Meiyo-Daini Seamount (station 11 in this cruise), which belongs to the above seamount chain. About 1000 rock fragments, including about 800 andesitic lavas and 150 rhyolitic lavas, were obtained. In this paper, preliminary petrological results of the andesitic lava will be reported.

Whole Rock Chemistry

Nine relatively fresh specimens were chosen for XRF whole rock chemical analysis. Contamination of seawater was carefully removed. The XRF analysis was carried out at Earthquake Research Institute, University of Tokyo with fused glass diluted by $Li_2B_4O_7$ with a weight proportion of 1:10. Major element compositions of whole rock are listed in table 9-6-1. SiO_2 contents of analyzed specimens range from 56.5% to 60.3% and FeO*/MgO ratios of them are high, suggests that the andesites are differentiated. The andesites from Meiyo-Daini Seamount (hereafter, SMt) are characterized by mildly alkaline and quarz normative features. Fig. 9-6-1 shows SiO_2 versus total alkali variation. In fig. 9-6-1, the andesite belongs to alkalic suite defined by Miyashiro (1978).

Petrography

The specimens of andesitic lava were examined under the microscope. The chemical compositions of constitute minerals were determined with electron microprobe analyzer at Ocean Research Institute, University of Tokyo. The data correction procedure was based on Bence & Albee (1968). Representative microprobe analyses are shown in table 9-6-2.

The specimens are vesicular and the modal volume of vesicules is up 15%. In all specimens, phenocryst assemblage is plagioclase + clinopyroxene $\pm$ olivine. Modal volume of phenocrysts are generally 10%.

The groundmass consists of abundant plagioclase and subordinate clinopyroxene, magnetite, and glass. Although constitute minerals and glass are generally fresh, chlorites sometime occur filling in vesicules and/or replacing to groundmass glass. Olivines are altered to be iddingsites in their rim.

Random analyses of core composition of phenocryst were carried out in a few specimens. Anorthite content of plagioclase, forsterite content of olivine, and Mg# vs Al content variation of clinopyroxene are shown in figs.9-6-2, 3, and 4, respectively. As is clear from these figures, all phenocryst phases can be divided into two groups by apparent compositional gap. 1)Evolved Group: sodic plagioclase(An_{40-60}) + fayalitic olivine(Fo_{55-61}) + Al-poor clinopyroxene. 2)Refractory Group: calcic plagioclase(An_{75-91}) + forsteritic olivine(Fo_{78-87}) + aluminous clinopyroxene. No systematic correlation is recognized between composition and size in all phenocryst phases.

Details of both group phenocrysts are described below.

Evolved Group Phenocryst:

Plagioclases of this group occur as euhedral form. They contain large amount of glass inclusions, showing skeletal morphologies. Their compositional zonings are irregular and their compositional range is from An_{40} to An_{60}. Olivines show euhedral to vermicular form and have fayalitic composition, Fo_{55} to Fo_{61}. Clinopyroxenes of this group occur as euhedra. Their Mg# and Al mole are below 0.7 and 0.1, respectively.

Refractory Group Phenocryst:

Phenocrysts of this group have unusually refractory composition for host differentiated andesite: plagioclase (An_{75-91}), olivine (Fo_{78-87}), clinopyroxene (Mg#'s are up to 0.88). Clinopyroxene of this group has much aluminouscomposition (fig. 9-6-4). Phenocrysts of this group often occur as clotof monophase or polyphase, merely containing all three phases, sometimes showing cumulative texture. In such case, pargasitic amphiboles characteristically occur as intercumulus and/or interstitial phase.

In this group phenocrysts, most striking feature is that various disequilibrium natures with host rock are always observed. This group phenocrysts show rounded form. They are always isolated from host rock by thin overgrowth("mantle") or aggregate consists of fine grained crystals of plagioclase, clinopyroxene, and magnetite. Mantles have much more evolved composition than their cores. The compositions of mantles are shown in figs. 9-6-2, 3, and 4, comparing to that of core of both group phenocrysts. It is noteworty that, in all three phases, the composition of mantlesare similar to that of core of Evolved Group phenocrysts.

Above disequilibrium natures are observed in only margin of clot when

phenocrysts of this group form crystal clot. Furthermore, in the case of that a clot contains both olivine and clinopyroxene, Fe-Mg partition coefficients between olivine and clinopyroxene keep to close unity within a single clot. It suggests that olivine and clinopyroxene were equilibrated under near 1000°C (Obata et al. 1974). Consequently, it is considered that all three phases of Refractory Group are in equilibrium each other.

Interrelation Between Both Group Phenocrysts and Host Rock:

It is noteworty that, within a thin section, coexistence of two group phenocrysts is commonly observed. Figs. 9-6-2 and 3 apparently show that two group phenocrysts coexist within a single specimen. In order to determine the relationship between host and phenocrysts of both groups, Fe-Mg partitionings between olivine and host were examined. Recall that modal volume of phenocrysts is generally 10%. Thus $Fe/Mg_{whole\ rock}$ may represents Fe/Mg_{magma}. In fig. 9-6-5, lower cluster is cores of Refractory Group, and upper cluster is cores of Evolved Group and mantles of Refractory Group. Fig. 9-6-5 apparently shows that Evolved Group and mantle of Refractory Group can be in equilibrium with host, while core of Refractory Group can not.

Above observations and the disequilibrium natures of Refractory Group, described before, suggest that Refractory Group phenocrysts are xenocrysts incorporated into host andesitic magma, and that Evolved Group and mantle of Refractory Group crystallized from host magma in equilibrium.

Remarks

The andesites from Meiyo-Daini SMt are differentiated mildly alkaline rock. Refractory Group phenocrysts are identified as xenocrysts as described before. In contrast, Evolved Group phenocrysts and mantle of Refractory Group might crystallized in equilibrium from host andesitic magma, after Refractory Group "xenocrysts" had been incorporated into host. Refractory Group "xenocrysts" are considered to be congnate cumulate because of following characteristics. They often occur as crystal clots, sometimes showing cumulative texture. Suggesting in Fe-Mg partitionings between olivine and clinopyroxene, such clots show no evidence of reequilibrium under low temperature within crust.

References

A.E,Bence and A.L,Albee, 1968, Empirical correction factors for the electron microanalysis of silicates and oxides, J.Geol., vol.76, 382-403

Kaneoka,I., 1986, Constraints on the time of the evolution of the Japan Sea floor based on radiometric ages,

J.Geomag.Geoelectr.,38,475-485

KH84-3 on board scientists, 1984MS, KH84-3 cruise report, Ocean Research Institute, Univ. of Tokyo

Miyashiro,A., 1978, Nature of alkalic volcanic rock series, Cont.Min.Petr.,66,91-104

Obata et al., 1974, The iron-magnesium partitioning between naturally occurring coexisting olivine and Ca-rich clino-pyroxene: an application of the simple mixture model to olivine solid solution, Bull.Soc.Fr.Min.Cryst.,97,101-107

Otofuji et al., 1986, Brief review of Miocene opening of the Japan Sea; paleomagnetic evidence from Japan arc, J.Geomag.Geoelectr.,38,287-294

Roeder,P.L. and Emslie,R.F., 1970, Olivine-liquid equilibrium, Contr.Mineral.and Petrol.,29,275-289

Takahashi,E. and Kushiro,I., 1983, Melting of a dry peridotite at high pressure and basalt magma genesis, Amer.Miner.,68,859-879

Table.9-6-1 Whole rock major element composition

Specimen	A020	A051	A135	A128	A069	A123	A059	A201	A300
SiO2	56.46	57.25	58.41	58.72	58.84	59.10	59.14	59.25	60.29
TiO2	1.06	0.99	0.97	0.94	0.98	0.93	0.97	0.95	0.97
Al2O3	20.53	21.30	19.33	18.61	20.30	18.27	19.22	18.39	19.88
FeO*	7.05	5.57	6.58	6.76	4.68	6.48	5.35	6.26	3.71
MnO	0.11	0.11	0.14	0.15	0.09	0.16	0.12	0.15	0.09
MgO	1.69	1.41	1.57	1.71	1.03	1.66	1.72	1.47	0.90
CaO	6.00	5.71	5.18	5.06	5.64	5.09	5.52	5.08	5.36
Na2O	4.57	4.96	4.63	4.67	5.23	4.85	4.89	4.95	5.35
K2O	2.19	2.40	2.92	3.12	2.87	3.20	2.78	3.24	3.14
P2O5	0.35	0.30	0.26	0.26	0.33	0.27	0.30	0.27	0.31
Total	100.00	100.00	100.00	100.00	100.00	100.00	100.00	100.00	100.00
FeO*/MgO	4.17	3.95	4.18	3.96	4.56	3.90	3.11	4.25	4.10

Recalculated to 100% and all iron as FeO

Table.9-6-2 Representative microprobe analyses

	Plagioclase		
	1	2	3
SiO2	46.26	55.96	55.37
Al2O3	33.78	28.44	28.29
FeO	0.47	0.43	0.38
CaO	17.90	11.21	11.15
Na2O	1.30	5.18	5.54
K2O	0.07	0.31	0.25
Total	99.78	101.53	100.98
Si	2.138	2.490	2.481
Al	1.840	1.491	1.494
Fe	0.018	0.016	0.014
Ca	0.886	0.534	0.535
Na	0.116	0.447	0.481
K	0.004	0.018	0.014
Total	5.003	4.996	5.020
An	0.880	0.535	0.519
Ab	0.116	0.447	0.467
Or	0.004	0.018	0.014

	Olivine		
	7	8	9
SiO2	39.33	35.53	35.95
FeO	14.20	34.64	33.68
MnO	0.20	1.02	1.01
MgO	45.51	27.59	28.83
CaO	0.22	0.26	0.15
NiO	0.10	0.04	-
Total	99.56	99.08	99.62
Si	0.990	0.999	0.998
Fe	0.299	0.813	0.781
Mn	0.004	0.024	0.024
Mg	1.708	1.156	1.194
Ca	0.006	0.008	0.004
Ni	0.002	0.001	-
Total	3.010	3.001	3.002
Fo	0.851	0.587	0.604

	Clinopyroxene		
	4	5	6
SiO2	50.76	50.98	51.15
TiO2	0.53	0.60	0.59
Al2O3	4.63	2.36	1.84
FeO	4.97	10.14	12.17
MnO	0.07	0.43	0.90
MgO	15.77	13.51	11.76
CaO	21.62	20.75	20.69
Na2O	0.29	0.35	0.41
Cr2O3	0.30	-	-
Total	98.94	99.12	99.51
Si	1.880	1.929	1.949
Ti	0.015	0.017	0.017
Al	0.202	0.105	0.083
Fe	0.154	0.321	0.388
Mn	0.002	0.014	0.029
Mg	0.871	0.762	0.668
Ca	0.858	0.841	0.845
Na	0.021	0.026	0.030
Cr	0.009	-	-
Total	4.011	4.014	4.008
Mg#	0.850	0.704	0.633

1,4,7: core of Refractory Group phenocryst
2,5,8: mantle of Refractory Group phenocryst
3,6,9: core of Evolved Group Group phenocryst

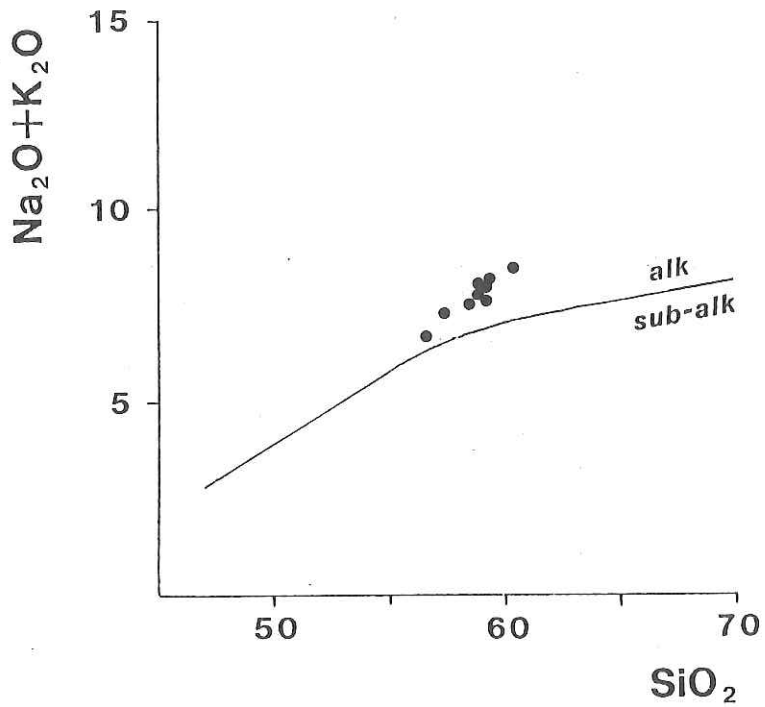

Fig.9-6-1. SiO_2 vs total alkali diagram. Boundary between alkaline and sub-alkaline suite is taken from Miyashiro(1978).

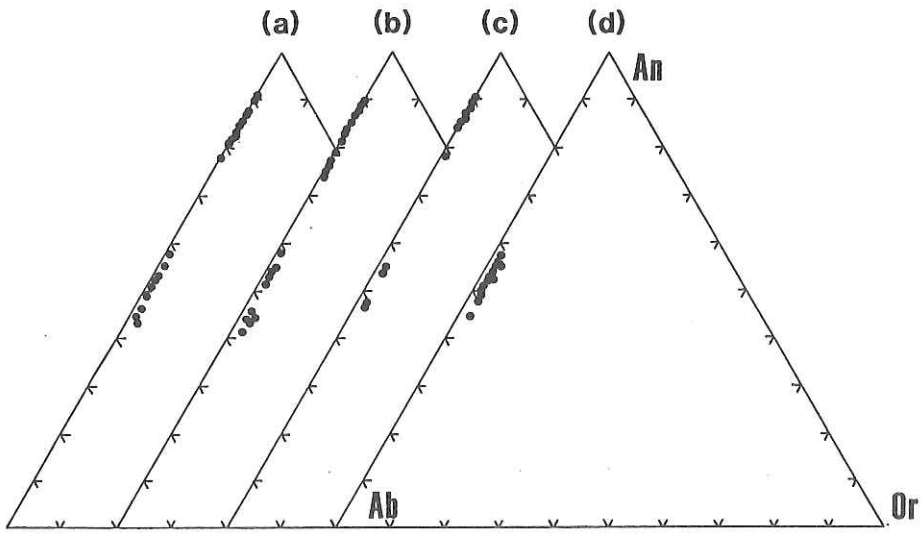

Fig.9-6-2(a)-(d). Compositions of plagioclase. **(a),(b)**, and **(c)** show core of phenocrysts in specimen 201,126, and 114 respectively. **(d)** shows mantle of Refractory Group phenocryst.

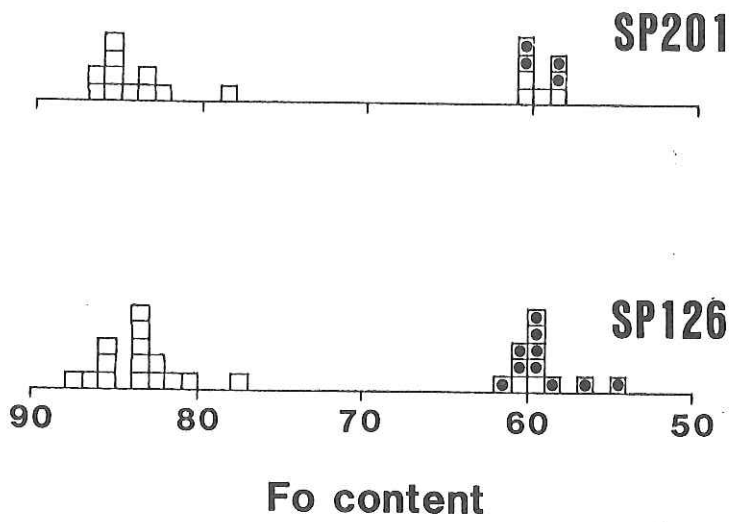

Fig.9-6-3(a),(b). Forsterite content of olivine in specimen 201**(a)**, 126**(b)**. Open square shows core composition of phenocryst. Square with dot shows composition of mantle of Refractory Group.

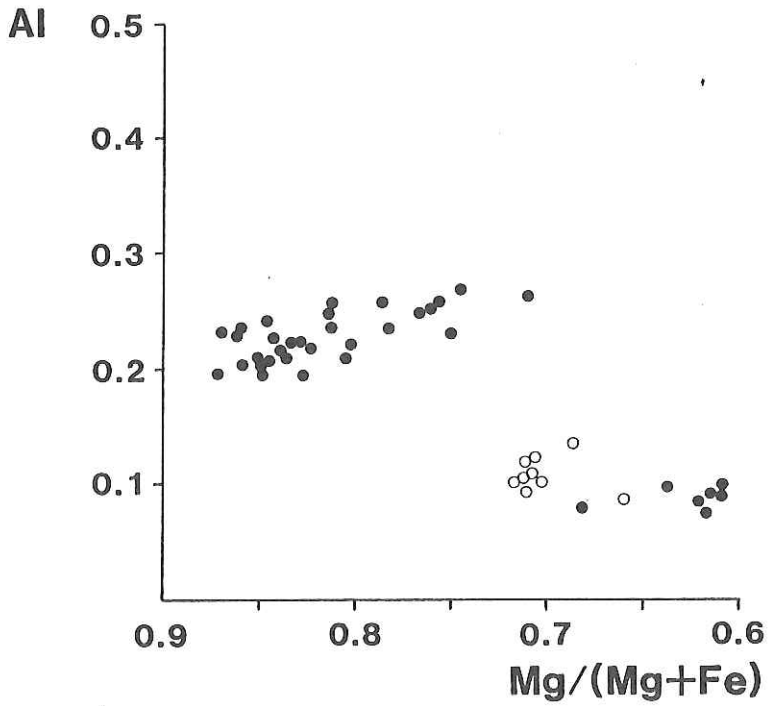

Fig.9-6-4. $Mg^{\#}$ vs Al content variation of clinopyroxene in a few specimens where Mg number $Mg^{\#}$ = Mg/(Mg+Fe). Close circle: core of phenocryst. Open circle: mantle of Refractory Group.

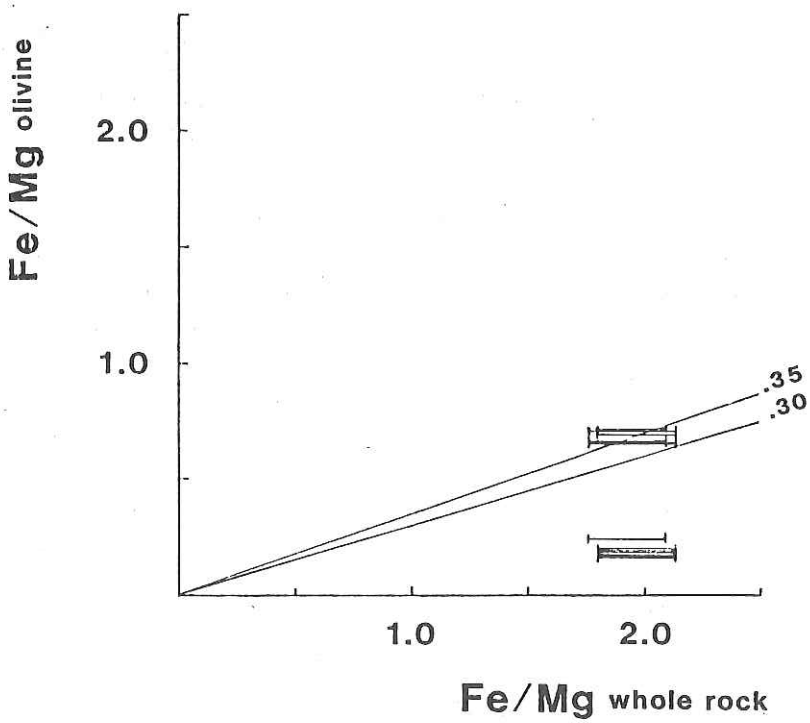

Fig.9-6-5. Fe-Mg partitioning between olivine and host whole rock. Partitioning coefficients determined by Roeder & Emslie(1970) and Takahashi and Kushiro(1983) are followed. Upper cluster of plots shows Evolved Group phenocryst and mantle of Refrac-tory Group phenocryst. Lower cluster is core of Refractory Group phenocryst. Bar means possible range of Fe/Mg in whole rock, where Fe_2O_3/FeO ratio is 0.00 to 0.35 by weight.

9-7. FIRST TRIAL USE OF DREDGE PINGER-TRANSPONDER (DPT-1030) FOR DREDGE HAULS DURING KH 86-2

T. Ishii, T. Furuta, M. Watanabe and M. Nakanishi

Dredge Pinger-Transponder system was prepared to confirm for dredge to hit sea bottom. The system consists of the following two units.

1) Under water system

Kaiyodensi Model DPT-1030, Dredge Pinger-Transponder

Rated water depth : 6000 m

Rated distance between DPT-1030 and R/V : approx. 10,000 m

Rated distance between DPT-1030 and sea bottom : 3.0 - 187.4 m

2) On board system

Kaiyodensi Model TP601 Transponder on board system

Theabove on board system was previously prepared for transponder system with three ocean bottom and one subnavigation transponders by Furuta et al. (1984). On the other hand, the Dredge Pinger-Transponder (DPT-1030) with both facilityof pinger and transponder was newly designed to monitor the three dimensional position of dredge equipments from the control room of research vessel during dredge hauls. Position of dredge equipments will be accurately estimated within several tens of meters in the transponder-net of properly distributed three transponders in the very steep bottom topography as well, up to 6000 m deep. It will be used for pin-point collecting of rock samples by dredge at the geologically interested critical stations.

The DPT-1030 was used during two dredge hauls and one wired deep sea camera work. It was installed at one and three hundred meters above the dredge equipments during KH 86-2-2 and KH 86-2-11 dredge hauls, respectively. The latter was more convenient to control the wire-winch without hitting of the DTP-1030 on the sea bottom. Reasonable results were obtained and some examples are shown in Table 15-1. This system is still improving. Its precise specifications and operation will be reported elsewhere.

Acknowledgements

We thank Mr. A. Murakami, Kaiyodenshi K.K., for his development of the DPT-1030, and Ms. D. Van de Rijt and T. Mizutani in typewriting.

References

Furuta, T., H. Fujimoto, Y. Tomoda, K. Kobayashi and H. Murakami, 1984. A handy acoustic transponder navigation system; development and operation. J. Geod. Soc. Jap., 30, 313-322.

Table 9-7--1. Examples of record of the Dredge Pinger-Transponder (DPT-1030) at KH 86-2-11 dredge haul.

L : distance from DPT-1030 to transduser
Tp: traveling time of sound wave between DPT-1030 and sea bottom
D : distance from DPT-1030 to sea bottom; D(m)=750(m/sec) x Tp(sec)
W.O.: wire out, W.D.: water depth by PDR

			W.O.	W.D.
L=2422m	Tp=203.9msec	D=153.0m	2710m	2110m
L=2424m	Tp=193.8msec	D=145.3m	"	"
L=*****m	Tp=***.*msec	D=***.*m	"	"
L=2423m	Tp=183.3msec	D=137.5m	"	"
L=2421m	Tp=***.*msec	D=***.*m	"	"
L=2479m	Tp=155.9msec	D=117.0m	"	"
L=2423m	Tp=187.4msec	D=140.6m	"	"
L=2425m	Tp=200.4msec	D=150.3m	"	"
L=2426m	Tp=194.6msec	D=146.0m	"	"
L=2426m	Tp=201.1msec	D=150.8m	"	"
L=2427m	Tp=198.4msec	D=148.8m	"	"
L=2428m	Tp=207.1msec	D=155.3m	"	"
L=*****m	Tp=***.*msec	D=***.*m	2710m	2120m
L=2468m	Tp=218.2msec	D=163.6m	"	"
L=2424m	Tp=206.8msec	D=155.1m	"	"
L=5239m	Tp=***.*msec	D=***.*m	"	"
L=2424m	Tp=191.0msec	D=143.3m	"	"
L=2425m	Tp=198.2msec	D=148.6m	"	"
L=*****m	Tp=***.*msec	D=***.*m	"	"
L=2424m	Tp=182.1msec	D=136.6m	"	"
L=2423m	Tp=183.3msec	D=137.5m	"	"
L=2515m	Tp=179.0msec	D=134.3m	"	"
L=2422m	Tp=173.7msec	D=130.3m	"	"
L=2423m	Tp=182.8msec	D=137.1m	2710m	2120m
L=2421m	Tp=174.6msec	D=131.0m	"	"
L=*****m	Tp=***.*msec	D=***.*m	"	"
L=2422m	Tp=175.5msec	D=131.6m	"	"
L=2423m	Tp=186.4msec	D=139.8m	"	"
L=2428m	Tp=***.*msec	D=***.*m	"	"
L=2502m	Tp=***.*msec	D=***.*m	"	"
L=2426m	Tp=198.6msec	D=149.0m	"	"
L=2427m	Tp=204.1msec	D=153.1m	"	"
L=2547m	Tp=137.0msec	D=102.8m	"	"
L=2426m	Tp=140.4msec	D=105.3m	"	"
L=2420m	Tp=111.2msec	D=083.4m	"	"
L=2418m	Tp=105.2msec	D=078.9m	"	"

10. DEEP-SEA PHOTOGRAPHY IN THE CRUISE KH 86-2

M. Watanabe, S. Kuramoto and H. Tokuyama

10-1. DEEP-SEA CAMERA SYSTEM AND OPERATION

Constitution of deep-sea camera system used during this cruise was the same as in the KH 86-1 cruise, that is, two cameras, one strobo, pinger and compass (Fig.10-1-1). Four deep sea camera operations were attempted during this cruise. Table 10-1-1 shows the operation logs at each station except for KH 86-2-4. This first operation, at the Erimo Seamount, was not successful in taking photography, since delay-time-counter in an electrical timer circuit board was set in an erroneous position.

Deep-sea compass, made by Kaiyo-Denshi Co. Ltd., memorized direction of the camera unit at each shot. These data were printed out by the computer onboard the ship.

10-2. LOCATIONS OF CAMARA OPERATION

Locations of camera stations in both this and the former cruise (KH84-3) are shown in Figs. 10-2-1 and 10-2-2. Arrows in Fig. 10-2-2 show the towing direction of the system. All the stations are located near or west of the Okushiri Ridge, northeastern margin of the Sea of Japan.

10-3. SELECTED PHOTOGRAPHS WITH EXPLANATION

(1)Stn. KH 86-2-7 (phote. 10-3-1, 10-3-2)

These photographs were taken at the east-central portion of the Japan Basin. Bottom is flat as a whole and covered with thick sediments. Photographs show many foot-marks of benthic organisms. Core samples taken from this region also indicate strong benthic activities by bioturbation structures in the bottom sediments.

(2) Stn. KH 86-2-8 and KH 86-2-12

These stations are located on the same seismic survey line (KH 86-2 Line #9). A few reverse faults are clearly recognized in the seismic reflection profile (see Chapt.13 of this report). Some bottom-surface features of these faults are directly observed in the present deep-sea photographs and proved to be now active, since the surface sediments are clearly offset in such an area with fast sedimentation rates.

Stn. KH 86-2-8 (41°16.8'N, 138°31.2'E to 41°16.6'N, 138°31.6'E)

Three different kinds of sediments are observed in the photographs; basement rock with white-gray and partly white-brown color, probably siltstone, outcropping on sea bottom. Thin dark gray to black colored, bioturbated soft sediments overly the basement. In a certain place, some gravels and sands are deposited (photo. 10-3-3). In photo 10-3-4, probably a siltstone boulders and gravels with their major diameter of approximately 40-50 cm are observed. Around the gravels, coarse sand to granule gravels are deposited over the siltstone.

In photo. 10-3-5, the white colored linear tuff or siltstone, is deformed under a shear strength. The lineation seen in the upper right corner of the photo 10-3-6,is probably a part of fault or joint plane. Coarse sediments are deposited along the fracture. Grain size of the sediments decreases and bioturbation becomes greater as distance from the fracture increases. In photo. 10-3-7, a white-brown part of the basement is offset and coarse sediments are deposited along the dislocated part.

Stn. KH 86-2-8 is close to a fault scarp. Semi-consolidated basement siltstone, is dislocated and outcrops. In some places rocks are fragmented to boulder grabels and, in other places, are weathered into fine-grained sand or silt. Some fault scarps were observed to be covered by very thin soft sediments. It was very difficult to judge the sense of these fault movements from these photographs only. The present observations strongly suggest that these reverse faults interpreted in the seismic porfiles are now active.

Stn. KH 86-2-12 (41°12.7'N, 138°27.0'E to 41°12.7'N, 138°27.9'E)

This station is located SW of stn. KH 86-2-8. There are gray soft sediments thicker than at stn. KH 86-2-8. Linear feature of outcropping basement siltstone may be controlled by its bedding plane topography. In photo. 10-3-8, basement rock is displaced with a minor offset and fractured at the criff. The fragmented siltstones are deposited as insitu gravels which are distributed linearly along the displacement. In photo. 10-3-9, basement siltstone is bounded by joint planes and covered by coarse soft sediments.

Stn. KH 86-2-12 is a fault zone. The fault has minor offsets and forms small scarps. The scarp is fractured and deposited as grabels. This observation shows that these faults are now active. The overlying soft sediments, however, are thicker than at stn. KH 86-2-8, suggesting possible difference in degree of activity.

Tabel 10-1-1. Operation logs of deep sea camera.

Date	1986.4.28	1986.4.30	1986.5.10
Station No.	KH 86-2-7	KH 86-2-8	KH 86-2-12
Location	Japan Basin	Foot of the Matsumae Platau	Foot of the Matsumae Platau
Weather	Fine	Fine	Fine
Wind	270° 5m/sec	230° 3m/sec	220° 10m/sec
Sea condition	Good	Good	Good
Bottom topography	Flat	Flat & up slope	Flat & up slope
Water (start)	3700m	3650m	3700m
depth (finish)	3700m	3500m	3450m
Film & Film length	Kodak 5294(100ft)	Kodak 5294(100ft)	Kodak 5294(100ft)
Battery No.	No. 81-03	No. 86-01	No. 86-01
Lens (camera A)	1.2m	1.2m	1.2m
focussed (camera B)	1.2m	1.2m	1.2m
Iris (camera A)	11	11	11
(camera B)	11	11	11
Shot interval	6sec	6sec	6sec
Compass	Ext trigger(6sec)	Ext trigger(6sec)	Ext trigger(6sec)
Time lowed	17:12	17:02	17:03
& location	42°12.8N 137°41.0E	41°16.3N 138°30.8E	41°12.4N 138°26.7E
Shot start time	18:17	18:04	17.56
& location	42°13.2N 137°40.1E	41°16.8N 138°30.2E	41°12.7N 138°27.0E
Shot finish time	19:32	19:19	191:11
& location	42°13.3N 137°40.3E	41°16.6N 138°31.6E	41°12.7N 138°27.9E
Time surfaced	20:19	20:10	20:08
& location	42°13.2N 137°40.4E	41°16.7N 138°32.0E	41°13.1N 138°28.0E
Result	Photo 10-3-1,10-3-2	Photo 10-3-3 ~10-3-7	Photo 10-3-8,10-3-9
Remarks	Added to SUB-NAV transponder	Combine with Piston core KH 86-2-8	Combine with Heat-flow KH 86-2-12

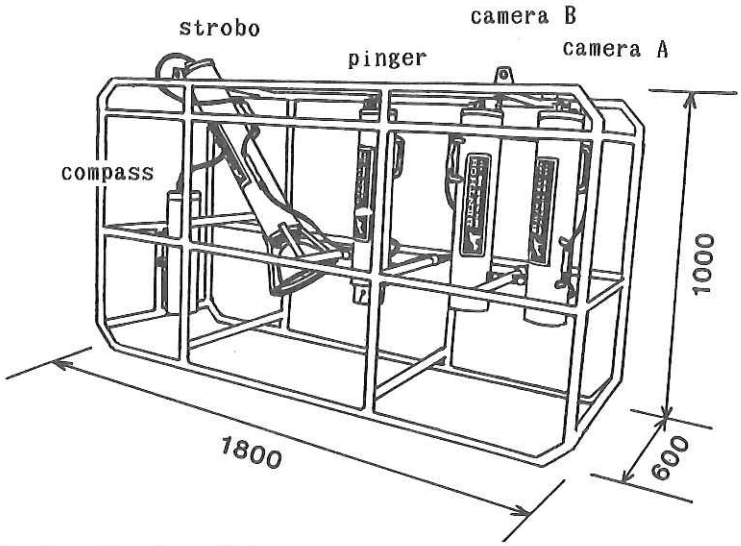

Fig. 10-1-1 Constitution of deep-sea camera system.
Camera: Benthos type 372, Strobo: Benthos type 382 flash,
Pinger: Benthos type 2216, Compass: Kaiyo-Denshi memory compass

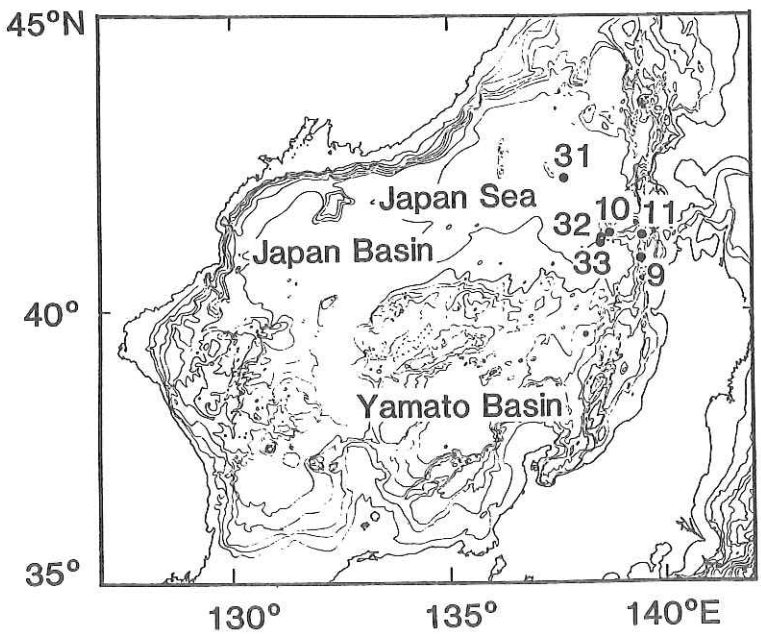

Fig. 10-2-1 Positions of camera stations (this cruise and others in the near district).
9: KH 84-3-32; Okushiri Ridge, **10**: KH 84-3-35; Matsumae Plateau
11: KH 84-3-36; Kojima Bank,
31: KH 86-2-8; Eastern Japan Basin,
32: KH 86-2-8; Southwestern flank of Matsumae Plateau,
33: KH 86-2-12; Southwestern flank of Matsumae Plateau,

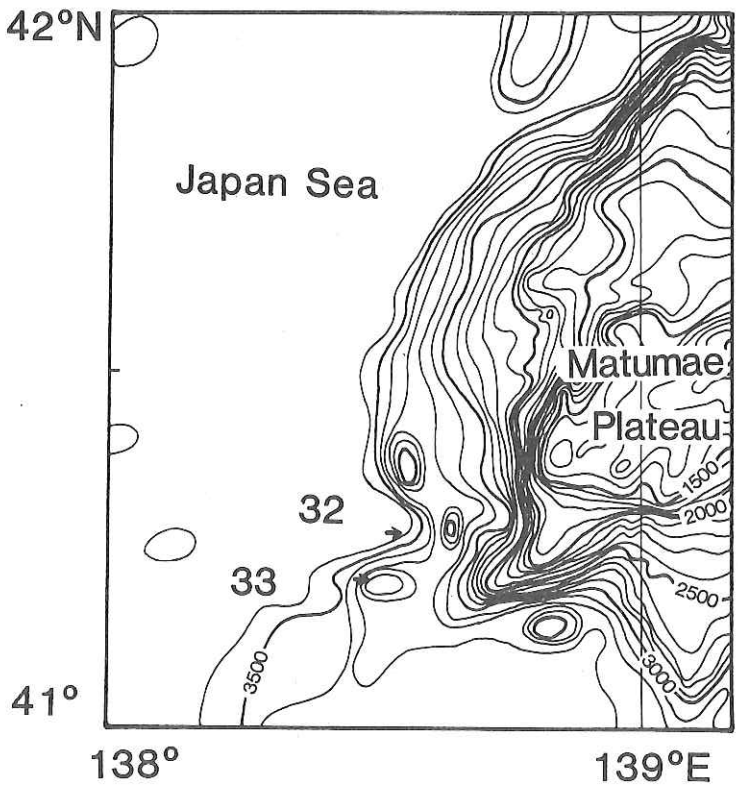

Fig. 10-2-2 Detailed locations of canmara stations KH 86-2-8 (32) and KH 86-2-12 (33) with bathymetric contours of the Matsumae Plateau. Contour interval: 100 m.

Photo. 10-3-1
KH 86-2-7
Japan Basin
Water Depth:
3,700 m
Time: $18^{h}13^{m}20^{s}$

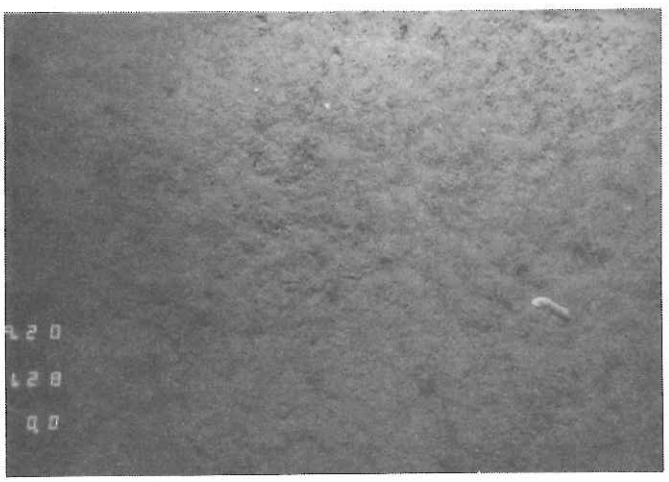

Photo. 10-3-2
KH 86-2-7
Japan Basin
Water Depth:
3,700 m
Time: $19^{h}20^{m}07^{s}$

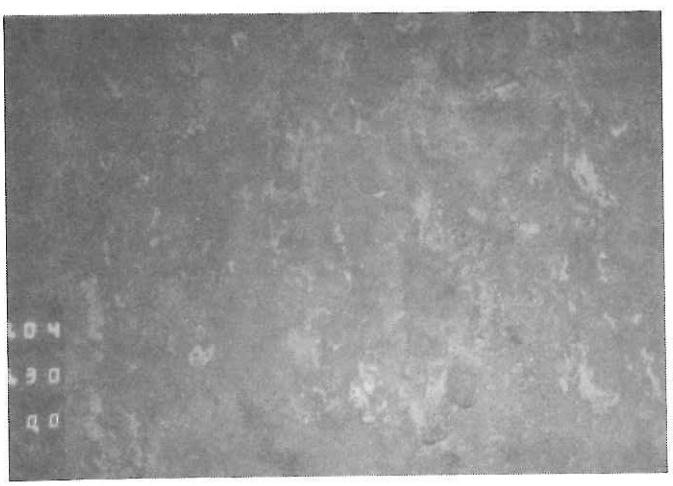

Photo. 10-3-3
KH 86-2-8
SW flank of
Matsumae Pl.
Water Depth:
3,500 m
Time: $19^{h}04^{m}56^{s}$

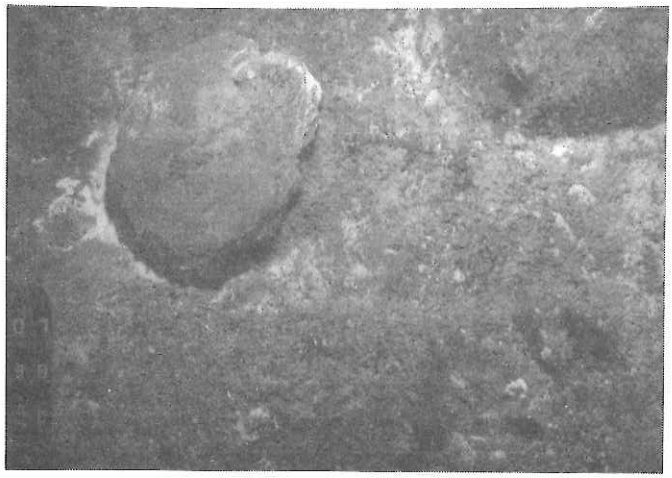

Photo. 10-3-4
KH 86-2-8
SW flank of
Matsumae Pl.
Water Depth:
3,500 m
Time:$19^{h}07^{m}32^{s}$

Photo. 10-3-5
KH 86-2-12
SW flank of
Matsumae Pl.
Water depth:
3,500 m
Time:$19^{h}08^{m}20^{s}$

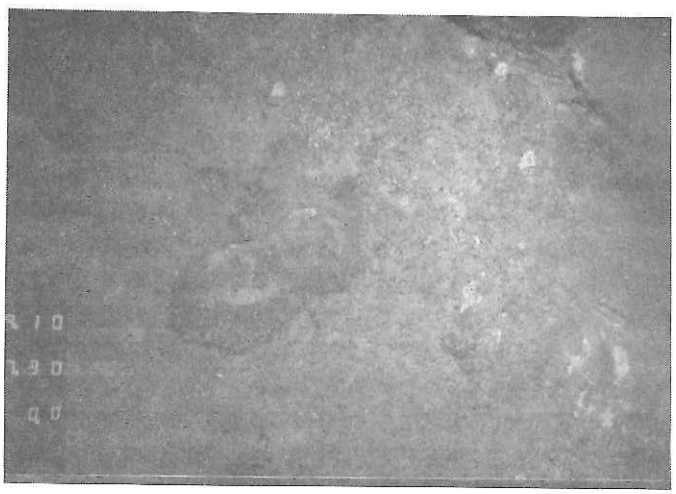

Photo. 10-3-6
KH 86-2-12
SW flank of
Matsumae Pl.
Water Depth:
3,500 m
Time:$19^{h}10^{m}37^{s}$

Photo. 10-3-7
KH 86-2-12
SW flank of
Matsumae P1.
Water Depth:
3,500 m
Time: $19^{h}16^{m}37^{s}$

Photo. 10-3-8
KH 86-2-12
SW flank of
Matsumae P1.
Water Depth:
3,500 m
Time: $18^{h}59^{m}24^{s}$

Photo. 10-3-9
KH 86-2-12
SW flank of
Matsumae P1.
Water Depth:
3,500 m
Time: $19^{h}03^{m}30^{s}$

11. SEA FLOOR ELECTROMAGNETIC MEASUREMENTS

J. Segawa, K. Koizumi, H. Toh, R. V. Iyengar
and J. L. Oubina

Instruments

We prepared 4 ocean bottom magnetometers and 1 ocean bottom electric field recorder for this cruise. Ocean bottom magnetometers include 3 fluxgate type three-component ocean bottom magnetometers(OBM's) and 1 Overhouser type ocean bottom proton magnetometer(OBP). As for the ocean bottom electric field recorder, we manufactured a string type vertical electric field sensor(OBE-Z) which is 110m long. An Aanderra current meter was also installed together with the electric field recorder. The total length of this system sums up to 270m long, and it weighs 400kg in air. The magnetometers we used here are spherical type OBM's, i.e. OBM-S1, OBM-S3 and OBM-S4 that weigh 80kg each in air and have 60cm§60cm in the maximum size, and a cylindrical type OBP that weighs 200kg in air and is 120cm in height. Each OBM's, OBP and OBE-Z are respectively equipped with a beacon, a flasher and an acoustic release system.

We can determine the conductivity structure beneath the sea floor by making use of three component magnetic fields obtained by the OBM's according to geomagnetic depth sounding method. The geomagnetic depth sounding reveals the direction of the conductor below and the relative magnitude of its conductivity. In addition, since OBP was installed simultaneously with the installation of OBM, calibration of OBM data can be made by using OBP data. Moreover, as a detailed survey of magnetic lineation by use of a towed proton magnetometer was made on the second leg of this cruise, the OBP data can be used to carry out the epoch reduction of magnetic total force.

The OBE-Z was also an equipment that was installed for the first time. It was used to know the electromagnetic induction of ocean current. That is, the purpose of OBE-Z is to estimate the influence of the dynamical velocity field in the ocean upon OBM's. Of course the effect of oceanic motion cannot be estimated by simple comparison of OBE-Z and OBM data. We take the correlation between OBE-Z and Aanderra current meter and between Aanderra and OBM-S4 all of which were installed at almost the same site(See the map of installation points). We think that we can get the first data which contain electromagnetic field and dynamical velocity field in the ocean simultaneously.

Installation and Recovery

As for the detailed information of both installation and recovery, refer to the map of installation points (Fig. 11-1) and the observation logtable (Table 11-1). Installation and recovery were carried out sequentially in the order of JK1 through JK5, respectively.

Thanks to the calm weather, the actual operation of both installation and retrieval resulted in a success although there occurred a little trouble with the connector between the acoustic controller and the hydrophone just before the retrieval. It took about twelve hours to recover all of five instruments and during the retrieval all the flashers and beacons worked correctly. With regard to the direction finder, it was proved that careful adjustment of the receiving antenna was very important. At both installation and recovery we stayed on the spot and followed the motion of each instrument acoustically until we were able to assure its arrival at and departure from the sea floor. Downward and upward velocities of each instrument were as follows:

Site	Instrument	downwards(cm/sec.)	Upwards(cm/sec.)
JK1	OBE-Z	109	227
JK2	OBP	48	116
JK3	OBM-S4	53	71
JK4	OBM-S1	60	61
JK5	OBM-S3	60	49

Table of upward and downward velocities of each instrument

As to the OBM's there was no damage except the slightly wounded glasspherre of OBM-S1. Unfortunately, the period was only one week during which we could make measurement, but the data read on board were quite satisfactory. A fatal cable break, however, was found at the float end sensor of OBE-Z. Since data reading couldn't be made on the ship, we could not find out when the cable break had happened. But we suspect that it was caused by the extremely strong tension between the Kevler cable and the sensor at the beginning of sinkage. Fortunately, rest of the OBE-Z system including Aanderra current meter had been working correctly until recovery.

OBP retrieval was also successful. But the true data was not obtained as found by the test at the Kakioka geomagnetic observatory. It was realized that the Overhauser type proton magnetometer needed much more improvement.

Table 11-1. List of mooring stations of Ocean Bottom Magnetometer system in the cruise KH 86-2.

Equipment	Site	Position	Depth (m)	Code	Beacon (MHz)	Flasher	Installation Date
OBE-Z & Aanderra	JK 1	Hybrid 40° 59′ .7 N 138° 25′ .1 E	3400	3D	Taiyo 43.528	Taiyo Installed	1986 29th/April 14:20
OBP	JK 2	40° 59′ .7 N 138° 25′ .9 E	3400	3B	Taiyo 43.528	Taiyo Installed	29th/April 15:43
OBM-S4	JK 3	41° 00′ .2 N 138° 25′ .1 E	3380	3G	Taiyo 43.528	OAR Installed	6th/May 19:14
OBM-S1	JK 4	40° 49′ .0 N 138° 08′ .0 E	3610	3C	OAR 26.995	Taiyo Installed	7th/May 14:44
OBM-S3	JK 5	40° 39′ .2 N 137° 44′ .5 E	3320	3A	OAR 27.045	Taiyo Installed	7th/May 18:18

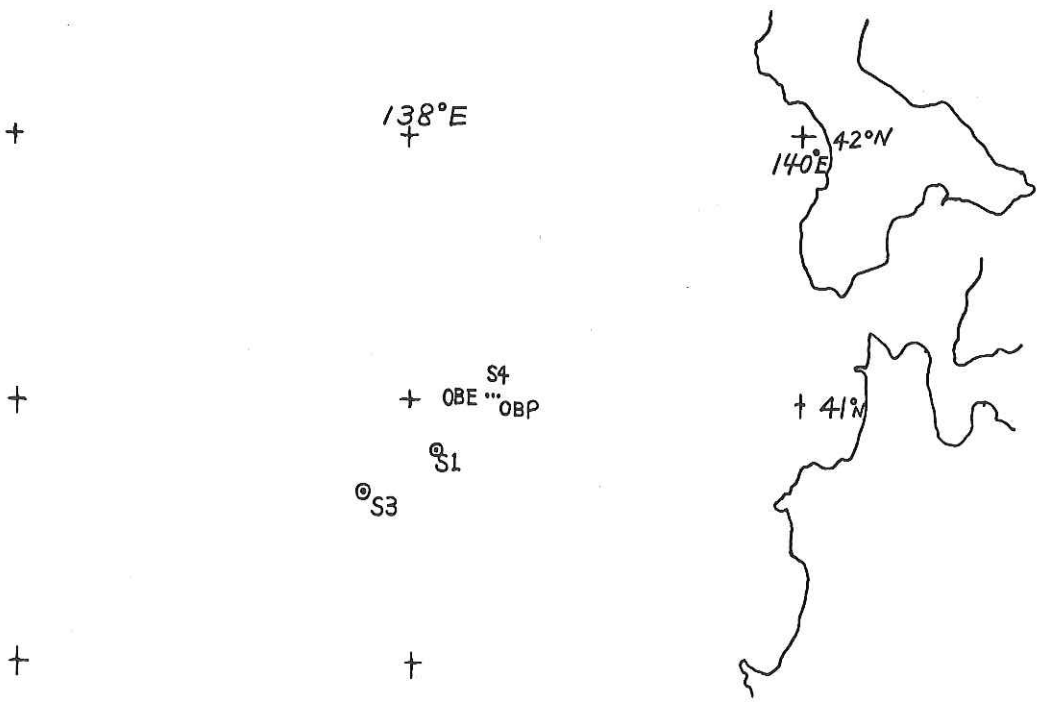

Fig. 11-1. Positions of OBM (S1,S3,S4), OBE and OBP moored in the Sea of Japan during the cruise KH 86-2.

12. 3.5 KHZ SUBBOTTOM PROFILING SURVEY

S. Kuramoto, H. Tokuyama, T. Asanuma and M. Suemasu

3.5 kHz subbottom profiling survey was carried out simultaneously with the seismic reflection survey. The purpose of this survey is for the precise understanding of the sedimentary features of the uppermost sediments.

The used survey system is composed of 3.5 kHz transducers, PRT 105B transceiver, CESP II correlation echo sounder processor and UGR recorder by Raytheon Co., Ltd.. The system was controlled by the program of the UGR recorder.

The obtained records have high qualities and are shown in Figs. 12-1, 2, 3 and 4. The vertical exaggeration of these profiles are not same as the single and multichannel reflection profiles, but about 50 at 10 knots ship speed. These 3/5 kHz records show detailed sedimentary sequences of uppermost parts, about 0.1 sec (two-way travel time) thick, which are not obviously recognized by the single and multichannel profiles because of the low frequency.

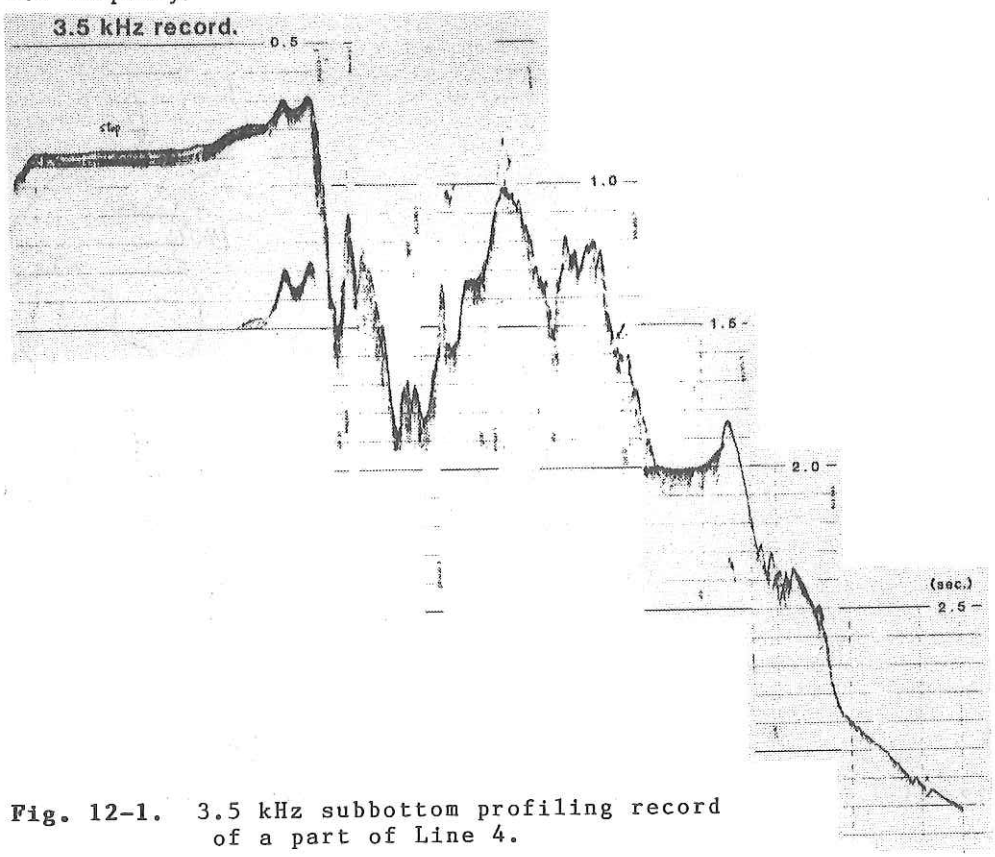

Fig. 12-1. 3.5 kHz subbottom profiling record of a part of Line 4.

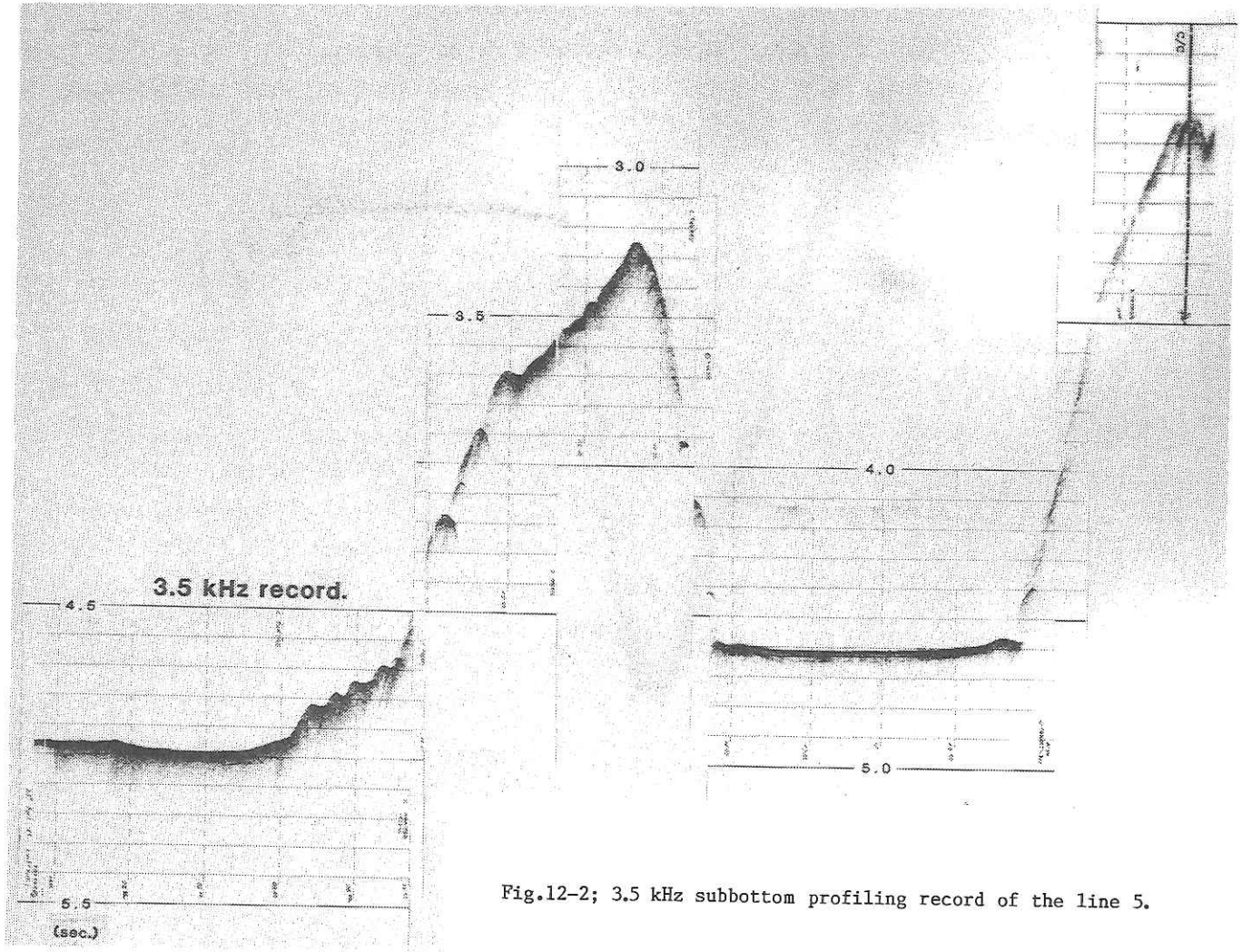

Fig.12-2; 3.5 kHz subbottom profiling record of the line 5.

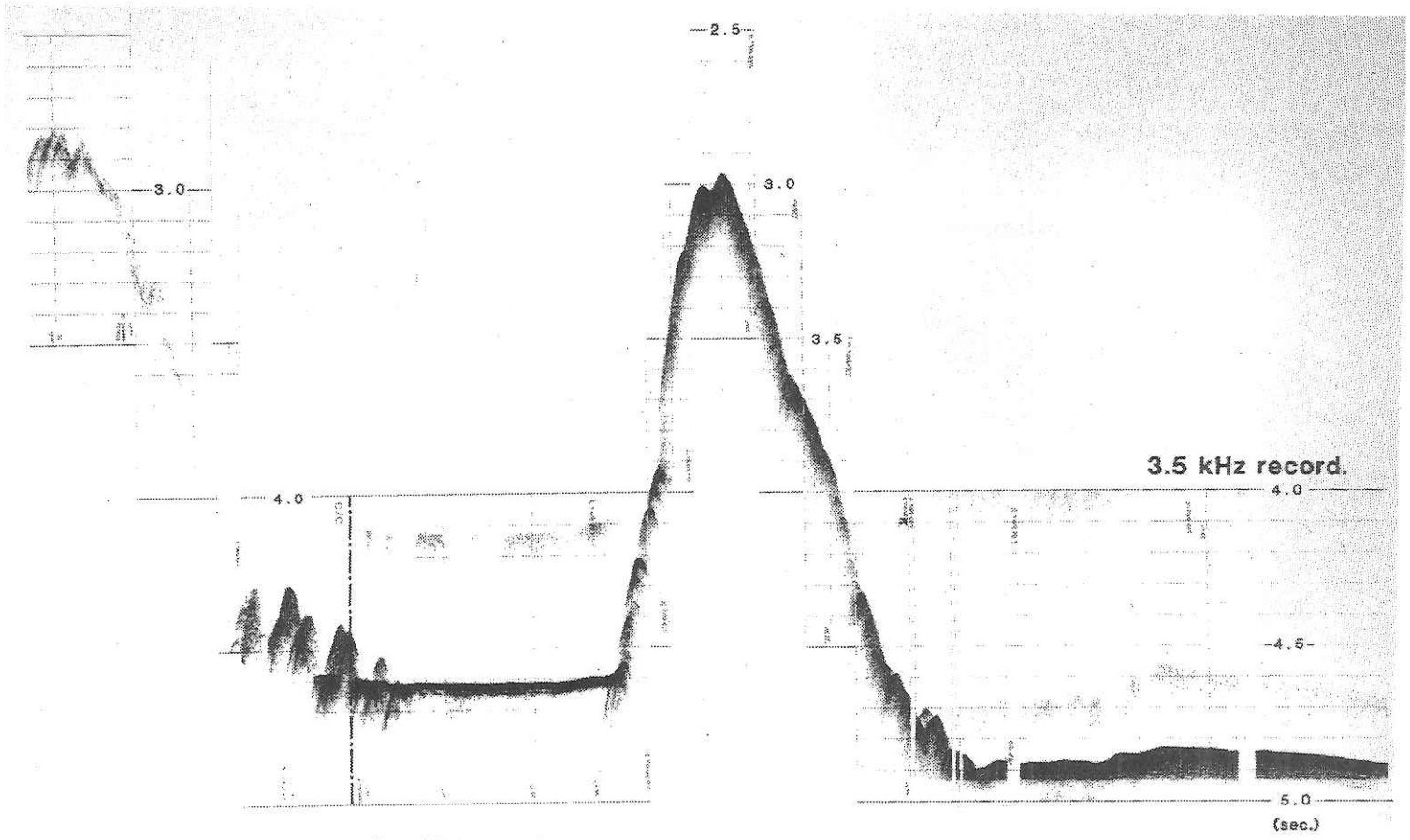

Fig.12-3; 3.5 kHz subbottom profiling record of the line 6.

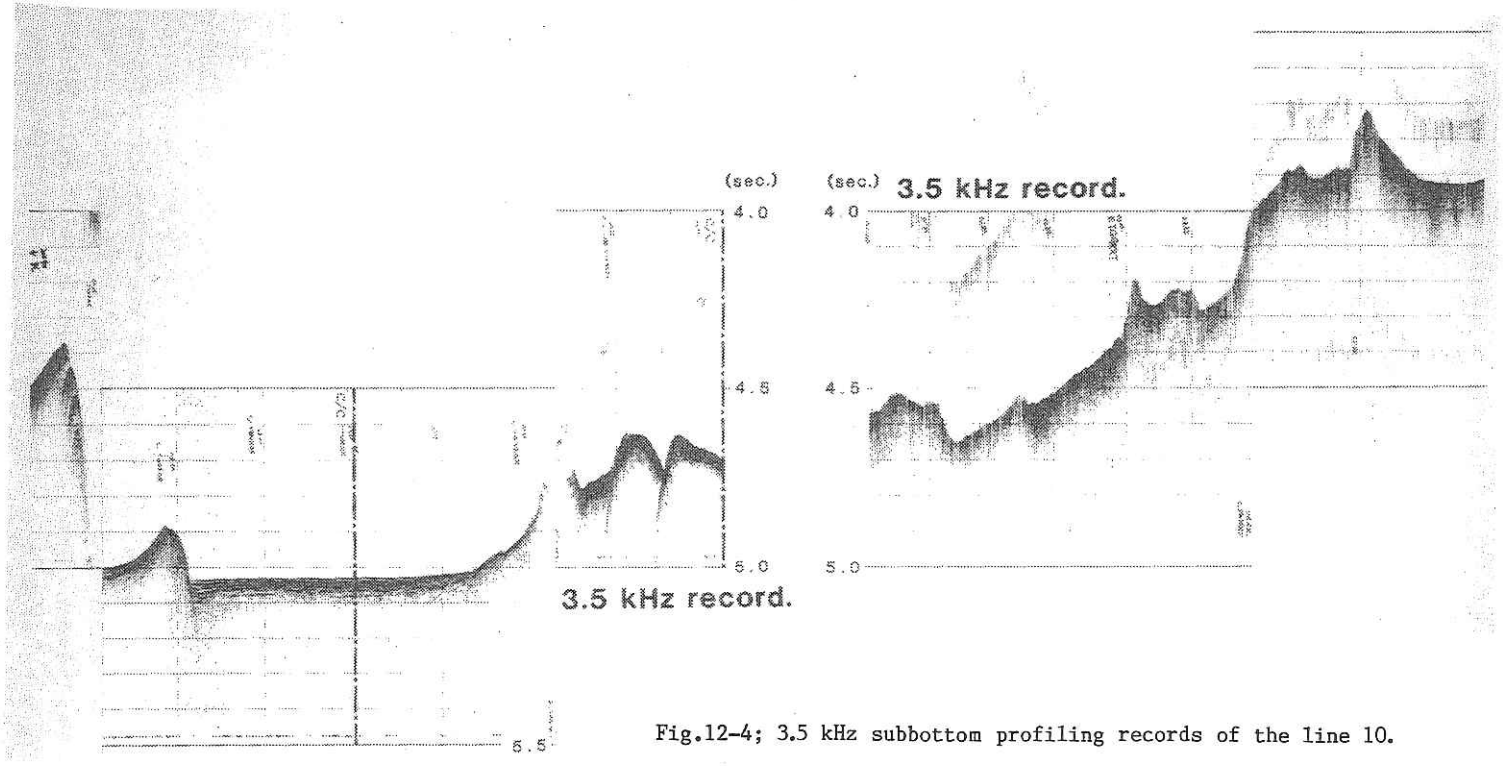

Fig.12-4; 3.5 kHz subbottom profiling records of the line 10.

13. MULTICHANNEL AND SINGLE-CHANNEL SEISMIC REFLECTION SURVEY

S. Kuramoto, H. Tokuyama, T. Asanuma and M. Suemasu

Introduction

Continuous seismic reflection surveys were carried out in the cruise KH 86-2 at two different tectonic settings; forearc slope and back-arc basin, which are located west and southeast off Hokkaido, respectively. These surveys were using not only single-channel seismic reflection but also multichannel recorders. Five each single-channel and multichannel profiles were obtained with good qualities visualizing interesting profiles of arc-trench system and Japan Basin structures. Ship's tracks for thesesurveys are shown in Fig. 13-1.

The lines 1, 2 and 3 are multichannel recording tracks situated in the forearc slope near the arc-arc junction of the Kuril and NE Japan arcs. Lines 4, 5 and 6 are running across as a morphological boundary between the Japan basin and Okushiri Ridge. Line 4 is a single-channel record and the other two are multichannel profiles. Lines 7,8,9 and 10 are single-channel profiles in the Japan basin. Precise locations of the surveyed lines and shot points are represented in Table 1.

Single-channel reflection surveys were carried out with a conventional streamer system composed of a single-channel hydrophone array, a lead-in cable and other accessory cables, with a ship speed of approximately 10 knots. A 1900C type air gun which produced by BOLT Co., Ltd. was used as a sound source. Multichannel survey system, on the other hand,is composed of a 600 meters long 12-channel streamer cable, an NE-128 digital recording system made by NEC Ltd. and a 1500C type air gun of BOLT Co., Ltd., with a ship speed of approximately 5 knots. All onboard monitor records are shown in Figs.13-2, 3, 5, 8, 9, 10 and 11. We will attempt to briefly describe and interpret these profiles in the following sections.

Lines 1, 2 and 3 (multichannel)

Lines 1, 2 and 3 (Fig. 2) are running across the forearc slope southeast off Hokkaido near the arc-arc junction of the Kuril and NE Japan arcs. This junction is supposed to be a collision zone where the Kuril forearc sliver is migrated southwestward and collides to the NE Japan arc with the oblique subduction of the Pacific plate along the Kuril trench axis (Kimura, 1986). This tectonic feature is an ongoing phenomenon supported by geological evidences (Kimura,1981;1986) and geodetic observations (Tada and Kimura,1987). One of the main objectives of the present survey was to reveal any evidence

of active collision features in this area.

The line 1 running from the Kuril trench to the forearc slope through the structural high (Fig.13-2). Many reverse faults that are inclined landward are visible in the line. The Kuril Trench is filled with thick sediments overlying the acoustic basement. Thickness of the sediments is about 0.4 sec (two-way travel time). The oceanward cliff of the structural high, about 2900m high, is composed of some thrust sheets, diping landward. In the forearc basin, some sediments are deposited horizontally. Upper slope is covered by 0.1 to 0.2 sec thick sediments parallel to the surface topography. The line 2 (Fig.13-2)are similar to the lines 1 and 3. Thick sediments, more than 1.0 sec thick, are observed in the center of profile. They consist of southwestward dipping and horizontally deposited sediments in ascending order. Moreover, there exist some vertically dipping faults. The top sediment on southwestern cliff is thinning northeastward,toward the forearc basin.

Line 3 running from the Kuril Trench to the NE Japan forearc slope is generally parallel to the kuril Trench axis. The bottom topography is roughly uneven with folding structures. Each block, either synclined or anticlined, is bounded with reverse faults that are active now. This is evidenced by the uppermost sediments rotated vertically and inclined.

Lines 4,5 and 6 (single- and multichannel)

Line 4 (Fig. 13-3) is a single-channel profile across the Okushiri Ridge trending north to south. The line is south-southeast to north-northwest through the shelf off Okushiri Island and ends at the Japan Basin. Water depth gradually increases toward the Okushiri Ridge from a zone west of the Tsugaru Straight in which thick sediments are accumulated. The acoustic basement is only traceable in the Japan basin that has some undulations.

Lines 5 and 6 (Fig.13-5) are running west to east in parallel with the 42°50' and 43°00' latitude lines across the Okushiri Ridge which separates the Japan Basin from the Shiribeshi Trough. The Japan Basin and Shiribeshi Troughhaveflat topography in this profile.The Okushiri Ridge isinclined westward, and has an irregular morphology at the western foot of the Ridge. The acoustic basement of the ridge is inclined in parallel to the bottom surface and can be traced to the Japan Basin. In the Shiribeshi Trough, it is seen that sediments near the Okushiri Ridge are deformed slightly with folding. These phenomena bring us to an idea that the boundary between the Shiribeshi Trough and Okushiri Ridge is composed of a Low angle reverse fault (thrust) dipping toward the west, which is probably active now. Line 6 runs east to west parallel to line 5. Its profile suggests the same fea-

tures as the line 5 except for an evidence that the angle of the inclined ridge is steeper.

Lines 7, 8, 9 and 10 (single-channel)

Lines 7, 8, 9 and 10 are all located in the Japan Basin. Topography of the Japan Basin is very flat, with water depth of about 3650m. Acoustic basement is distinctly traced, although surface of the basement has rugged topography in some places.

InLine 7 (Fig. 13-8) the basement depth is about 7.0 sec below the sea level. Thickness of the sediments, very stratified above the acoustic basement, is about 2.0 sec. These sediments are acousti-cally divided into two layers, upper opaque and lower transparent layers. The uppermost sediments are deposited very flatly, whereas the lower part in the upper opaque layer are weakly undulated.

Line8 (Fig. 13-9) has nearly the same features as Line 7. Toward the southeast end of the line, the acoustic basement gradually becomes shallower accompanied with thinning of overlying sediments. The line 9 (Fig. 13-10) is composed of 4 parallel lines trending northwest to southeast. On all the lines, the acoustic stratigraphy is divided into 5 layers; 2 opaque and 2 transparent layers and basement. They are acoustically very continuous and clearly traced. There are two en echelon type reverse faults (probably with strike-slip sense) in this area. The acoustic basement and overlying sediments are obviously cut and deformed with folding by these faults with an NE-SW trend. Offset by these faults have a variable range. The basement may outcrop at each fault scarp.
The fault must have beenactive when the overlying sediments were deposited.

Line 10 (Fig. 13-11) runs from the Japan Basin to Yamato Basin. In the northeastern portionof this line, the profile is nearly the same asLine 9 whereas in the southwest where the profile exists in the Yamato Basin, the acoustic basement becomes gradually shallower in harmony with the overling sediments. It can not be solved by these results whether or not the basement in the two basins is the same in structure and composition.

References

Kimura, G., 1981. Tectonic evolution and stress field in the southwestern margin of the Kuril Arc. J. Geol. Soc. Japan, 87, 757-768.

Kimura, G., 1986. Oblique subduction and collision. Geology, 14, 404-407.

Tada, T. and Kimura, G., 1987. Collision tectonics and crustal deformation at the southwestern margin of the Kuril arc. J. Seis. Soc. Japan, 40, 197-204.

Table 13-1. List of precise location and water depth of each shot point and survey line.

Line 1 (Apr. 24-25, 1986)

Shot #	Time	Latitude	Longitude	Water Depth
6	16:39	41°09.0' N	145°02.8' E	
100	17:09	10.7	144°53.6'	7080 m
200	17:42	12.5	50.4	7050
300	18:14	14.3	47.1	7000
2	18:41	15.5	44.9	6400
100	19:11	17.0	42.5	5100
200	19:44	18.5	39.0	4100
1	20:15	19.8	35.8	
100	20:47	20.9	32.6	4270
200	21:20	22.1	29.4	4800
300	21:52	23.1	26.4	3740
1	22:34	24.6	22.1	3480
100	23:07	26.0	18.8	2850
200	23:40	27.4	15.7	2890
300	00:12	29.2	12.3	2760
400	00:45	30.7	09.7	2150
1	00:47	30.9	09.6	
100	01:22	32.5	06.5	1600
C/C	01:30	32.9	05.8	1610

Line 2 (Apr. 25, 1986)

Shot #	Time	Latitude	Longitude	Water Depth
	02:00	41°34.3' N	144°07.9' E	1930 m
100	02:45	36.0	12.0	2630
200	03:18	37.4	15.1	2800
300	03:51	39.0	18.2	2760
400	03:23	40.6	21.1	2540
100	05:05	42.6	25.1	2270
200	05:38	44.1	28.1	2290
300	06:10	45.4	31.3	2460
363	06:31	46.1	33.1	2480
C/C	06:33			

Line 3 (Apr. 25, 1986)

Shot #	Time	Latitude	Longitude	Water Depth

1	06:52			
100	07:25	41°44.1' N	144°30.3' E	2580 m
200	07:57	41.9	28.5	2590
300	08:30	39.8	26.5	2760
400	09:03	37.4	24.6	3000
1	09:14	36.7	24.1	3000
100	09:47	34.3	22.5	2870
200	10:19	32.1	20.7	3100
300	10:52	29.7	18.8	2700
400	11:24	27.4	16.7	2770
1	11:36	26.7	16.1	2900
100	12:09	24.2	13.7	3420
200	12:41	21.9	11.7	3400
300	13:14	19.6	09.5	3330
400	13:46	17.3	07.2	3190
1	13:58	16.2	06.4	
100	14:29	14.1	04.4	3160
200	15:01	11.9	02.1	3100

Line 4 (Apr. 26, 1986)

Shot #	Time	Latitude	Longitude	Water Depth
1	12:51	41°09.0' N	139°53.4' E	530 m
57	13:00	10.3	52.4	900
237	13:30	14.6	48.9	1200
417	14:00	18.7	44.9	870
597	14:30	23.1	41.4	920
777	15:00	27.6	38.0	1140
957	15:30	31.5	34.0	1420
1137	16:00	35.8	30.3	1700
46	16:30	40.0	27.1	2100
226	17:00	44.6	23.4	2270
406	17:30	49.1	20.0	2400
586	18:00	53.4	16.4	2570
766	18:30	58.1	13.7	2500
946	19:00	42°03.3	12.1	2940
1126	19:30	08.4	10.4	3680
1	20:00	13.5	09.1	3700
177	20:30	18.7	08.2	4550

357	21:00	23.8	07.2	3200
537	21:30	28.8	06.0	3380
717	22:00	33.8	04.5	3500
897	22:30	38.8	03.1	3690
1077	23:00	43.8	01.7	3690
	23:30	48.8	00.2	3660
1280	23:34	49.4	00.5	3650

Line 5 (Apr. 27, 1986)

Shot #	Time	Latitude	Longitude	Water Depth
1	01:47	42°50.0' N	138°56.3' E	3650 m
100	02:19	50.0	139°00.1'	3640
200	02:52	50.1	03.9	3660
300	03:24	49.9	07.2	3640
400	03:57	50.2	10.9	3480
1	04:07	50.3	12.0	3450
100	04:39	50.3	15.5	2980
200	05:12	50.3	18.9	2650
300	05:44	50.3	22.6	2410
400	06:17	50.3	26.2	3050
100	06:59	50.2	30.8	3380
200	07:31	50.2	34.2	3380
300	08:04	50.6	37.5	3370
400	08:36	50.9	40.7	3050
415	08:42	50.9	41.2	2930
1	08:50	51.0	42.1	2670
100	09:22	51.0	45.3	2080
C/C	09:25	51.0	45.8	2050

Line 6 (Apr. 27, 1986)

Shot #	Time	Latitude	Longitude	Water Depth
200	09:55	42°53.4' N	139°44.9' E	2200 m
300	10:27	56.0	43.2	2770
400	11:00	58.6	41.5	3150
C/C	11:09			
1	11:13	59.6	40.9	3370
100	11:46	43°00.4'	37.3	3375
200	12.18	00.7	32.9	3380

300	12:51	01.0	28.6	3380
400	13:23	00.9	24.4	2870
100	14:06	00.8	19.0	2450
200	14:38	00.7	14.8	3140
300	15:11	00.5	10.7	3470
400	15:43	00.5	06.6	3580
100	16:27	00.5	01.1	3570

Line 7 (Apr. 27-28, 1986)

Shot #	Time	Latitude	Longitude	Water Depth
1	18:04	42°59.6' N	138°52.0' E	3590 m
155	18:30	57.6	47.1	3550
335	19:00	55.1	41.1	3630
515	19:30	52.2	35.7	3640
695	20:00	49.2	30.7	3650
875	20:30	47.5	24.4	3650
1055	21:00	45.2	18.2	3650
1235	21:30	42.9	11.9	3680
1282	21:38	42.3	10.3	3690
1	21:43	41.9	09.2	3690
103	22:00	40.5	05.8	3690
283	22:30	38.1	137°59.9'	3700
462	23:00	35.8	54.1	3700
643	23:30	33.6	48.0	3700
823	00:00	31.3	42.3	3700
	00:30	29.1	36.2	3680
	01:00	26.9	30.1	3690
56	01:30	24.7	23.9	3690
228	02:00	22.6	17.8	3690
408	02:30	20.6	11.9	3690
588	03:00	18.5	06.1	3680
768	03:30	16.3	00.3	3680
C/C	03:40	15.6	136°58.3'	
872	03:47	16.3	57.5	3680
948	04:00	18.2	58.8	3680
1127	04:30	22.6	137°01.8'	3680
1	05:00	26.5	05.1	3670
175	05:30	31.5	07.5	3670

355	06:00	35.2	12.2	3680
535	06:30	39.5	15.6	3680
C/C	06:50	42.5	17.5	
691	06:56	42.6	18.7	
895	07:30	38.0	21.6	3690
1075	08:00	33.5	24.4	3690
1255	08:30	29.1	27.4	3690
1284	08:35	28.3	27.8	3690
1	08:43	27.2	28.6	3680
102	09:00	24.7	30.2	3690
282	09:30	20.5	33.2	3700
462	10:00	16.2	36.0	3690
523	10:10	14.9	37.0	3690

Line 8 (Apr. 28-29, 1986)

Shot #	Time	Latitude	Longitude	Water Depth
81	23:38	42°15.9' N	137°40.5' E	3690 m
212	00:00	18.4	37.9	3690
357	00:24	22.4	37.8	
393	00:30	23.2	37.1	3690
573	01:00	27.7	33.8	3690
753	01:30	32.4	30.9	3690
90	02:00	36.8	28.0	3690
C/C	02:28	40.9	25.0	3690
288	02:33	41.0	24.2	3690
450	03:00	38.9	19.2	3690
C/C	03:18	37.3	15.6	3690
582	03:22	36.8	15.2	3690
630	03:30	35.5	16.2	3690
810	04:00	30.9	19.9	3690
990	04:30	26.4	23.5	3690
1170	05:00	21.5	27.4	3690
42	05:30	17.2	30.2	3690
222	06:00	12.2	34.0	3690
402	06:30	07.6	37.5	3690
582	07:00	02.9	41.0	3690
762	07:30	41°58.0'	44.8	3690
942	08:00	53.5	48.2	3690

1122	08:30	48.7	51.6	3690
	09:00	43.8	54.8	3690
170	09:30	40.1	57.1	3690
350	10:00	35.4	138°00.1'	3690
1	10:10	33.9	01.2	
120	10:30	30.8	03.4	3690
300	11:00	26.1	06.5	3700
480	11:30	21.3	09.7	3700
661	12:00	16.7	12.9	3690
843	12:30	12.3	16.3	3690
1020	13:00	07.6	19.7	3540
1200	13:30	02.8	22.7	3370
1260	13:40	01.3	23.6	3375

Line 9 (Apr. 29-30, 1986)

Shot #	Time	Latitude	Longitude	Water Depth
1	18:10	41°00.8' N	138°28.3' E	3420 m
119	18:30	01.6	32.6	3420
C/C	18:40	02.0	34.7	3420
209	18:45	02.6	35.0	3420
299	19:00	05.0	33.2	3410
478	19:30	09.6	29.5	3310
658	20:00	14.2	25.7	3660
838	20:30	18.8	22.3	3700
1018	21:00	23.5	19.2	3700
C/C	21:30	28.8	16.4	3700
1289	21:45	29.7	18.7	3700
1	21:50	30.2	20.1	3700
C/C	21:51			
60	22:00	29.4	21.3	3700
240	22:30	25.2	24.6	3705
420	23:00	20.9	27.7	3700
600	23:30	16.6	30.4	3600
780	00:00	12.1	33.4	3330
960	00:30	07.6	36.5	3410
C/C	01:00	03.0	39.5	3420
1169	01:04	02.7	40.5	
C/C	01:26	04.3	44.9	3410

5	01:30	04.9	45.1	3410
185	02:00	09.1	41.6	3410
365	02:30	13.4	38.4	3380
545	03:00	17.8	35.3	3230
725	03:30	22.3	32.4	3700
C/C	04:00	26.6	29.6	3700
929	04:04	26.8	28.9	3700
1085	04:30	24.4	23.8	3700
1265	05:00	21.6	18.1	3700
C/C	05:08	20.9	16.4	3700
27	05:12	20.4	15.9	3700
135	05:30	17.9	17.8	3700
315	06:00	13.0	21.4	3610
495	06:30	08.1	24.2	3570
675	07:00	03.8	27.2	3390
855	07:30	00.2	30.6	3430
901	07:37	40°58.4'	31.4	3440

Line 10 (Apr. 30 - May 01, 1986)

Shot #	Time	Latitude	Longitude	Water Depth
1	20:28	41°15.5' N	138°33.0' E	3240 m
C/C	20:35			
72	20:40	14.1	32.5	3300
192	21:00	14.1	29.3	3650
372	21:30	14.3	22.5	3610
552	22:00	14.3	16.0	3690
732	22:30	14.1	09.2	3690
912	23:00	09.3	11.4	3680
1092	23:30	04.4	14.7	3580
1272	00:00	40°59.9'	17.9	3400
146	00:30	55.3	21.2	3430
C/C	00:36	54.4	21.8	3450
	00:38	54.0	22.0	3460
327	01:00	50.2	21.4	3350
506	01:30	45.1	20.9	3330
686	02:00	39.9	19.9	3370
866	02:30	34.7	18.7	3310
1046	03:00	29.5	17.5	3150

1226	03:30	24.1	16.7	3090
99	04:00	18.8	15.9	2920
249	04:25	14.5	15.2	2840
279	04:30	13.7	15.1	2840
459	05:00	08.6	14.4	2740
538	05:13	06.3	13.9	2800

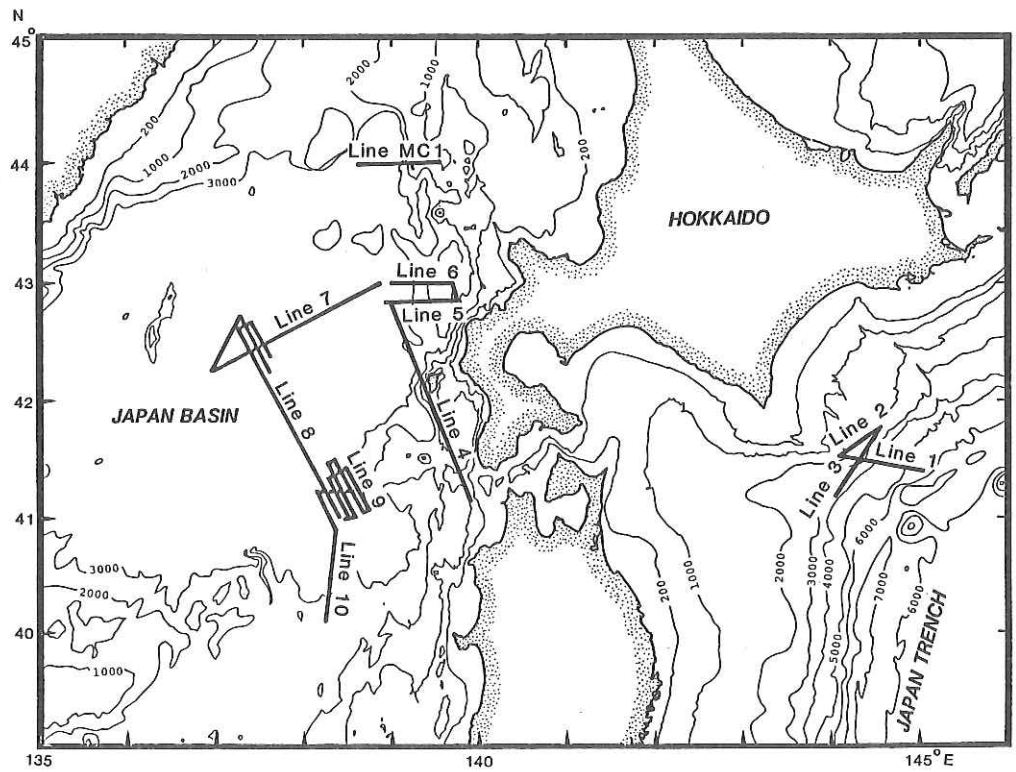

Fig. 13-1. Survey lines of seismic reflection in the KH-86-2 cruise except with Line MC1, the multichannel survey line of KT-87-6 cruise.

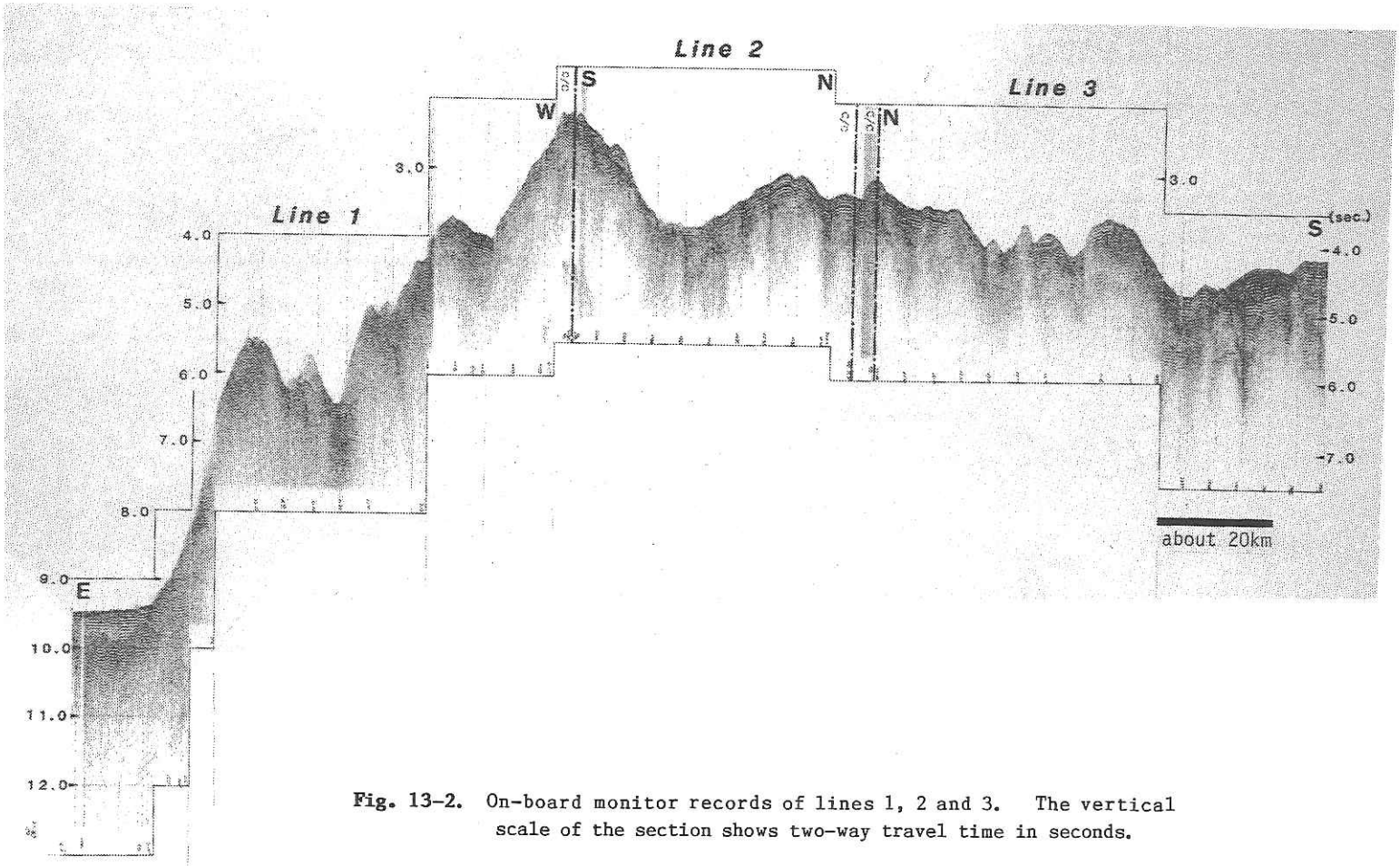

Fig. 13-2. On-board monitor records of lines 1, 2 and 3. The vertical scale of the section shows two-way travel time in seconds.

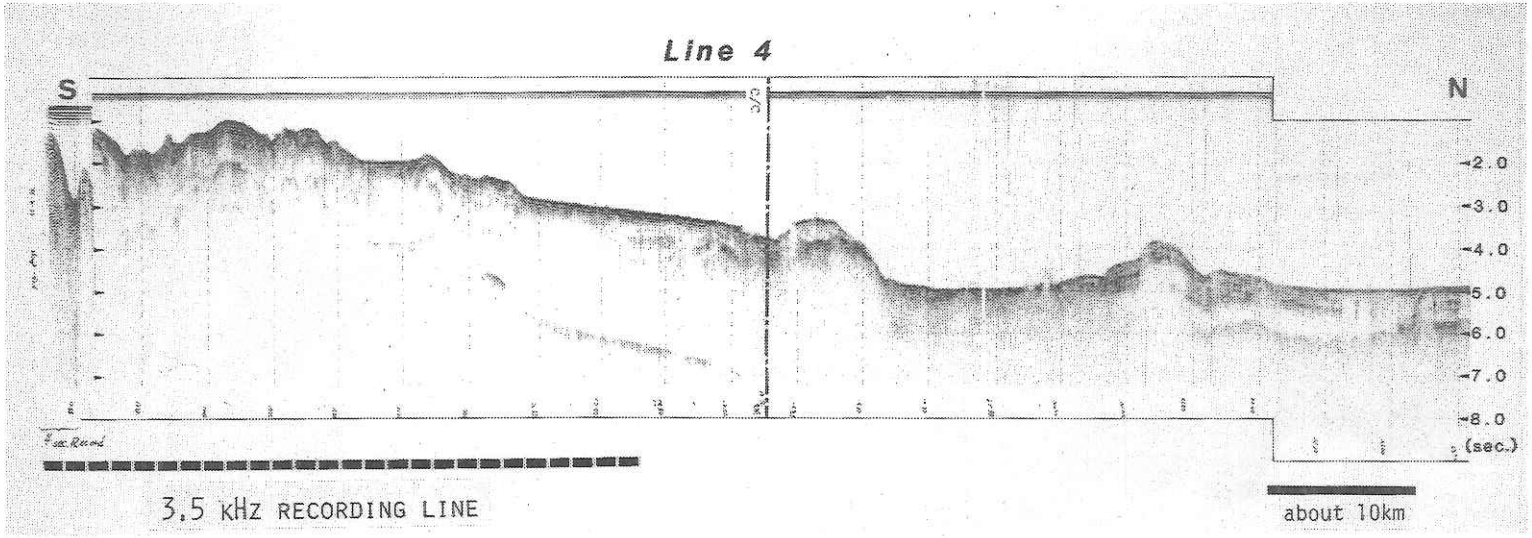

Fig. 13-3. On-board monitor record of line 4. Broken line indicates the 3.5 kHz recording line.

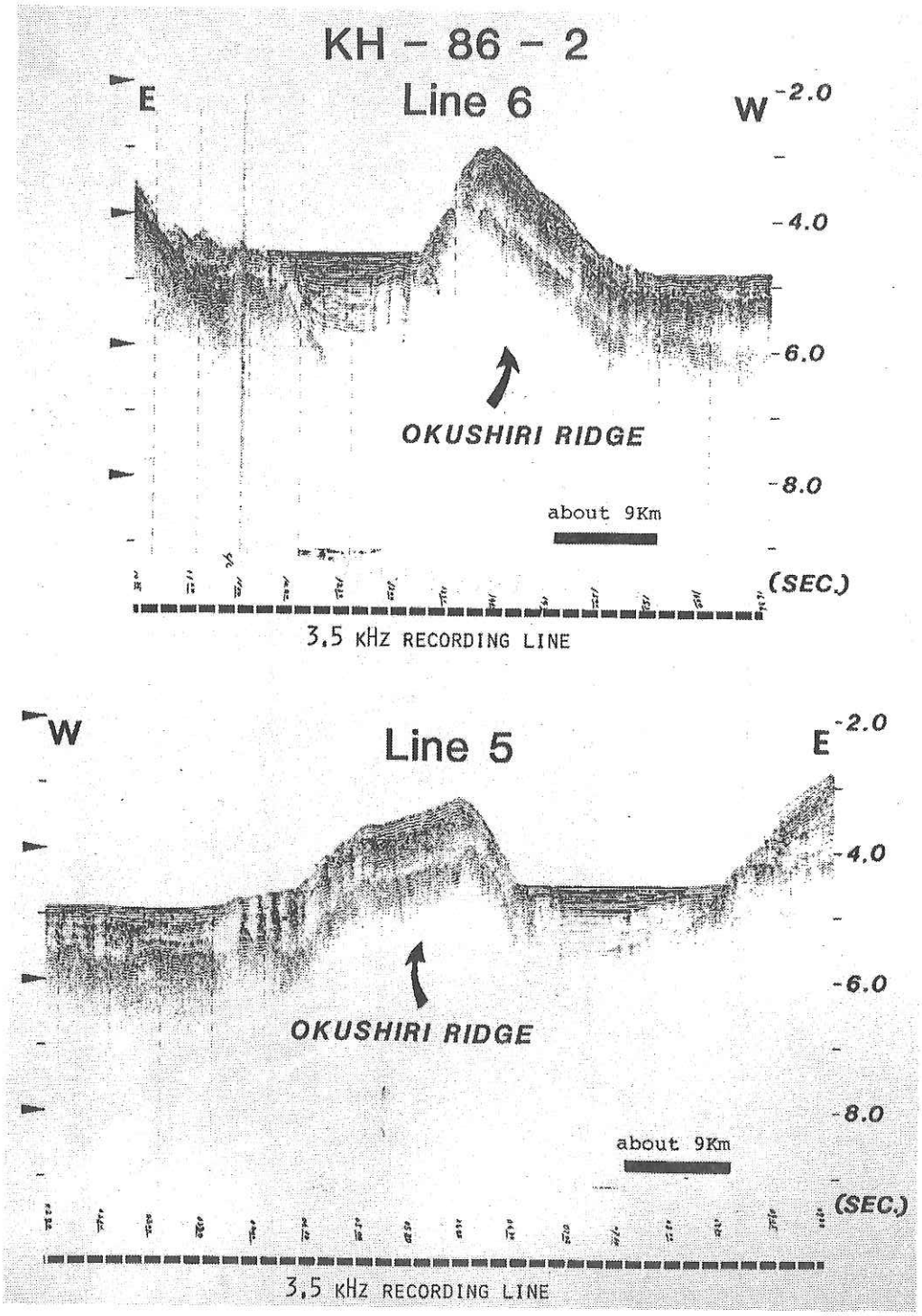

Fig. 13-4. On-board monitor records of lines 5 and 6. Broken lines show the 3.5 kHz recording lines.

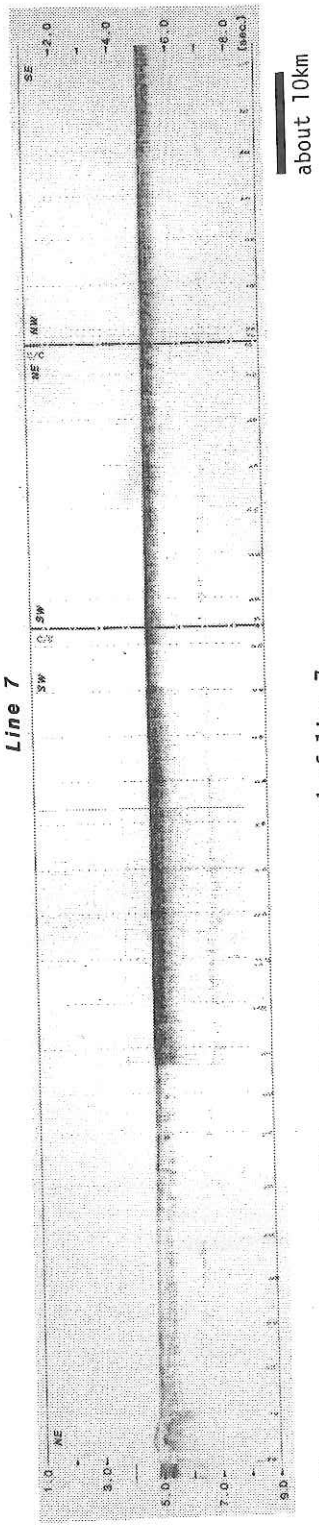

Fig. 13-5. On-board monitor record of line 7.

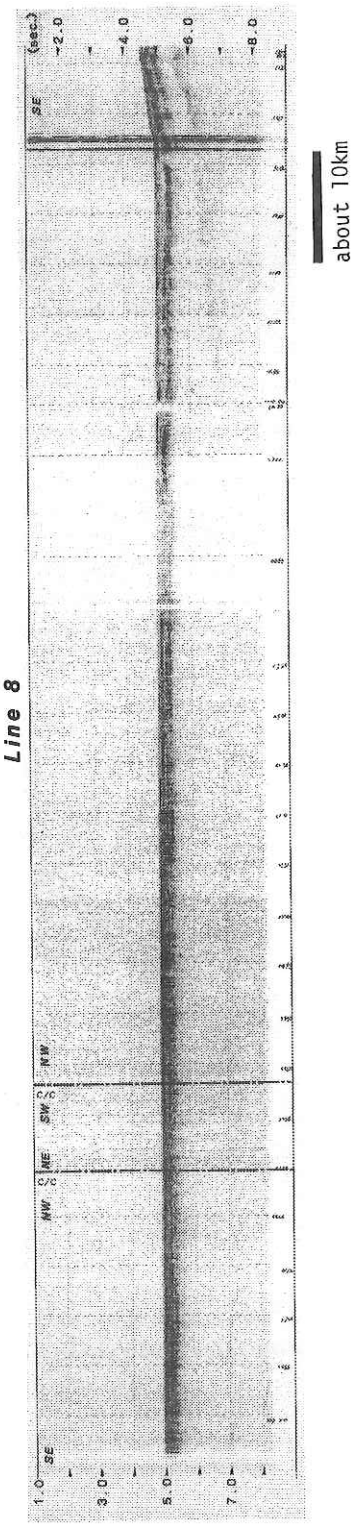

Fig. 13-6. On-board monitor record of line 8.

LINE 9

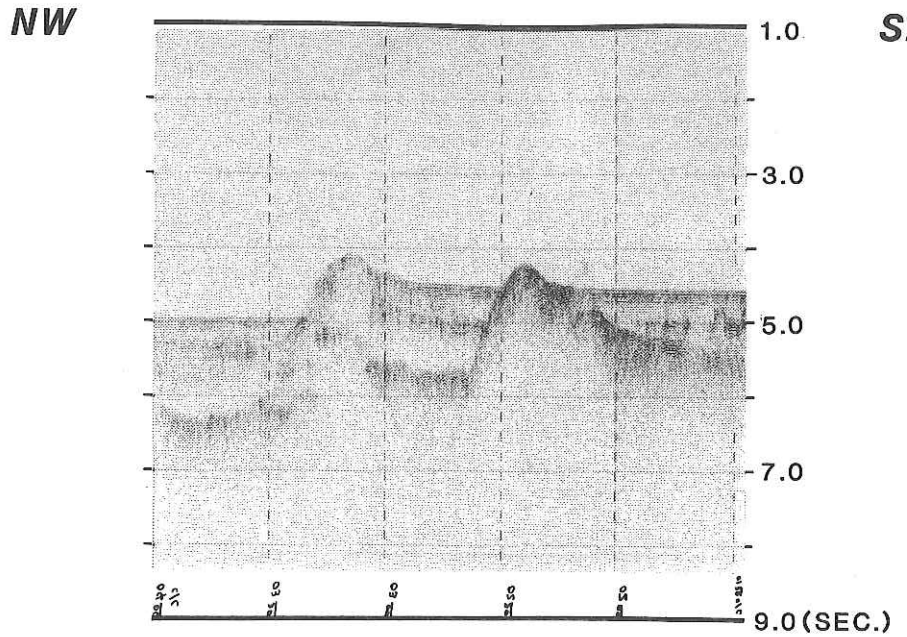

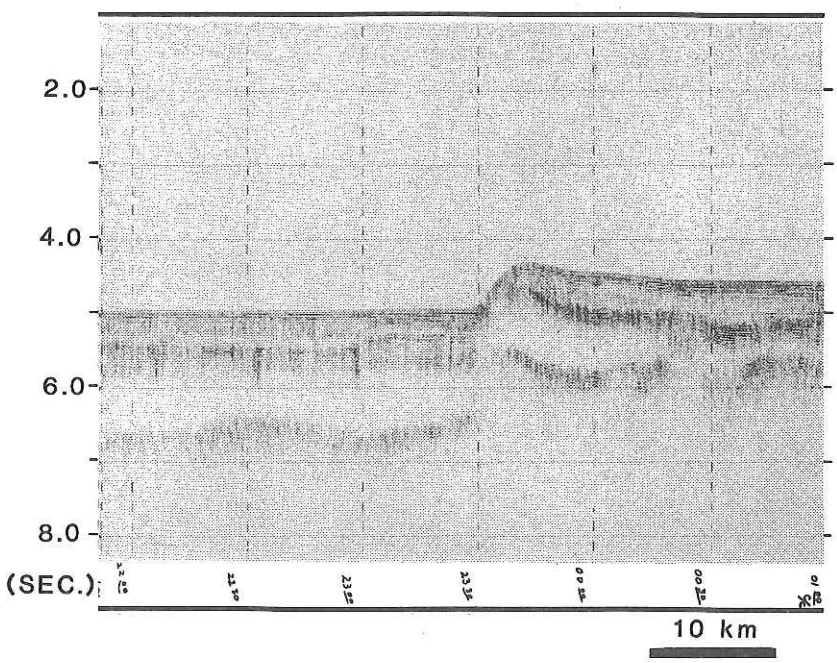

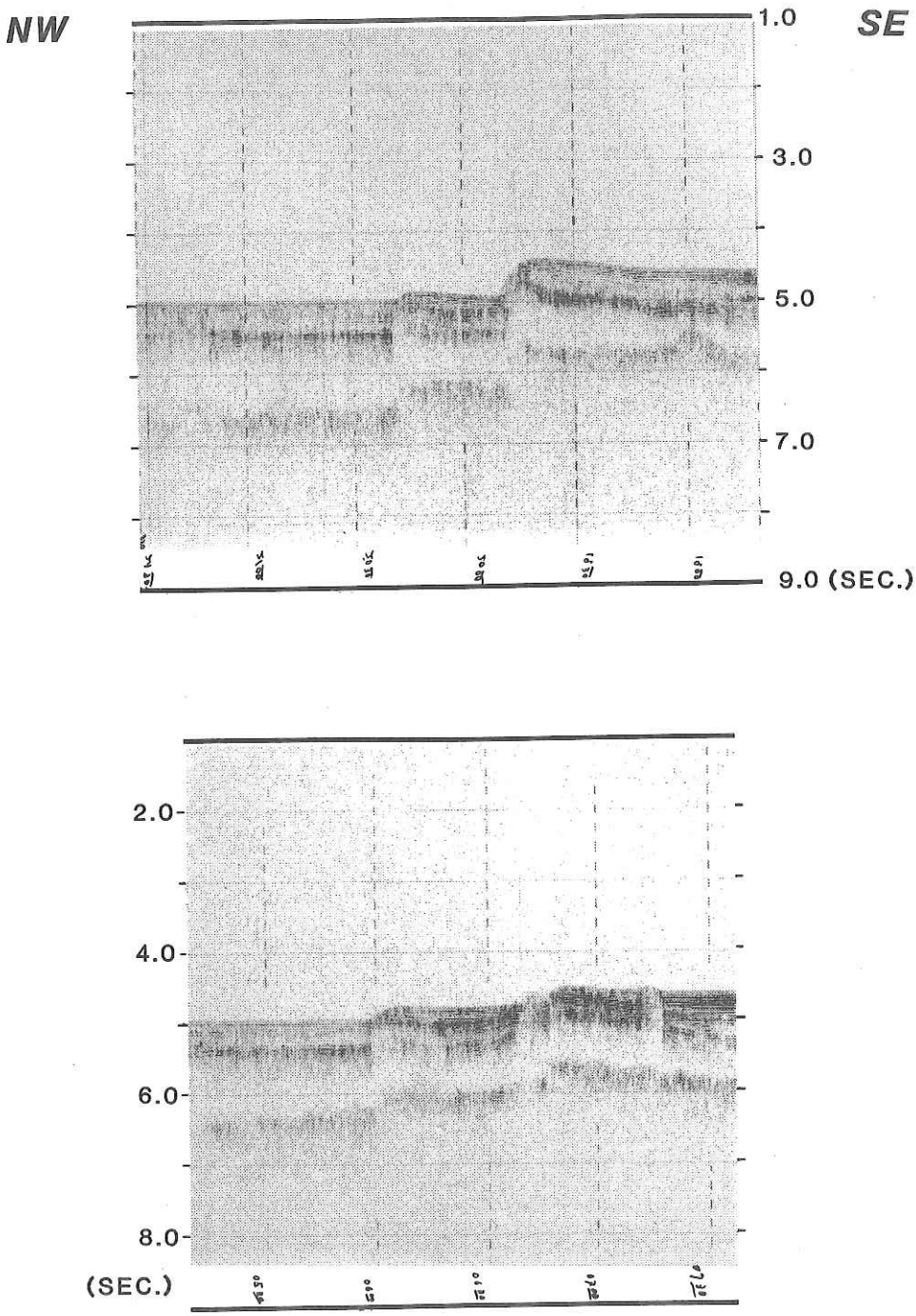

Fig. 13-7. On-board monitor record of line 9. (4 short lines)

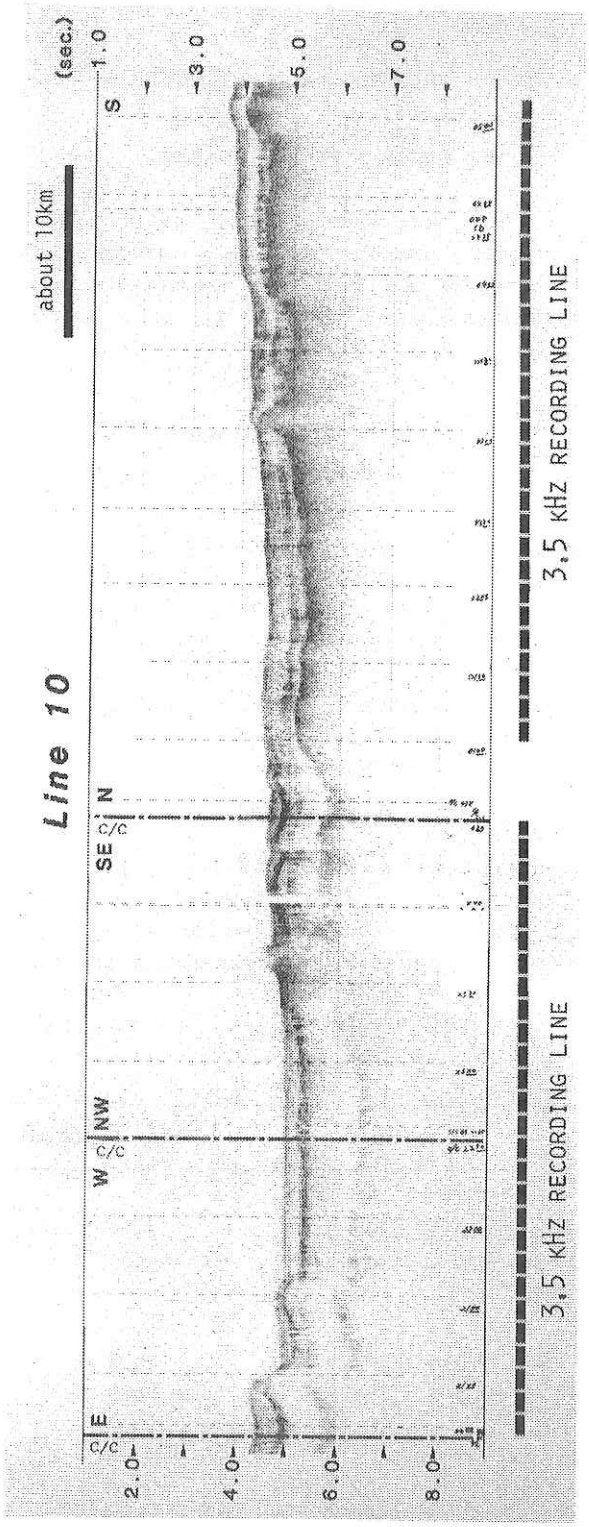

Fig. 13-8. On-board monitor record of line 10. Broken lines show the 3.5 kHz recording lines.

14. HEAT FOLW MEASUREMENTS

S. Nagihara and T. Asanuma

Heat flow measurements were made at three stations (St.7, St.8 and St. 12) during this cruise. At St.7 and St.8, thermal conductivity of the sediment was measured as well as temperature gradient. Thermal conductivity measurements were also made at other three stations (St.5, St.6 and St.10).

Method and Instrument

The heat flow measuring system used in this cruise is the one developed recently at Chiba University. It has an Ewing type probe (4m length) and permit multiple penetrations. Six thermistors are equipped on the probe for the temperature gradient measurements. This probe also has the ability of the in-situ thermal conductivity measurements. One of the six thermistors is specially applied for the purpose. Thermal conductivity was also measured on samples taken by a piston corer by the needle probe method at the five stations mentioned above (St.5-8 and St.10). The results of the both methods will be compared later.

Measurements

We tried two penetrations at each station. At St.7 and St.8, every penetration seemed successful. At St.12, however, the probe fell down when we tried the first. The three thermistors including the one for the in-situ thermal conductivity measurement were not in the mud at the second time.

TABLE

Station	Location		Water Depth(m)
St. 7			
HF1-A	42°13.6'N	137°40.2'E	3690
B	42°13.6'N	137°40.1'E	3690
St. 8			
HF2-A	41°19.9'N	138°29.4'E	3690
B	41°19.8'N	138°29.4'E	3690
St. 12			
HF3-A	41°12.4'N	138°27.2'E	3670
B	41°12.4'N	138°27.3'E	3670

ANNEX

PRELIMINARY REPORT OF TANSEI MARU CRUISE KT 87-6

May 29 - June 4, 1987
(Aomori - Akita)

1. SCIENTISTS ABOARD THE R.V. TANSEI MARU FOR THE CRUISE KT 87-6

TAMAKI, Kensaku	(Chief Scientist) Ocean Research Institute, University of Tokyo
FURUKAWA, Masahide	Department of Earth Sciences, Kobe University
ITODA, Chizu	Department of Earth Sciences, Kobe University
KURAMOTO, Shin-ichi	Ocean Research Institute, University of Tokyo
MIYASHITA, Sumio	Department of Geology, Niigata University
NAKANISHI, Masao	Ocean Research Institute, University of Tokyo
SAYANAGI, Keizo	Department of Earth Sciences, Kobe University (now at Ocean Research Institute, University of Tokyo)
TOKUYAMA, Hidekazu	Ocean Research Institute, University of Tokyo
TSUKUI, Masashi	Department of Earth Sciences, Chiba University
UNO, Ikuko	Department of Earth Sciences, Kobe University
YAMASHITA, Shigeru	Department of Earth Sciences, Chiba University

ANNEX: PRELIMINARY REPORT OF TANSEI MARU CRUISE KT 87-6 (Investigation on the Sea-floor Spreading Tectonics in the Northeastern Part of Japan Basin-ODP)

K. Tamaki, H. Tokuyama, S. Miyashita, M. Tsukui, M. Furukawa, K. Sayanagi, S. Kuramoto, M. Nakanishi, I. Uno, S. Yamashita, and C. Itoda

The research cruise (cruise code: KT87-6) for the geological and geophysical investigation of the northern part of the Japan Sea was carried out by R/V Tansei-maru of the Ocean Research Institute, University of Tokyo. R/V Tansei-maru departed from Aomori on May 29, 1987 and arrived at Akita on June 4, 1987. The duration was 7 days. The objectives of the research cruise were summarized into three categories as below.

(1) Detailed geomagnetic survey of the eastern part of the Japan Basin.
(2) ODP (Ocean Drilling Project) site survey of a proposed site J1d at the northernmost part of the Japan Basin.
(3) Bottom rock sampling of the Okushiri Ridge and an unknown seamount in the Japan Basin.

The weather condition was generally good except for last two days, June 3 and 4. Severe interruption against the multi channel seismic survey was often produced by groups of fishery boats for salmons and trouts. Only one and half lines of originally planned 6 MCS lines were successfully carried out. Other planned lines were abandoned because of widely spread groups of fishery boats on the planned lines.

Four scientists (Tamaki, Tokuyama, Miyashita, and Tsukui) and seven graduate students from four institutions in Japan joined the cruise. Survey tracks are shown in Fig. A-1.

Detailed geomagnetic survey

Detailed geomagnetic survey in the eastern part of the Japan Basin was conducted as a subsequent survey of KH 86-2 research cruise. 16 tracks for detailed geomagnetics had been done during KH 86-2 cruise in the eastern part of the Japan Sea. Geomagnetic record of three full transect lines and three half lines were obtained in the northeastern extension of the KH 86-2 survey area during the present cruise. One full track was added in the southwestward extension. Composite tracks of KH 86-2 and KT 87-6 cruises are shown in Fig. A-2.

The same proton magnetometer system as used for KH 86-2 survey was used during the present cruise. The observed data were logged every 30 seconds. On-board three component magnetometers of Kobe University

(Isezaki, 1986) were also operated all through the duration of the cruise. Two systems of the three component magnetometer were operated simultaneously this time for the comparison of the two systems.

Figure A-3 shows geomagnetic anomaly profiles along the ship's tracks of KT87-6. The magnetic anomaly lineations trending NEE that was observed in the detailed geomagnetic survey area of KH 86-2 are observed in the northeastward extension of the KH 86-2 area. Although composite analyses of the KH 86-2 and KT 87-6 data have not been done, general trends of magnetic anomaly lineations of NEE and the complex pseudofaults pattern (Kobayashi et al., 1986) are still valid.

The variation of amplitudes of magnetic anomalies are observed on Fig. 3. The amplitudes of magnetic anomalies in the detailed tracked area is about 100 nT, while those of the Yamato Basin is 150 to 400 nT. This difference is caused by difference of the basement depth in both basins. The basement depth in the central part of the Japan Basin is about 5000 m while that of the Yamato Basin is about 3500 m (Ishiwada et al., 1984; Tamaki 1986). The amplitudes of the magnetic anomalies at 41.6°N and 137.5°E reaches 250 nT. No seamounts and basement reliefs are observed at the site from the available seismic reflection data and gravity data. This kind of high amplitudes may reflect some anomalous crustal accretion during the seafloor spreading stage of the Japan Basin.

Multi-channel seismic reflection survey

One full track (Line MC1) and a half track (Line MC2) of multi channel seismic reflection survey was successfully carried out at the northernmost end of the Japan Basin (Fig. A-4). Line MC1 is planned as site survey for ODP drilling site J1d proposed by Tamaki et al. (1985). This site was selected as thin and transparent sediments at the site suggest easy access to the basement by drilling without meeting gas charged layer.

Data were recorded by NE128 digital recording system, manufactured by NEC Ltd., included 6 channels streamer cable which was composed of 12 hydrophone groups each length was 25 meters. The BOLT 1500C type airgun was used as a sound source which air chamber was remodeled to a capacity of 9 liters fired every 50 meters, about 20 sec. interval. The recorded digital data are carried back to the Ocean Research Institute and processed at once. The field data were converted from the SEG-B to the SEG-X formats, firstly. Geophysical signal processing methods, deconvolution, normal moveout collection and filtering, are carried out. The traces are completely stacked with the common depth point gather traces, and printed out continuously (Fig. A-5).

In the Line MC1, the Japan Basin is composed of three acoustic units, acoustic basement, lower sedimentary unit and upper sedimentary unit in ascending order. The upper two sedimentary units are bounded by very intense and continuous horizontal reflector. Near J1d site (proposed drilling site for ODP, shot#350-500), the depth of acoustic basement is relatively shallow and increasing the depth toward the Okushiri ridge and also to the westward. The basement is horizontally covered by the upper two sedimentary units. This kind of features are seen on the Okushiri ridge with same acoustic character although the sea-floor is inclined to the east. In the Japan Basin and the Okushiri ridge the acoustic stratigraphy is probably comparable. The boundary between the Japan Basin and the Okushiri Ridge forms steep cliff composed of the active eastward dipping thrust sheets that are identified by the offset of same acoustic unit, acoustic diffraction from the thrust planes (Kuramoto et al., 1987). The lower sedimentary unit of Japan Basin on the foot of the Okushiri Ridge is obviously dragged by the thrust activity. The border between the Okushiri ridge and the Musashi basin is probably bounded with westward dipping thrust (Tamaki and Honza, 1985). These tectonic phenomena with thrust faults are coincided with the mechanism solution of natural earthquake, E-W compression (Fukao & Furumoto, 1975).

Sampling of bottom rocks

Two dredge haul samplings (Sites D1 and D2 in Fig. A-4) were carried out the during the cruise. Both sampling were successful with abundant of solid rock samples. The dredge logs are represented in the next section.

Site D1

The target of Site D1 was to get the basement rocks and lower sedimentary sequence of the Okushiri Ridge. Hoyanagi et al. (1987) successfully sampled the basaltic rocks and silt stones by the dredge of the site a few miles south of Site D1. There is a possibility that the basement of the Okushiri Ridge was originally the oceanic crust of the Japan Basin. The western slope of the Okushiri Ridge is considered to be a large thrust fault (Tamaki and Honza, 1985). The basement of the Okushiri Ridge may be an uplifted blocks of the oceanic crust of the Japan Basin by thrust movements. There is, however, a possibility that the boundary between the Okushiri Ridge and the Japan Basin was an original ocean-continent boundary during the break-up of the continental crust and opening of the Japan Sea. The ocean-continent boundary may have been preferably selected as a suture of thrust fault.

Total number of the fragments sampled were 322 (Fig. A-7). These rock samples are divided into six groups as follows: (1) basaltic rocks (70 fragments), (2) shale I (70 fragments), (3) sandy shale (including some sand stones) (60 fragments), (4) shale II (112 fragments), (5) semi-consolidated clay (5 fragments), (6) allochthonous pebbles (5 fragments).

Shale I and shale II were divided on the basis of hardness. Shale I is harder than shale II. Shale II is as soft to be scratched by nails. This division is not so strict that there are some rocks with the intermediate hardness. The rock fragments of the groups (1), (2), and (3) are angular and those of the groups (4) and (5) are subangular or round which is considered to be rounded because of their softness. The abundant recovery of these rocks with angular to subangular shape strongly suggests in-situ occurrence of these sampled rocks on the western slope of the Okushiri Ridge at the depth range of 2750 to 2000 m.

The variable hardness of the recovered sedimentary rocks indicates that they are included into wide age range of sedimentary layers overlie the basement of the Okushiri Ridge. The recovered volcanic rocks are exclusively basaltic rocks. No rhyolitic and andesitic rocks were observed. This basaltic rocks may be related to the oceanic crust of the Japan Basin.

Site D2

Site D2 is on a unnamed seamount that was not charted on Hydrographic office bathymetric map No.6311. Relative height above seafloor is about 1200 m. The water depth of the summit of the seamount is about 2500 m. As the sediment thickness in the basin around the seamount exceeds 1500 m, then the relative height of the seamount reaches 2700 m. This seamount is characterized by weak geomagnetic anomaly (Tamaki et al., this volume). Tamaki and others (this volume) suggests that the origin of this seamount is an continental fragment trapped in the oceanic basin during the process of break up and subsequent seafloor spreading episodes fo the Japan Sea. We propose that this unnamed seamount dredged by R/V Tansei-maru for the first time is named the Tansei Seamount (Fig. A-7).

All the fragments larger than 4 cm diameter (65 fragments) were observed on board. 80 % of the fragments are tuff breccia and others are siltstone, pumice tuff, and sandstones (Fig. A-8).

The tuff breccia is dacitic and includes pumice with a diameter less than 1 cm and siltstone of round pebble, angular blocks, and unconsolidated blocks with a diameter less than 1 cm. The matrix of the tuff brec-

cia is sandy silt. The maximum size of the sampled tuff breccia is 25 cm in length.

The siltstone is divided into two groups. One is dark grey in color and semi-hard and the other is light grey in color and soft. The latter group of siltstone is included in the tuff breccia. The maximum size of the sampled siltstone is 25 cm in length.

The pumice tuff is composed of dacitic and white pumice. The maximum size of the sampled tuff breccia is 10 cm in length. Basaltic lava or scoria were not observed. The configuration of the sampled rocks suggests that tuff breccia and siltstone are in-situ samples. All these rock samples do not suggest volcanic origin of the Tansei Seamount. The further comparative study with rocks on shore of Tohoku and Hokkaido regions is needed.

REFERENCES

Hoyanagi, K., T. Sagayama, J. Ishii, S. Miyashita, T. Yamazaki, N. Tsuchiya, Y. Watanabe, S. Izu, and M. Iwashita, Middle Miocene siltstone fragments and rounded pre-Tertiary rocks collected from the seamount (Kaiyo-kaizan) in the Sea of Japan, Bull. College of Arts and Sci. at Sapporo, Tokai Univ., 7, 11-19, 1987.

Isezaki, N., A new shipboard three component magnetometer, Geophysics, 51, 1992-1998, 1986.

Ishiwada, Y., E. Honza, and K. Tamaki, Sedimentary Basins of the Japan Sea, Proc. 27th Intern. Geol. Congr., 23, 43-65, 1984.

Kuramoto, S., H. Tokuyama, and K. Tamaki, Geological structure of the transition zone between the Japan Basin and the Okushiri Ridge, Programme and Abstracts, Fall Meeting of Seismol. Soc. Japan, 1987 (in Japanese).

Tamaki, K., Age estimation of the Japan Sea on the basis of stratigraphy, basement depth, and heat flow data, J. Geomag. Geoelctr., 38, 427-446, 1986.

Tamaki, K. and E. Honza, Incipient subduction and obduction along the eastern margin of the Japan Sea, Tectonophys., 119, 381-406, 1985.

Tamaki, K., H. Kagami, E. Honza, and K. Kobayashi, ODP drilling proposal: tectonics of the Japan Sea, in Japanese ODP Proposals, Edition 1, edited by A. Taira and K. Kobayashi, 1985.

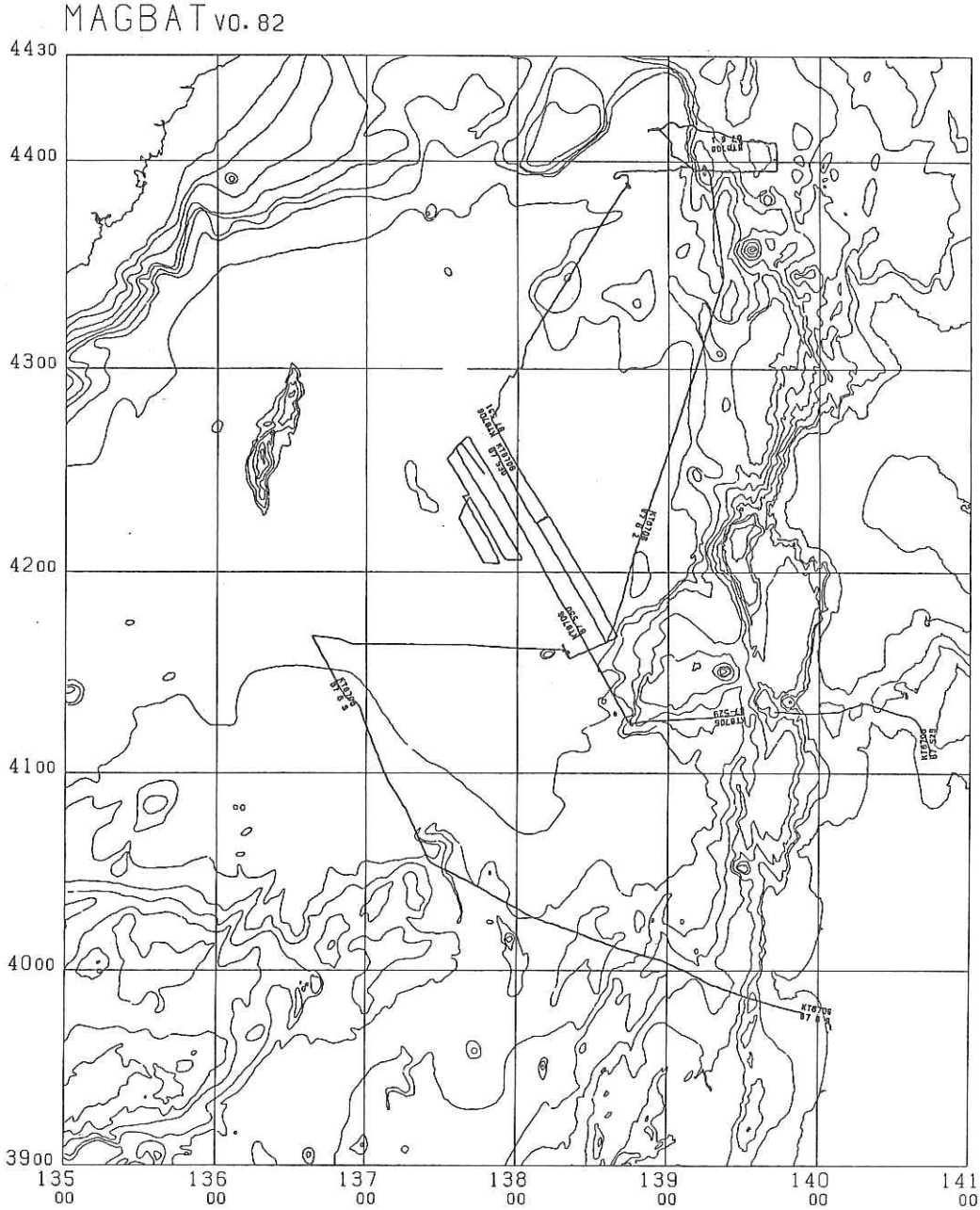

Fig. A-1. Ship's tracks for detailed survey of geomagnetic anomalies in the cruise KT 87-6. Interval of tracks are generally 4 n.m.

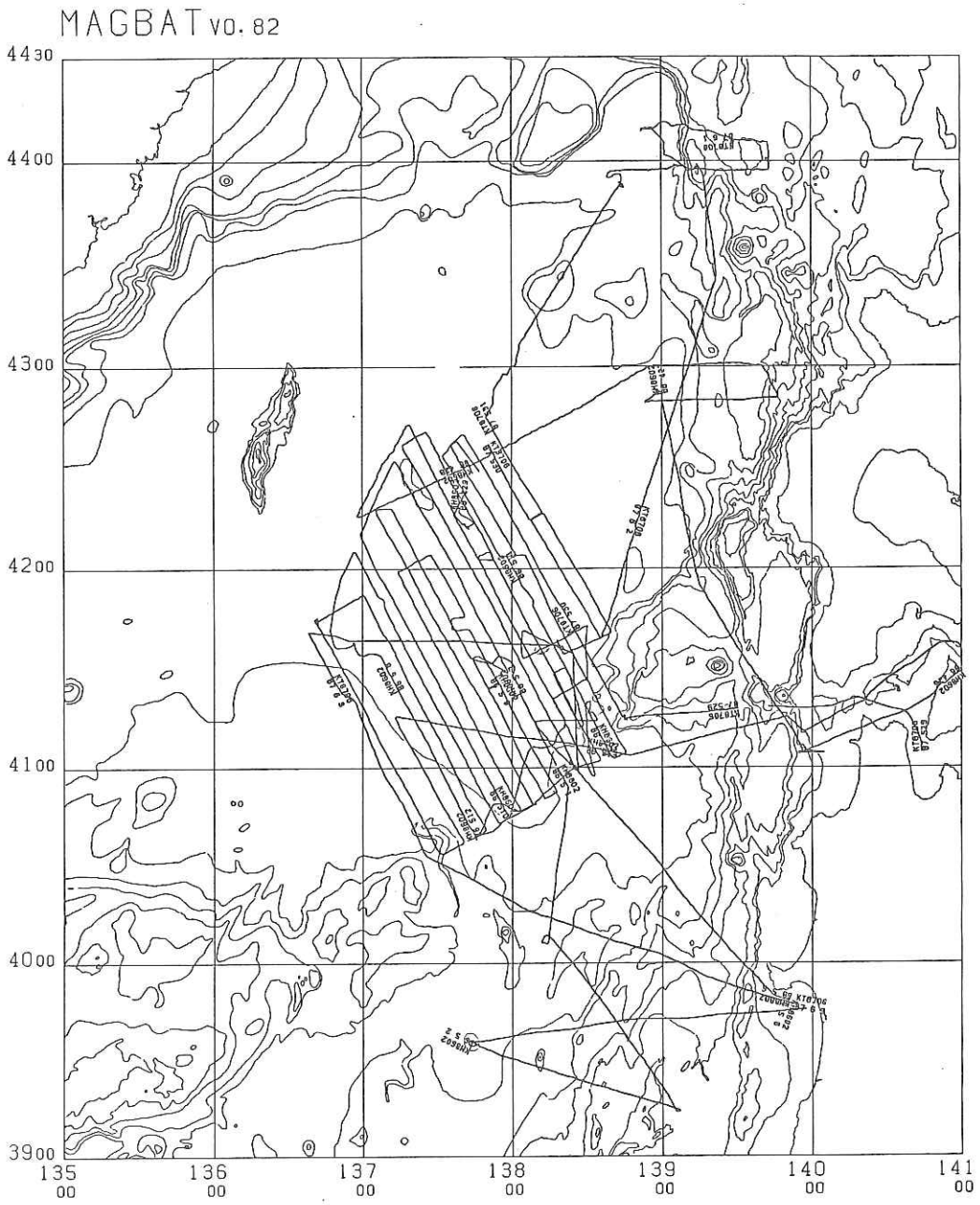

Fig. A-2. Composite survey tracks of KH 86-2 and KT 87-6 in the north-eastern Sea of Japan. Interval of tracks are generally 4 n.m.

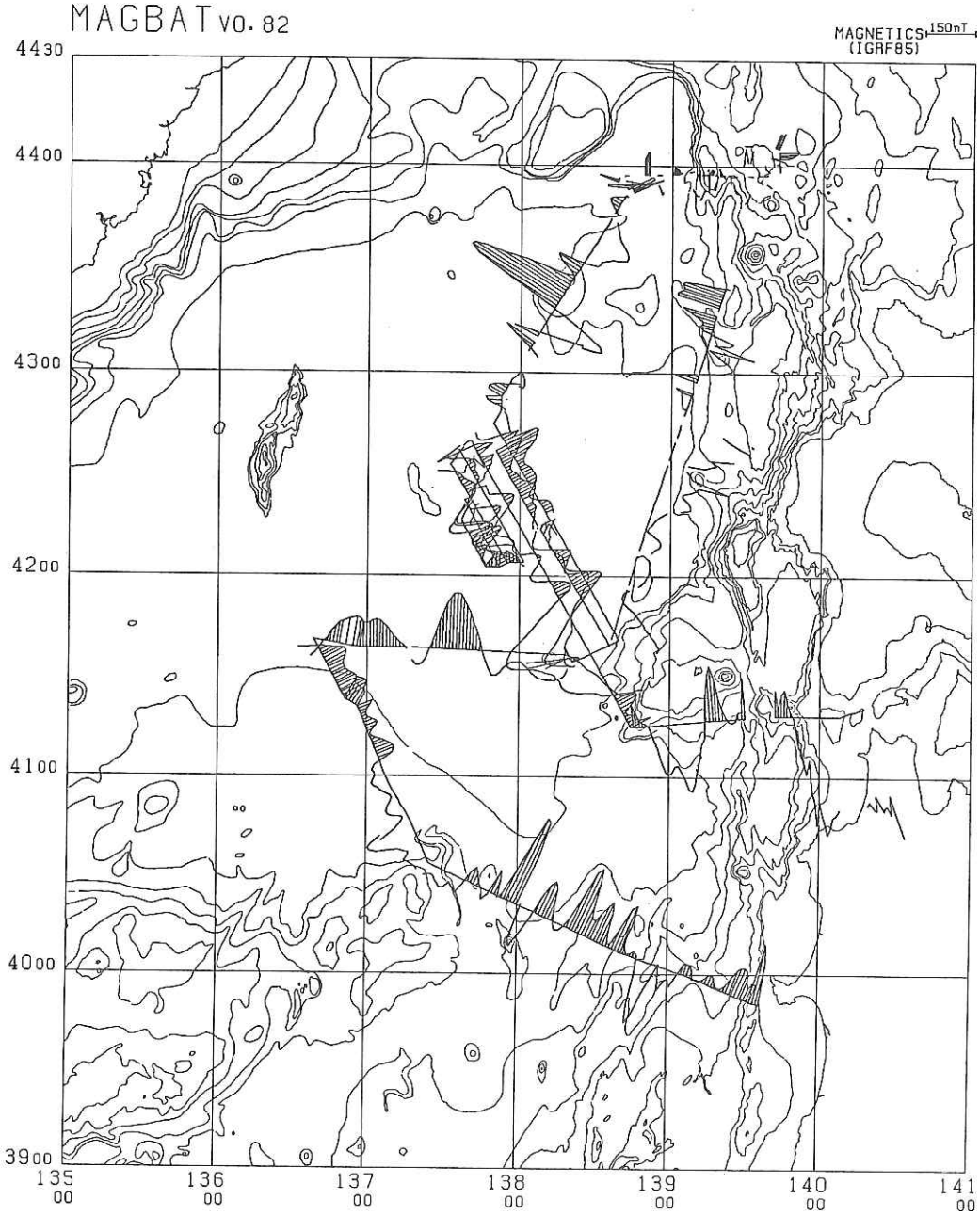

Fig. A-3. Geomagnetic anomaly profiles along ship's tracks of KT 87-6. Positive anomalies are hatched. Anomalies are calculated based upon IGRF 1985.

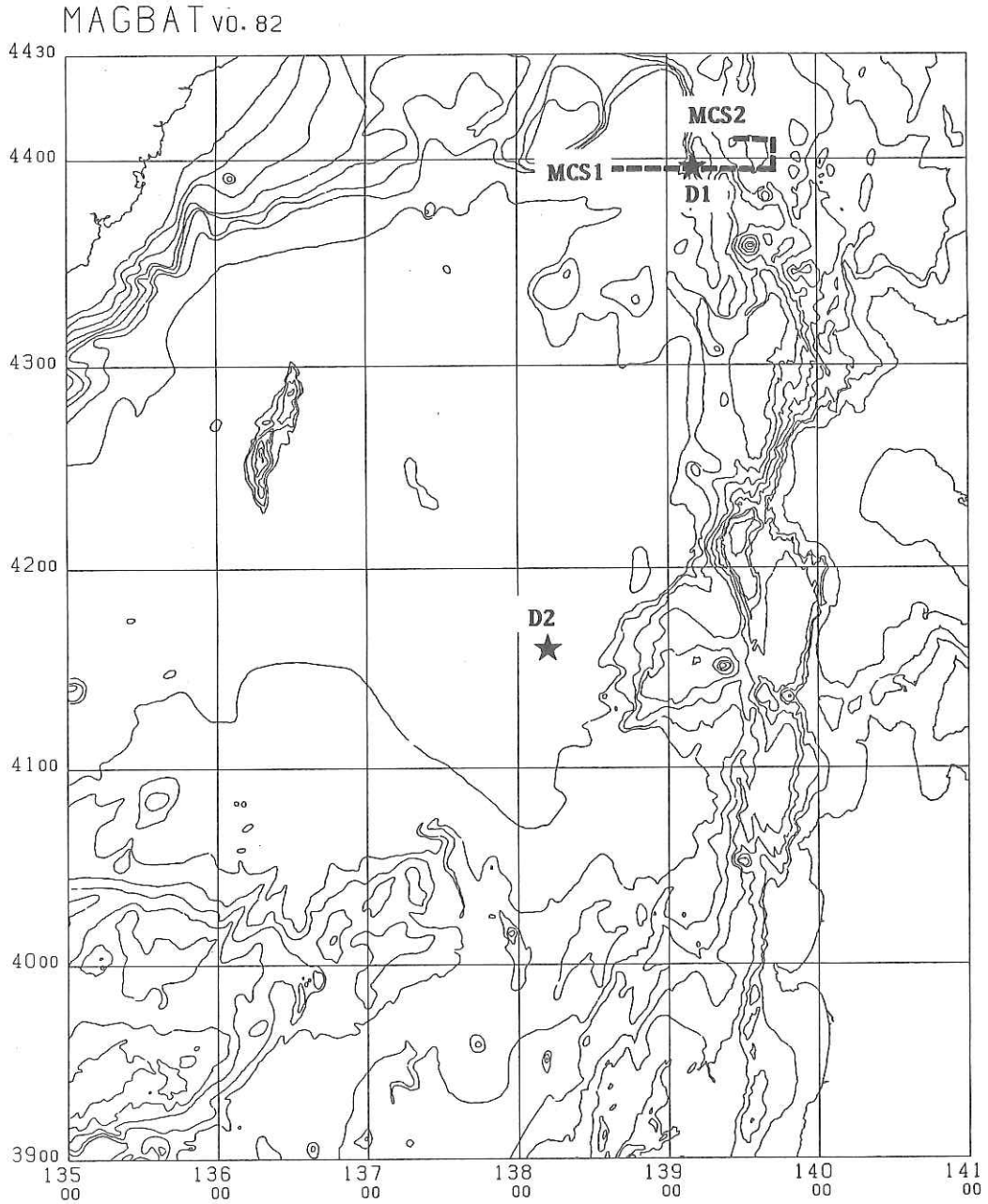

Fig. A-4. Multichannel seismic reflection survey lines and bottom sampling sites.

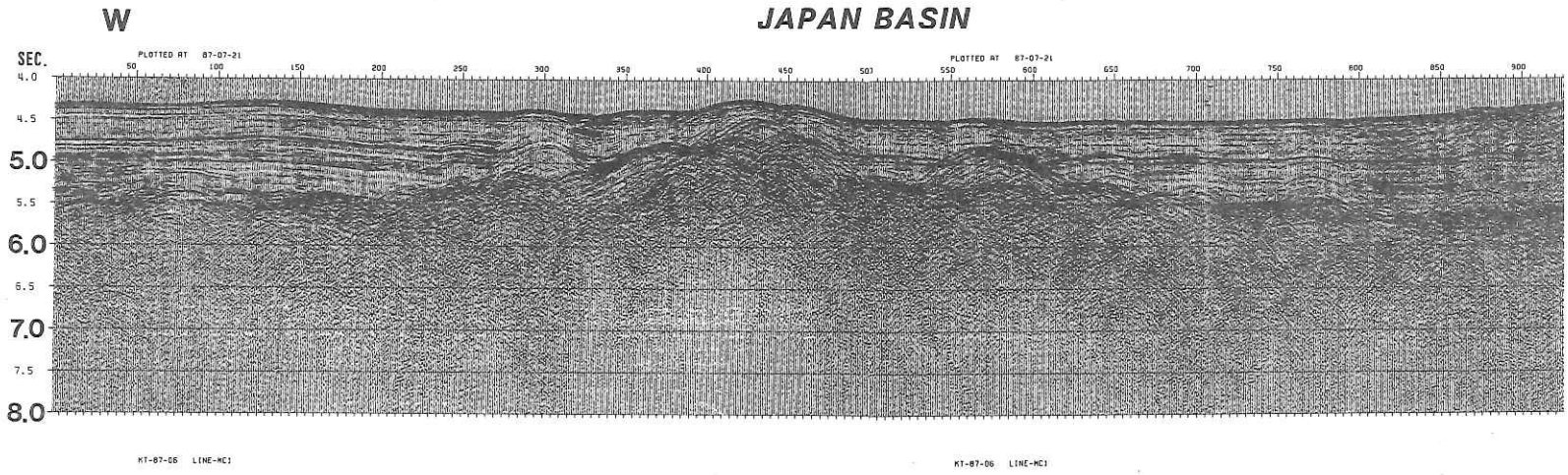

Fig. A-5. Stacked multichannel seismic reflection profile for Line MC1.
(a) Japan Basin

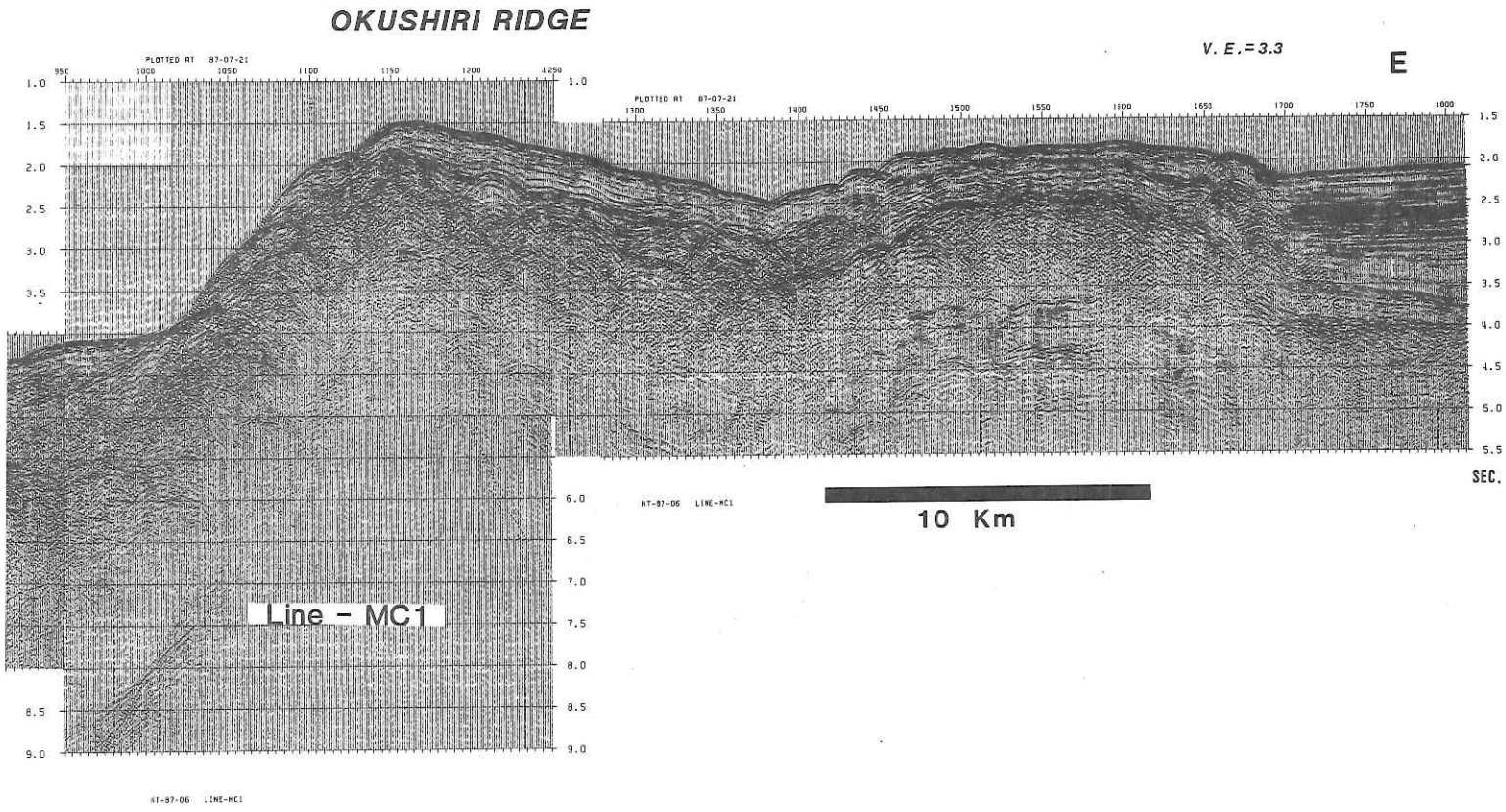

Fig. A-5. Stacked multichannel seismic reflection profile for Line MC1.
(b) Okushiri Ridge

Fig. A-6. Rock samples (all) recovered at site D1 (KT 87-6-1).

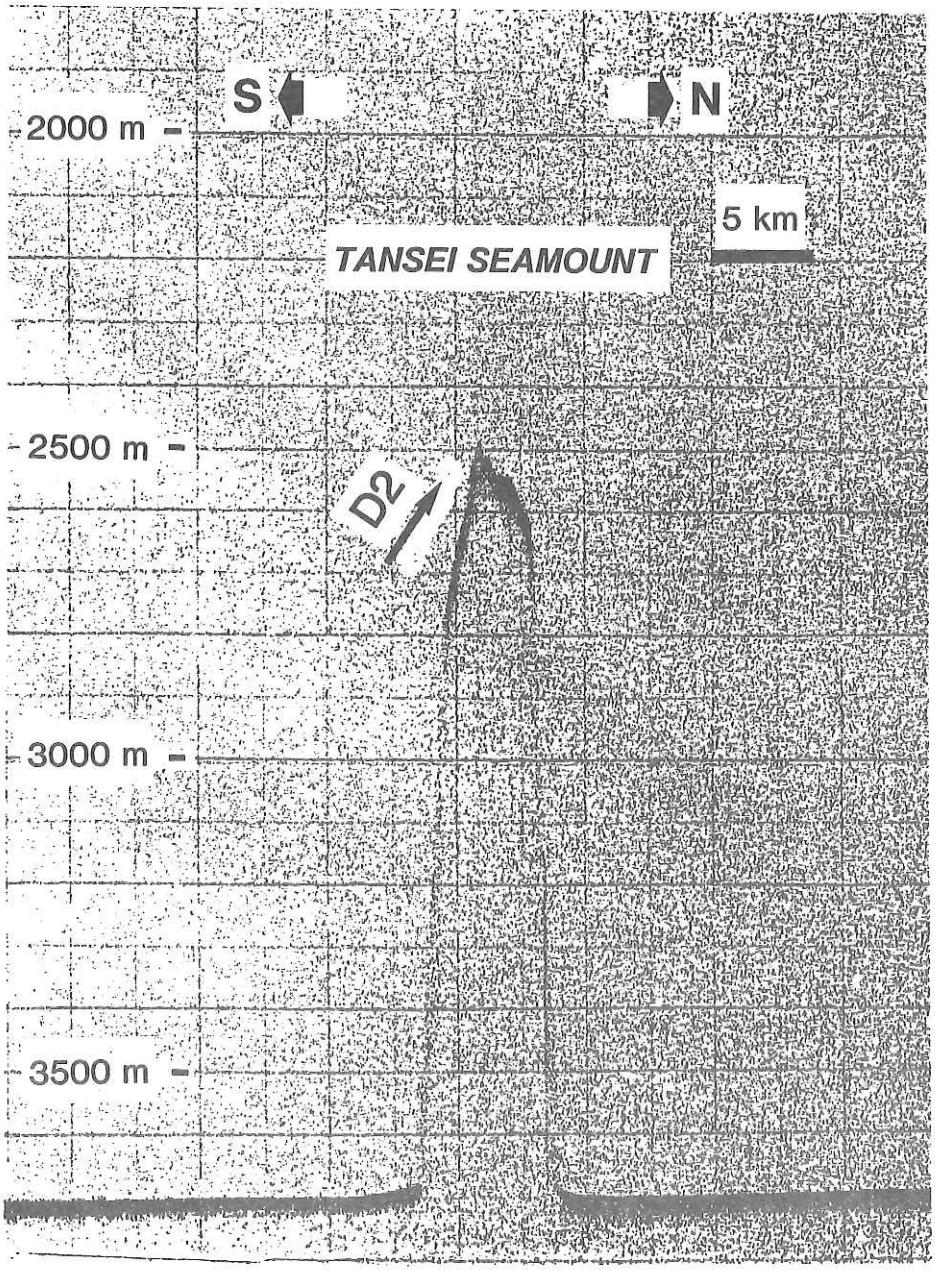

Fig. A-7. Bathymetric profile of the Tansei Seamount with site D2.

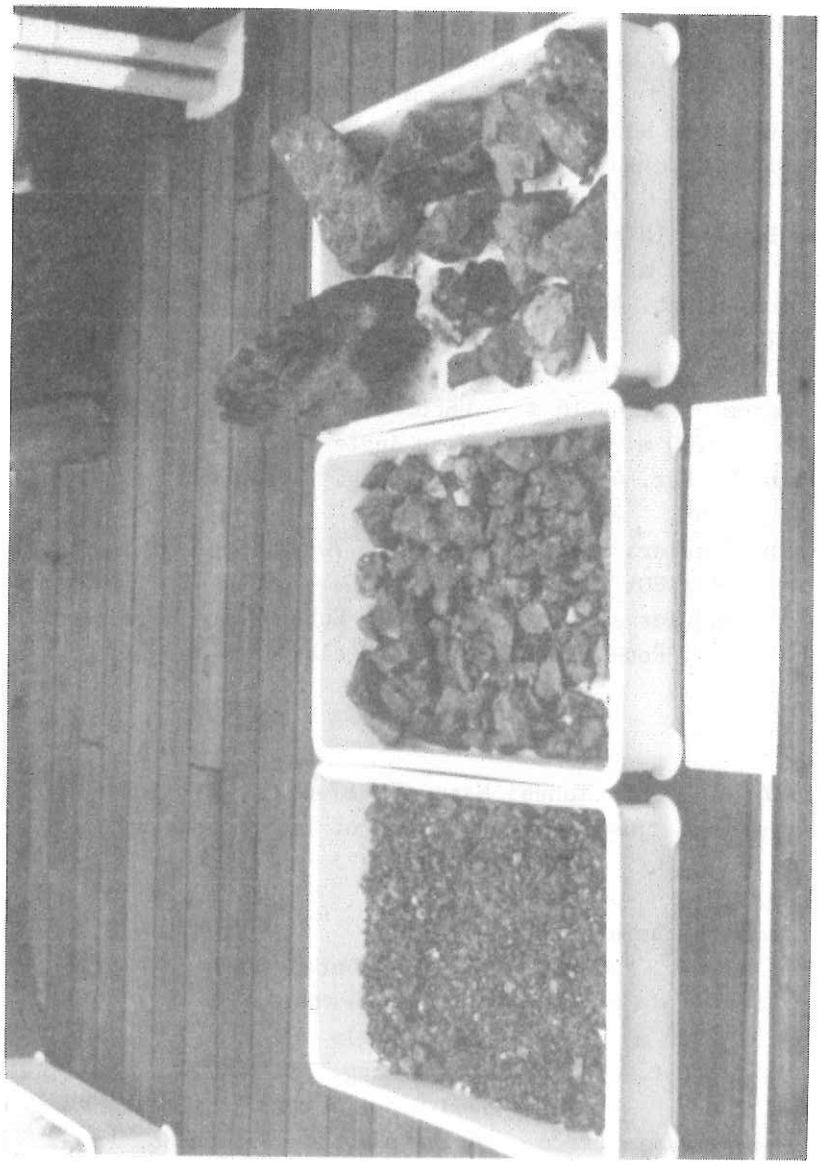

Fig. A-8. Rock samples (all) recovered at site D2 (KT 87-6-2).

DREDGE HAULS

OPERATION LOGS

Date June 1, 1987 Ship Tansei Maru KH 87-6 Station No. D1
Location Western slope of Okushiri Ridge
Weather cloudy Wind 210° 10 m/s Sea swell
Bottom Topography steep slope
Typeof Dredge Nalwalk chain bag with backet Add.Wt. 0 kg
Time Towered 10 h 03 m Uncorr. Water Depth 2860 m
Initial Time on Bottom 10 h 58 m Uncorr. Water Depth 2752 m
Wire Length 2990 m Wire Angle 0°
Ship Position Lat. 44°00'005 Long. 139°09'387
Direction of Haul 90 ° Ship Speed 0.5-1.0 kt. (till 11 h 49 m)
Speed Wire-in 60 m/min(from 11 h 58 m) Winch No. 1
Final Time on Bottom 12 h 16 m Uncorr. Water Depth 1996 m
Wire Length 2200 m Wire Angle
Ship Position Lat. 44°00'465 Long. 139°10'359
Time Surfaced 12 h 40 m
Dredged Materials Angular basalt fragments: 70 pieces (Max. pebble: 260x180x110 mm), Angular shale I(hard): 70 pieces, Angular sandy shale: 60 p., Subangular shele II(soft): 112, Rounded semisolidified clay: 5 pieces.

Date June 2, 1987 Ship Tansei Maru KH 87-6 Station No. D2
Location Southern slope, just L-low the crest of Tansei seamount
Weather cloudy Wind 120° Sea calm
Bottom Topography
Type of Dredge Nalwalk chain bag Add.Wt. 0 kg
Time lowered 13 h 36 m Uncorr. Water Depth 2771 m
Initial Timeon Bottom 14 h 18 m Uncorr. WaterDepth 2683 m
Wire Length 2943 m Wire Angle 0°
Ship Position Lat. 41°36'698 Long. 138°16'754
Direction of Haul 330° Ship Speed 0.5-1.5 kt. (till 14 h 55 m)
Speed Wire-in 60 m/min (from 14 h 46 m) Winch No. 1
Final Time on Bottom 15 h 08 m Uncorr. Water Depth 2640 m
Wire Length 2663 m Wire Angle
Ship Position Lat. 41°36'841 Long. 138°16'605
Time Surfaced h m
Dredged Material Abundant rock flagments, consist of mainly tuff breccia and subordinate tuff and siltstone

List of dredged materials during KT 87-6

Sample No.	Diameter(mm) L	M	S	Round-ness	Wt(g)	Mn-coating(mm)	Lithology & Remarks
D1-001	260	180	110	A	n.d.	0	basalt
002	100	50	50	A	"	0	"
003	100	80	40	A	"	0	"
004	90	45	60	A	"	0	"
005	70	55	30	SA	"	0	"
006	55	50	35	A	"	0	"
007	60	50	30	A	"	0	"
008	85	60	25	A	"	0	"
009	60	45	35	A	"	0	"
010	45	40	35	A	"	0	"
011	50	45	30	SA	"	0	"
012	95	80	55	A	"	0	basalt breccia
013	70	55	65	A	"	0	"
014	60	65	45	A	"	0	"
015	55	45	35	A	"	0	"
016	55	45	30	A	"	0	"
017	60	40	35	A	"	0	basalt
018	85	30	30	A	"	0	"
019	70	45	35	A	"	0	"
020	75	65	55	SA	"	0	basalt andesite?
021	75	50	30	A	"	0	basalt
022	70	50	30	A	"	0	"
023	55	45	25	SA	"	0	"
024	75	50	30	A	"	0	"
025	75	40	28	A	"	0	"
026	74	60	40	SA	"	0	"
051	118	110	64	SA	"	0	shale
052	114	105	42	A	"	0	"
053	175	153	88	A	"	0	"
054	96	54	50	A	"	0	"
055	116	78	42	SA	"	0	"
056	76	50	27	SA	"	0	"
057	108	76	52	A	"	0	"
058	66	48	40	A	"	0	"
059	98	85	24	SA	"	0	"
060	95	75	50	SA	"	0	"
061	120	65	63	A	"	0	"
062	77	50	25	SA	"	0	"
063	95	46	20	A	"	0	"
064	125	96	40	SA	"	0	"
065	78	55	37	A	"	0	"
066	132	80	40	SA	"	0	"
067	108	78	62	A	"	0	"
068	70	45	30	A	"	0	"
069	75	56	42	SA	"	0	"
070	90	68	28	A	"	0	"

Sample No.	Diameter(mm) L	M	S	Round-ness	Wt(g)	Mn-coating(mm)	Lithology & Remarks
D1-101	126	95	33	A	n.d.	0	sandy shale, typical
102	77	58	50	A	"	0	sandy shale
103	105	74	42	SA	"	0	"
104	60	66	30	SA	"	0	"
105	65	58	30	A	"	0	"
106	78	60	39	A	"	0	"
107	130	100	55	SA	"	0	"
108	90	80	36	A	"	0	"
109	60	40	28	R	"	0	typical sand stone
110	70	60	40	SA	"	0	sandy shale
111	66	50	70	SA	"	0	"
112	70	50	39	A	"	0	"
113	90	45	40	A	"	0	"
114	110	65	37	A	"	0	sandy shale, grading
115	75	55	35	SA	"	0	"
116	80	60	12	SA	"	0	"
151	110	75	50	SA	"	0	shale(medium hard)
152	70	65	50	SA	"	0	"
153	100	105	50	SA	"	0	"
154	66	45	50	SA	"	0	"
155	80	60	45	SA	"	0	"
156	70	55	22	SA	"	0	"
157	105	55	30	SA	"	0	"
158	80	35	30	A	"	0	"
159	67	45	43	SA	"	0	"
160	67	45	43	SA	"	0	"
161	70	40	32	SA	"	0	"
162	65	53	25	A	"	0	"
163	75	60	26	R	"	0	"
164	56	52	32	R	"	0	"
165	80	53	30	A	"	0	"
166	65	40	27	SA	"	0	"
167	57	52	30	SA	"	0	"
168	63	55	22	R	"	0	"
169	58	48	23	SA	"	0	"
170	40	58	35	A	"	0	"
201	250	90	85	R	"	0	semi solidified cray
202	130	80	65	R	"	0	"
203	100	65	40	SA	"	0	"
204	76	70	35	R	"	0	"
205	130	55	54	R	"	0	"
206	60	50	50	R	"	0	"
251	85	45	30	WR	"	0	chert?
252	80	45	20	WR	"	0	basalt
253	78	50	30	WR	"	0	s.s
254	62	38	23	WR	"	0	s.s?
255	55	43	8	WR	"	0	basalt

Sample No.	Diameter(mm) L	M	S	Round-ness	Wt(g)	Mn-coating(mm)	Lithology & Remarks
D2-001	290	180	140	A	n.d.	0	shale
002	120	110	35	A	"	0	"
003	100	80	65	A	"	0	siltstone
004	70	45	35	A	"	0	"
005	55	50	20	A	"	0	"
006	60	55	20	A	"	0	"
007	75	45	25	A	"	0	"
008	45	40	25	A	"	0	"
009	65	35	25	A	"	0	"
010	45	35	17	A	"	0	"
011	210	120	90	A	"	0	tuff breccia
012	220	110	90	A	"	0	"
013	170	110	90	A	"	0	"
014	130	75	70	SA	"	0	"
015	110	65	55	A	"	0	"
016	85	65	45	A	"	0	"
017	140	110	50	A	"	0	"
018	110	85	40	A	"	0	"
019	110	80	40	A	"	0	"
020	115	65	40	SA	"	0	"
021	100	70	50	A	"	0	"
022	70	55	35	A	"	0	"
023	100	65	65	SA	"	0	"
024	90	55	35	SA	"	0	"
025	100	55	25	SA	"	0	"
026	80	55	55	A	"	0	"
027	70	60	45	SA	"	0	"
028	70	65	35	A	"	0	"
029	85	50	45	A	"	0	"
030	80	60	45	A	"	0	"
031	80	55	40	A	"	0	"
032	65	45	30	A	"	0	"
033	70	50	45	A	"	0	"
034	70	50	30	A	"	0	"
035	75	55	40	A	"	0	"
036	70	65	35	A	"	0	"
037	75	45	30	SA	"	0	"
038	75	45	20	SA	"	0	"
039	75	70	25	A	"	0	"
040	70	45	35	A	"	0	"
041	70	50	25	A	"	0	"
042	80	50	35	A	"	0	"
043	55	35	30	A	"	0	"
044	75	45	20	A	"	0	"
045	65	45	30	A	"	0	"
046	75	35	30	A	"	0	"
047	60	45	30	SA	"	0	"
048	60	55	35	SA	"	0	"
049	75	40	30	A	"	0	"
050	65	45	30	SA	"	0	"
051	65	40	30	A	"	0	"
052	70	35	25	SA	"	0	"

Sample No.	Diameter(mm) L	M	S	Roundness	Wt(g)	Mn-coating(mm)	Lithology & Remarks
D2-053	75	35	35	A	n.d.	0	tuff breccia
054	60	40	30	A	"	0	"
055	45	30	25	SA	"	0	sandstone
056	55	35	15	A	"	0	siltstone + tuff breccia
057	25	15	15	A	"	0	scoria?
058	110	75	70	A	"	0	pumice tuff
059	100	85	65	SA	"	0	"
060	45	35	30	A	"	0	"
061	40	30	15	A	"	0	"
062	40	30	20	A	"	0	"
063	35	30	20	A	"	0	"
064	35	20	18	SA	"	0	"
065	30	25	20	A	"	0	"
	90	45	35	SA	"	0	

the others 6 max 35

Note: Roundness -- A=angular SA=subangular R=rounded WR=well round